High-Conductance Measurement with the Heat Flow Meter Apparatus

A thesis submitted in fulfilment of the requirements for the degree of Doctor of Philosophy

Robin Edward Clarke

BSc (Hons) (Physics)

School of Engineering

College of Science, Engineering and Health

RMIT University

May 2017

DECLARATION

I certify that except where due acknowledgement has been made, the work is that of the author alone; the work has not been submitted previously, in whole or in part, to qualify for any other academic award; the content of the thesis is the result of work that has been carried out since the official commencement date of the approved research program; any editorial work, paid or unpaid, carried out by a third party is acknowledged; and, ethics procedures and guidelines have been followed.

The work has encompassed five journal or conference papers comprising Chapters 2 to 6, all of which have involved co-authors.

In the case of the three papers that comprise Chapters 2, 3 and 5, my contribution to the published work comprised 100% of the experimental component, 100% of the analysis and 95% of the writing and editing. As co-authors, my supervisors contributed to the editing.

In the case of the paper that comprises Chapter 4, my contribution to the published work comprised 80% of the experimental component, 90% of the analysis and 90% of the writing and editing. The second author, Andrew Pianella, was responsible for sample preparation and also contributed to the analysis, writing and editing. As additional co-authors, my supervisors also contributed to the editing.

In the case of the paper that comprises Chapter 6, my contribution to the published work comprised 100% of the experimental component, 95% of the analysis and 95% of the writing and editing. Assistance in the initial setup of the ANSYS model was provided by Cameron Stanley. As co-authors, my supervisors contributed to the editing.

Robin Edward Clarke

January 2017

ACKNOWLEDGEMENTS

I gratefully acknowledge my Senior Supervisor, Gary Rosengarten. My candidature became possible through his willingness to supervise a topic that was not precisely aligned with his research interests. Its success is a tribute to his capabilities and breadth of knowledge. It has also been very rewarding to be part of the active research group that has rapidly developed under his tutelage. He and my Associate Supervisor Bahman Shabani have both provided incisive criticism of my work which has greatly improved its quality. Andrew Pianella was most helpful with the work described in Chapter 4, particularly in the timely preparation of test specimens. Timely assistance was also provided by Cameron Stanley in setting up ANSYS for thermal modelling for the work described in Chapter 6.

The path that led me to undertake a higher degree began with my commencement as a new graduate with CSIRO in 1978. I am grateful to Leon O'Brien and Ron Ballantyne for offering me employment in the Thermal Group and for their many years of inspirational mentoring. Bill Clarke provided much the same in matters of electronics and instrumentation. To these I must add John Peirce who provided sterling technical support over many years and Harry Trethowen whose intellectual vitality was always inspirational, despite his distant location at BRANZ. More recently, I am grateful of the opportunity provided by Sukhvinder Badwal to join his research team, in which all members were encouraged and supported to do good science and to publish. My candidature became practical when Mark Burgess created a part-time position for me in commercial thermal conductivity testing at CSIRO and was happy to allow simultaneous study towards a higher degree.

Many CSIRO staff have been of assistance over many years. During my candidature, Peter Haggar has been most helpful and supportive in fitting commercial testing around my use of CSIRO facilities. Ian Cox-Smith of BRANZ has helped greatly in the development of ideas and perspectives over our numerous conversations.

All of my family and friends have provided encouragement and support. This is especially true of my close friend Chris Jablonski and my siblings, Barbara, Pauline and Graham. They mirror the encouragement I always received from my parents, Ted and Josie, when they were alive and which my wife's mother Joyce continues to provide with optimism and affection. Most importantly, I am blessed by the support of my wife Susan, who has been patient, understanding and sympathetic through this long period of study and stress, during which many sacrifices have been made and alternative pursuits neglected or postponed.

CONTENTS

LIST OF TABLES

LIST OF FIGURES

ABSTRACT

Measurement laboratories must be mindful of equipment limitations and increasing uncertainty as the extremes of operational range are approached. In the measurement of more highly-conductive materials, which may include lower-performing insulations, the prominent issue is that of interface resistance. Equipment is generally based on the heat flow meter or the guarded hot plate apparatus, both of which measure the heat flux between flat parallel plates held at different temperatures with the test specimen located between them. Interface resistance occurs between the test specimen and the plates that it contacts. Standards prescribe lower limits of specimen thermal resistance, typically 0.1 m^2.K/W. However whilst interface resistance may already be significant at this thermal resistance, measurement is often sought for more-conductive products. This dissertation considers a number of aspects of such measurements, in all cases proposing the use of flexible buffer materials at the interface between the test specimen and the apparatus plates in order to provide lower interface resistance. The use of this solution is seldom reported although it is described in some standards where it is also suggested that buffers of very low thermal resistance are required in order to minimize errors. However this would require them to be very thin and potentially ineffective. An alternative prospect has been explored, that of using thicker, softer interface materials to ensure good specimen contact. Separate measurement of the interface materials, in conjunction with an error analysis allows thermal resistance to be calculated as the difference between these measurements with known uncertainty.

Chapter 2 describes a study using the difference approach to measure twelve highly-conducting specimens in conjunction with four foamed plastic buffer materials, based on PVC, silicone, EVA and nitrile. The specimens ranged from aluminium sheet to fluted plastic board. Compared with direct measurement, thermal resistance values via difference

measurement were lower by between 0.003 and 0.01 m^2.K/W, depending on specimen and buffer choice. Silicone sponge gave the most uniform results. Compression tests showed that it also displayed the lowest deformation hysteresis. An analysis of the difference calculation is given, showing it to be numerically inexact since there are residual interface-resistance terms that are not present in both measurement cases.

Chapter 3 describes a further study of the difference technique in conjunction with flexible buffer materials, extending the procedure to materials of higher thermal resistance and to thinner, harder buffers. An alternative difference calculation is proposed to eliminate residual resistance terms through comparing results for the unknown specimen and for a reference specimen with similar surface characteristics and known properties, measured using the same buffers. Specimens of expanded polystyrene board and cast acrylic sheet were measured in the heat flow meter apparatus using two alternative silicone-based buffer materials, one solid and the other a sponge. Analysis also includes earlier measurements of twelve more highly-conducting specimens, adjusting for the residual error terms. Across all of these, thermal resistance values obtained by the difference method were lower by between 0.008 m^2.K/W and 0.016 m^2.K/W, attributable to removing the contribution of interface resistance.

In Chapter 4, a technique incorporating buffer materials is proposed for measuring the thermal conductivity of moist earthen and granular loose fill materials. Transient methods involving needle and other probes are also reviewed but it is concluded that a steady state approach offers reliable uncertainty estimation and a test method that is widely accepted in industry. Variations to the standard loose-fill method are proposed, including the use of a rigid holding frame with stiff base and silicone sponge buffer sheets, in conjunction with difference measurement to factor out the contributions from base, buffers and contact resistance. Using this approach, consistent results were obtained for loose-fill earths based on scoria, terracotta and furnace-ash at different moisture contents. Thermal resistance ranged from 0.08 to 0.4 m^2.K/W. Thermal conductivity fitted well to linear regression plots against moisture content. Further comparative measurements of a single specimen showed that direct measurement was less consistent than difference measurement, and that indicated thermal resistance was higher by 0.023 m^2.K/W, this effectively being a measure of the interface resistance.

Chapter 5 explores earlier evidence that high-conductance materials with rough surfaces, (such as many building boards), are measured to have higher thermal resistance and higher test thickness when measured with harder buffers. Results from an experimental study of nine materials and four buffer types are reported. Thermal resistance was higher by up to 0.01

m^2.K/W and thickness by up to 0.5 mm using the hardest buffer relative to the softest. An analytical model was developed, allowing measured roughness to be expressed as flat high and low areas of varying height and area fraction so that thermal resistance and height variations could be predicted as a function of roughness. Predictions were consistent with optical roughness measurements. The model further predicted that interface-resistance errors are proportional to surface roughness and are always present with harder buffers, typically reaching 010 m^2.K/W for a mean roughness amplitude (S_a) of 200 μm. However with softer buffers these errors are absent below an onset level, typically at an S_a value of 60 μm.

Chapter 6 describes heat flow meter measurements and transient thermal modelling using ANSYS of a webbed, hollow-cored panel with silicone sponge buffer materials chosen to provide boundary conditions comparable to standard surface coefficients. Surface temperatures were also measured at eight locations for an uninsulated configuration as well as with bulk insulation filling. Measured and modelled temperature-time plots agreed well after corrections for web and airspace thermal conductivity. Modelled spatial variation in heat flow exceeded 200% for one insulated case but was only about 2% for the uninsulated panel. Modelled values for heat flux and overall thermal resistance agreed well with standard analytical calculations. However heat flows indicated by the apparatus were consistently higher than the modelled and calculated values by up to 8%, expected to be due at least partially to specimen non-homogeneity. Nevertheless results suggest a useful role for the apparatus in providing temperature measurement under controlled conditions and helping to validate thermal modelling.

1 INTRODUCTION

1.1 Overview

This dissertation concerns measurement of the thermal properties of certain building products and industrial materials. Such measurements are necessary in order to determine how well thermal insulation and other building components effectively control the flow of heat and comply with thermal performance requirements. The properties typically measured include thermal resistance (R-value) and thermal conductivity, from which several other properties may be derived. For manufacturers, designers, regulators and end users alike, achieving the highest possible accuracy and precision is important. This requirement contributes to the significant technical challenges that are present in many aspects of the work. This dissertation concerns those that arise in the measurement of materials and products of high conductance (poor insulation value). It proposes solutions to control errors due to the presence of interface resistance which are the largest obstacle to achieving satisfactory accuracy and precision in the measurement of high-conductance materials. The experimental work was undertaken at a commercial thermal measurement facility operated by CSIRO. The work is encompassed within five published papers which are reproduced as Chapters 2 to 6.

1.2 A History of Thermal Properties Measurement

Measurement of the thermal properties of industrial and building materials is of growing importance in a world where products and components are increasingly engineered for purpose rather than specified on ad hoc principles. Within the building industry, engineering data requirements are likely to include structural, acoustic and fire properties and potentially

others, with thermal properties being just some among many. Initial interest in thermal properties measurement was associated with the early refrigeration industry and was bolstered by the need to calculate air-conditioning loads when cooling systems for buildings started to become common in the 1950s (Robinson and Powlitch, 1954; Zarr, 2001). The energy crisis of the 1970s ensured interest would flourish (Tye, 1990). In recent times, the ubiquity of computational methods ranging from pre-calculated look-up tables to full numerical simulations has meant that that the impact of improving the thermal performance of a single component can be assessed in terms of a building section or even a whole building almost instantaneously, and is therefore of recurrent interest. Running in parallel with this, particularly within the building industry, has been the steady march of regulation. Minimum energy performance requirements now often mean that a wall or ceiling must meet a specific performance target, which places the focus directly on the properties of each component. Thermal properties may be embodied not just in thermal performance areas but also for comfort, liveability and safety. Examples of this are the fire-retardant boards used behind fireplaces and cooktops which in some situations are required to have specified thermal performance to prevent overheating of the building fabric.

Methods for making such measurements do not have a particularly long history. In the USA, at the forefront of post-war development, the first thermal properties measurement standard was issued in 1945. It was the first description of the guarded hot plate method, ASTM C 177. Similar European standards were in development at around the same time. The first major report of inter-laboratory comparison between laboratories using C 177 was published in 1952 (Robinson and Watson, 1952). Early instrumentation meant that the method was slow and laborious. Measurement became easier as the capability of electronic instrumentation improved. The development of stable, sensitive heat flux transducers added an alternative approach, the heat flow meter method, under the designation ASTM C 518. Although a secondary method, reliant upon calibration against reference materials, it was eventually recognized as sufficiently precise for commercial measurement and its expediency in use was compelling. Supporting standards also arose, giving additional provisions for particular materials, sampling procedures and other aspects of measurement. Large scale methods such as the guarded and calibrated hot boxes arose in parallel. The ensuing 40 years have seen the introduction of commercial instruments built to comply with the testing standards, and the emergence of computer control and automated operation. A number of measurement issues have attracted attention and controversy, including the “thickness effect” wherein apparent thermal conductivity is seen to be thickness dependent (Shirtliffe, 1980; Hollingsworth, 1980; Albers and Pelanne, 1983), anomalous results with multiple reflective

airspaces (Desjarlais and Yarbrough, 1991), aging effects in plastic foams (Booth et al., 1995) and in vacuum panels (Wegger et al., 2011). Work by measurement communities and standards laboratories in developing and characterizing reference materials is ongoing (De Ponte, 1984; Tye and Salmon, 2001; Zarr et al., 2014). However the research base is this field is relatively small and the number of years over which efficient and reproducible measurement capabilities have been available has not been great. It is therefore not surprising that many gaps exist in collective knowledge, relating both to the properties of the materials themselves, as well as to issues specific to the measurement process. This dissertation has a focus on those issues particular to high-conductance measurements.

1.3 CSIRO Research Activities

Study of the thermal properties of materials was a major area of focus for the Building Research Laboratories (BRL), when first established in the Melbourne suburb of Highett in 1945. The first project undertaken involved a compilation of the thermal conductivities of building materials (Williamson, 2013). Report R2, Thermal Conductivities of Building Materials, was published in the following year (Barned, 1946). It included a compendium of thermal properties data amassed from overseas sources. The laboratories became part of the Commonwealth Scientific and Industrial Research Organisation (CSIRO) in 1949 with interests expanded to include building thermal design and analysis. By the mid-1960s, experimental facilities included a guarded hot plate apparatus. A revised edition of Report R2 published in 1970 included a significant number of results from the Highett apparatus (Barned and O'Brien, 1970). The first edition of the AIRAH Design Data Manual (AIRAH, 1978) contained a further-enlarged listing. The CSIRO apparatus was a conventional double-sided (two-specimen) design based on ASTM C 177 with 305 mm (1 ft) square plates. It utilized a precision potentiometer with Weston cell reference for thermocouple voltage measurement.

Also in 1980, a one metre square heat flow meter apparatus became operational at Highett. It was constructed by CSIRO and was rotatable, allowing horizontal or vertical measurement. It incorporated a set of four 254 mm square heat flux transducers in one plate and provided automated measurement of specimens up to 220 mm thick. Instrumentation included a precision data logger in combination with a desktop computer. Notable research based on this apparatus included an investigation into the slow equilibration times of moisture adsorbing materials (Clarke and Delsante, 1993), a broad study of the conductivity of compressible insulation materials (Symons et al., 1995) and a study of the properties of local clay bricks (Zsembery et al., 1996).

In 1999, similar instrumentation was integrated into a commercial “k-Matic” apparatus to allow automated operation. This instrument was an earlier implementation of the heat flow meter method produced by the Dynatech Company, with 305 mm square plates and a single 100 mm square heat flux transducer. The plate temperatures, which were un-adjustable as standard, were made variable through controller modifications. A Fox 600 heat flow meter apparatus (TA Instruments, 2016) began operation in 2011. The experimental work described in this dissertation was performed using either the Fox 600 or the k-Matic apparatus.

1.4 Research Gaps - The Interface Problem

The performance of insulation materials has improved over time. Measurement candidates now frequently include very low conductivity rigid plastic foams based on polyurethane, phenolic or polyisocyanurate, with thermal conductivity typically below 0.02 m^2.K/W before aging (Stovall, 2014). Accurate measurement can be problematic, especially with the increasing use of these products at greater thickness which results in very low output voltages from the heat flux transducers, relative to the values at calibration. Measurement accuracy may therefore suffer although the effect on uncertainty can be difficult to calculate. A compounding issue is the limited availability of reference materials in this range. Traditional reference materials are typically glass fibre with thermal resistance of the order of 1 m^2.K/W. In contrast a block of plastic foam 200 mm thick might exceed 10 m^2.K/W.

At the same time, there is steady demand for assessment of highly-conducting building products. These may be engineered products with primary attributes other than their insulation performance. Thermal properties may nevertheless be of interest and may be required for compliance with codes or for design calculations.

Some of the calibration issues that exist for high thermal resistance measurement are also present for low-resistance cases. Whereas high-resistance specimens may be an order of magnitude higher in thermal resistance than an available calibration reference, a high-conductance board may be an order of magnitude lower. At least the heat flows are large in the case of high-conductance materials, so that some uncertainty issues related to their measurement are less significant. The current version of ASTM C 518 (ASTM, 2015) pays considerable attention to calibration. In the first instance it states that the apparatus shall be calibrated with materials having similar characteristics and thicknesses as the materials to be evaluated. This is only practical to a limited degree since the apparatus is expected to accommodate a large variety of material types over a large range of thicknesses. The available calibration reference materials cover a much smaller range.

Accurate measurement of building insulations and low-conductance materials relies principally on the guarded hot plate and heat flow meter methods (ASTM, 1985). The differences between these two approaches are not great, amounting to the ways that temperatures are controlled and how heat flow is measured. Fundamental to both is the presence of two parallel plates of adjustable separation, held at different temperatures to create a uniform temperature gradient across the test specimen that is located between them. The guarded hot plate also allows for a double-sided, three-plate design which accommodates two specimens but is otherwise similar.

These geometries can provide test conditions that are close to optimum. Provided the plates are large relative to specimen thickness, a uniform pattern of heat flow can be established from plate to plate, precisely normal to the plane of the specimen. A large plate area also allows for heat flow to be measured over a relatively large area which provides helpful averaging of small variations as well as a large heat flow signal for accurate measurement. Hot and cold plate temperatures are uniform and can be precisely measured. For compressible and uniform rigid materials, test thickness can be precisely defined as the spacing between two accurately flat and parallel plates. The accurately known values of heat flow, temperature and thickness are all that is required to determine the thermal properties with an accuracy that is typically within 2-3% relative to a calibration reference specimen (Bomberg, 1994), (Zarr, 2010).

Difficulties emerge however with rigid specimens that are not truly flat. Plate separation no longer accurately reflects specimen thickness. Lack of contact with the plates in some areas also means that neither temperatures nor heat flows may remain spatially uniform. The large measurement area becomes a liability because it makes flatness hard to achieve. The scale of error introduced is related to the conductivity of the test specimen. The non-contacting areas are effectively small insulating airspaces and so would have an insignificant effect on measurement of an insulation material that had a thermal conductivity similar to air, 0.026 m^2.K/W at ambient temperature. Some of the better-performing insulations do have thermal conductivities around this value whilst for some conductive materials the thermal conductivity might be ten times higher. For a thin, conductive specimen, a simple calculation might reveal the potential for an error of around 20% due to interfacial airspaces. For thicker specimens the plate interface is relatively less important and the potential error is lower.

The problem of poor contact due to uneven surfaces is effectively one of interface resistance, introduced in association with the unwanted airspaces. It may be minimized by ensuring the specimen is very flat, possibly by surface grinding both faces. However this may

be impractical with some specimens and, in any event, presumes that the apparatus plates are also very flat, something that is difficult to ensure for a class of apparatus with plates often exceeding 500 mm square. The guarded heat flow meter, ASTM 1530 (ASTM, 2011) is an alternative measurement method with some overall similarities to the heat flow meter method, but which relies on small specimens (typically 50 mm round), very high flatness, high clamping pressure and a calibration technique that includes allowance for interface resistance. It is a preferable method for specimens that can accommodate its requirements. Many however are too thick or cannot tolerate either surface grinding or the high clamping forces.

1.5 Research Objectives – Solutions based on Interface Buffers

The provisions of the heat flow meter standard, ASTM C 518, deal with the prospect of interface resistance in part by suggesting that the default location for temperature measurement should be the surface of the test specimen, not the apparatus plate that is in contact with it. Using the surface temperatures should result in a measurement that does not include the interface resistance. However it would require provision for wiring to external temperature sensors, a feature with limited availability in commercial test apparatus. Temperature measurement at the plates is commonly the only option. A single external measurement point is available in some apparatus, forcing reliance on the assumption that the degree of imperfect contact between specimen and plates is uniform and that temperature is not spatially variable. This assumption may not be warranted, especially considering the difficulties in making precise measurements of surface temperatures in the presence of significant heat flow. A key aspect of this dissertation is the idea of using an alternative approach to this difficulty. If a flexible interface material, herein termed a buffer material, is placed between the specimen and each plate, it provides improved contact, potentially reducing the spatial temperature variation and heat flow non-uniformity. In addition, if the two interface materials are measured separately, their thermal resistance may be subtracted from the measured total leaving a difference value that does not include the contact resistance. This option is foreshadowed in C 518, proposing the use of a “thin sheet of suitable homogeneous material”, measured separately. However the standard gives little significant detail on its application, suggesting only that the interface material should have low thermal resistance relative to the specimen. That practice is not followed in this dissertation. Instead, reliance is placed in the formal uncertainty determination in order to assess the significance of buffer thermal resistance along with all other factors that contribute to overall uncertainty.

This dissertation is therefore an examination of the limitations arising in direct measurement of several high-conductance material types using the heat flow meter apparatus and an evaluation of the extent to which the use of thick buffer materials, a technique not accommodated in current standards, is able to deliver acceptable measurement solutions. An implicit objective is therefore also to illustrate certain limitations in existing standards and to provide some suggestions for change and improvement.

1.6 Scope

The work described in this dissertation has been undertaken as five interlinked research projects, embodied as five published research papers addressing the objectives described in the previous section. The five publications are presented as Chapters 2 to 6 and constitute the complete research content of this dissertation. The published versions of these papers have some variation in style according to the requirements of the publishers. However the chapters are presented in a harmonized style, representing the final word-processor version of the submitted paper, along with editorial changes as a result of the review process. Each chapter contains a facing page describing any specific issues related to the particular paper.

Chapter 2 describes a study into the use of buffer materials and the subtraction (difference) approach referred to in the previous section. Four alternative buffer materials were assessed in the measurement of twelve highly-conducting sheet materials. The buffers were all foamed plastics, including EVA, nitrile and silicone sponge. The sheet materials included aluminium, some rigid plastics, two extruded fluted plastics, a cementitious board, a fibre board and several composites. The difference technique was demonstrated to be effective although results were dependent upon the characteristics of the specimens, especially roughness, as well as the buffer type. Compression and hysteresis tests were undertaken in order to correlate the buffer-related differences with their physical characteristics. The chapter also presents an analysis of the difference approach and considers the material and interface resistance terms that are present in the buffer measurements with and without the specimen present.

Chapter 3 is an extension of the work described in Chapter 2 to specimens of higher thermal resistance, for which the possibility of significant interface resistance might not be anticipated. The materials studied were a smooth-faced, PMMA (acrylic), and an EPS foam with some surface roughness in its wire-cut surface. Having established silicone sponge as a buffer material with good performance, two alternative types of silicone-based buffer were compared. One was a medium soft sponge, the other an un-foamed (solid) sheet. Being also

thinner, it was much less compressive and had a much lower thermal resistance. The latter brought it more in line with the prescriptions of ASTM C 518 that the buffer should have a low thermal resistance. Analysis of results also introduced a refinement to the difference measurement. If the first measurement is of the unknown specimen whilst the second is of a known high-conductance reference material, the subtraction of the two no longer includes residual terms such as the interface resistance of direct buffer-to-buffer contact. This does entail the presumption that the interface resistances of the specimen and the reference are similar, linked to the presumption that they have similar roughness. This is supported by the results obtained for different materials having roughness that is apparently similar based on visual inspection. Consideration of these matters is expanded in Chapter 5 which deals with quantitative assessment of roughness. The alternative procedure using a reference specimen for difference measurement was then compared with the original method, with consistent results, giving correction factors that allowed the results described in Chapter 2 to be recalculated according to the new method. This produced a consistent range of interface resistance values, higher overall than the Chapter 2 results, which are presented. Small but consistent differences between results produced by the different buffers are noted.

Chapter 4 concerns the application of buffer materials in the measurement of earthen and granular loose fill materials. These materials are often used outside the building industry, where alternative transient methods involving needle and other probes are common. A review of the competing methods is presented although it is concluded that the steady state methods offer the advantages of an uncertainty that can be reliably estimated and a test method that is widely accepted in industry. However, variations to the standard loose-fill measurement method are also proposed, including the use of a rigid holding frame with stiff base and the use of silicone sponge buffer sheets, in conjunction with difference measurement to factor out the contributions from base, buffers and contact resistance. The softest, most compliant available buffer was proposed for the upper surface of the granular loose fill. Depending upon coarseness and composition, this surface may be very rough and have very poor contact with the abutting surface. An experimental program involving nine sets of three near-identical specimens is described. Very consistent thermal conductivity results are reported for loose-fill earths based on scoria, terracotta and furnace-ash at different moisture contents. The study also included multiple re-measurements of one specimen, alternately by direct and difference measurement. This provided an indication of the effective interface resistance. It also provided an indication of the variability produced by direct contact with the random high points of a rough surface, in comparison with the more uniform contact provided by a soft buffer. Since publication of these steady-state results, a paper comparing them to results

obtained with transient probe results with the same specimens has also been published (Pianella et al., 2016).

Chapter 5 further extends the work on interface resistance described in Chapters 2 to 4. In Chapter 3 it was noted that when measuring with buffers and calculating the thermal resistance by difference, indicated thermal resistance tended to be slightly higher as measured with the harder buffers, which were based on solid (un-foamed) silicone rubber sheet. Subsequent measurements of highly-conducting materials had confirmed this effect and shown it to be very significant when specimen surfaces were also very rough. The chapter reports on an experimental study of nine mostly-rough materials and four buffer types to demonstrate and quantify the effect of buffer hardness on measured thermal resistance as well as on apparent overall thickness. The correlation between these two properties was investigated, and associated with independent measurement of surface roughness provided by confocal microscopy. The relationship between interface resistance and surface roughness was studied through the development of an analytical model which allowed measured roughness to be expressed as flat high and low areas of varying height and area fraction so that thermal resistance and height variations may be predicted as a function of roughness using a simple two-zone (binary) model of buffer compression and heat flow. A simple geometric transformation was also developed to allow generalized roughness to be expressed in terms of the binary model, allowing a general relationship between roughness and interface resistance to be developed. Findings are discussed, including the implication that measured thermal properties have some inherent dependency on the roughness of the interfacial material used in their measurement.

Chapter 6 considers the thermal assessment of a webbed hollow-cored building panel using the heat flow meter apparatus. Although non-homogeneous materials are outside the scope of the method, an initial series of measurements showed results to be independent of the position of webs relative to the heat flux transducer. This suggested that such measurements might be practical. It was recognized that a potential role for buffers in these measurements was to create boundary conditions similar to those that exist in a hot box apparatus where surface coefficients exists between the panel under test and the isothermal conditioned space on either side. Hot box standards allow for non-uniform specimens on the basis that air to air temperatures provide a single value of the overall thermal resistance which automatically accommodates the panel irregularities. Buffers may provide the same effect and so were chosen to have a thermal resistance similar to typical indoor and outdoor surface coefficients. The panel was instrumented with fine-gauge thermocouples at eight surface locations. The measurement procedure involved pre-conditioning under isothermal conditions in the heat

flow meter apparatus followed by a step function placing 33 ºC on the hot side and 13 ºC on the cold side. The step response was modelled using ANSYS running in transient thermal analysis mode. These measurements were performed with the original uninsulated panel as well as with the addition of two levels of fibrous insulation to the cores which provided much greater spatial variability. Measured temperatures were used for refinement of some of the modelling properties data. It was then possible to compare results from numerical modelling with temperature measurement, with standard analytical calculation of bridging heat flow for the panels and with heat flow and thermal resistance results from the apparatus. These results are presented.

2 FLEXIBLE BUFFER MATERIALS TO REDUCE CONTACT RESISTANCE IN THERMAL INSULATION MEASUREMENTS

Conference Paper:

Clarke RE, Rosengarten G and Shabani B. (2014) Flexible Buffer Materials to Reduce Contact Resistance in Thermal Insulation Measurements *Thermal Conductivity 32 / Thermal Expansion 20, Proceedings of the 32th International Thermal Conductivity Conference and 20th International Thermal Expansion Symposium.* West Lafayette, Indiana: Purdue University Scholarly Publishing Services, DOI: 10.5703/1288284315544

Additional Information for Chapter 2

The following pages of this chapter present, in the formatting style of this dissertation, a paper published in the Proceedings of the 32th International Thermal Conductivity Conference. Revision based on reviewer comments has been incorporated.

There are some formatting and editorial differences in the published version which utilized a two-column format.

For inclusion in this dissertation, section numberings have been amended to incorporate the chapter number.

American spellings were required by the publisher and have been retained.

Figures in the submitted version were in monochrome (black and white) as required by the conference organizers at the time of initial submission. New colour figures have been prepared for this dissertation to improve and harmonize appearance. There are slight differences in the colour figures, relative to the monochrome versions in the published document.

A harmonized reference style based on Sage Harvard has been used in the presentation of this paper, as throughout this dissertation. However this is not the style used by the publisher. DOI numbers have been included where available.

FLEXIBLE BUFFER MATERIALS TO REDUCE CONTACT RESISTANCE IN THERMAL INSULATION MEASUREMENTS

Robin E Clarke[1,2], Bahman Shabani[3] and Gary Rosengarten[1]

[1]School of Engineering, RMIT University, Melbourne, VIC, Australia

[2]CSIRO Australia, Clayton South, VIC, Australia

[3]School of Engineering, RMIT University, Bundoora, VIC, Australia

Corresponding author:

Robin E Clarke, CSIRO Australia, Private Bag 10, Clayton South, VIC 3169, Australia.

Email: Robin.Clarke@csiro.au

Keywords

thermal resistance; measurement; test methods; contact resistance; interface resistance

Abstract

Thermal insulation test methods approach their lower limits as thermal resistance falls below 0.1 m^2.K/W. This is the minimum value specified in ASTM C 518 (ASTM, 2010b) whilst ASTM C 177 (ASTM, 2010a) proposes about 0.06 m^2.K/W. Nevertheless these are the test methods, along with their ISO equivalents, required by Australasian building codes and directed at many products and materials with thermal resistances below 0.1 m^2.K/W. Alternatives such as ASTM E 1530 (ASTM, 2011) cover much lower resistances but require carefully-prepared small specimens and very-high contact pressures and are therefore largely unsuitable for both technical and compliance reasons. For these low resistances, the insulation test methods face large errors due to interface resistance between specimen and the apparatus hot and cold plates. Staying with C 518, the problem can be avoided by using direct measurement of the test specimen surface temperatures but this is difficult, has its own accuracy issues, and is often impractical for commercial laboratories. This technique is generally used in conjunction with interface materials such as flexible foam between the specimen and the hot and cold plates, to enhance contact and also provide an access path for temperature sensors. We have studied the alternative prospect of using these interface materials to ensure good specimen contact, in conjunction with a simple two-step thermal

resistance determination based on the difference between presence and absence of the test specimen.

This paper presents results of a study using this difference approach for the measurement of twelve highly-conducting materials, including sheets of aluminum, phenolic, HDPE, MgO, bonded rubber and cork granules, PMMA and compressed wood fiber. For each material, repeated measurements have been performed with 4 different interface or "buffer" materials; PVC, silicone, EVA and nitrile. Silicone sponge gave the most uniform results, consistent with a measurably lower hysteresis. The difference technique yielded a lower indicated thermal resistance than direct measurement by between 0.003 and 0.01 m^2.K/W, with some variation depending on the specimen surface characteristics and to a lesser extent on the choice of buffer. Larger differences were associated with bowed, uneven or roughly-surfaced specimens. The difference-technique results have greater variability but they may be seen as better estimates of the actual specimen resistance since contact resistance is much lower for soft-surface interfaces. An interface resistance of up to 0.01 m^2.K/W is large enough to be of significance in many thermal measurements.

2.1 Introduction

A laboratory seeking to have a capability for thermal resistance measurement around and below 0.1 m^2.K/W, might consider the option of an ASTM E 1530 apparatus. However E 1530 covers the range 0.001 to 0.04 m^2.K/W, leaving a gap up to the low end of C 518 where neither method is optimum. E 1530 has a strong focus on interface resistance. Test specimens, typically 50 mm in diameter, are required to have tightly-controlled flatness (± 0.025 mm). Gimbal joints are required at the load application points to maintain an even contact pressure of at least 70 kPa, and typically over 200 kPa, which is 100 times higher than C 518 contact pressures. A heat-transfer medium is recommended for the contacting faces. Finally the calculation method is by comparison with a known similar material measured under similar conditions so that extraneous sources of thermal resistance, from the interface as well as internal to the apparatus, are automatically accommodated.

The attention that E 1530 affords to issues of interface resistance serves to highlight the absence of such considerations in the insulation standards, where the focus is on high-performance materials. However, energy performance regulations require data to be available for all building elements, not just insulations. In Australia, the primary source for standardized tabulations of such data is the AIRAH Handbook (AIRAH, 2013). It lists the thermal resistance of 10 mm gypsum plasterboard, for example, as 0.059 m^2.K/W. Numbers

such as this are typical of the raw data required for building thermal modelling software. In general, it is also a requirement that such data be obtained by measurements in compliance with the Australasian & New Zealand insulation standard, AS/NZS4859.1 (Standards Australia, 2006). This standard in turn calls up the ASTM test methods C 518 and C 177 and their ISO equivalents. Australian Building Regulations are also tied directly to AS/NZS4859.1. This provides a disincentive for the use of alternative techniques such as E 1530 or the laser flash standard E 1461 (ASTM, 2013c) which might not be completely excluded but have "last resort" status at best. In any event, there are definite advantages with the "insulation" test methods, which assess a sizeable sample of a "product" rather than a small, carefully-prepared test specimen. Real-world products may be composite, textured, layered, profiled or otherwise complex, they may have uneven surfaces, and they may lack small-scale uniformity. These are all manageable issues with the insulation test methods, particularly the larger apparatus.

It is therefore not surprising that the CSIRO thermal laboratory has an ongoing focus on the thermal insulation test methods, ASTM C 518 in particular, and that we also have a particular interest in accurate measurement of low-resistance specimens. This study of the use of flexible buffer materials, and measurement by difference, is indicative of this emphasis and has provided an opportunity for closer scrutiny of a technique we have used for some time.

2.2 Background

2.2.1 Measurement Techniques

From a technical perspective, a C518 apparatus optimized for operation up to 10 m^2.K/W might be expected to struggle with measurement more than two orders of magnitude lower. Unfortunately this is not widely acknowledged. The specifications for commercial apparatus often quote conductivity range rather than resistance and do not generally impose low-resistance limits. Lower thermal resistances are associated with higher heat flows, which would seem to be no harder to measure accurately. This rational of course ignores the issue of interface resistance.

ASTM C 518 does contain a clause requiring rigid or high-conductance specimens to have careful surface preparation. It states that surfaces should be made flat and parallel to the same degree as the heat flow meter and that plate-mounted temperature sensors "may" be used if thermal resistance is sufficiently high. In fact few test specimens could be supplied, or

modified, to achieve this flatness. As for temperature sensors, commercial apparatus generally have only the plate-mounted option. In order to use external sensors, the laboratory must set up a separate measurement system running in parallel with the built-in instrumentation. This introduces data management and calibration issues, especially for thermocouples where a different wire calibration and a different cold junction compensation system would be required. The European standard, EN 12664 (BSI, 2001) has a focus on materials of medium to low thermal resistance and presents considerable detail on techniques for external temperature measurement which are suggested for thermal resistances of up to 0.5 m^2.K/W in some cases. EN 12664 also emphasizes specimen uniformity, especially flatness.

Despite the difficulties, the use of external temperature sensors is an effective technique to bypass interface resistances. In order to accommodate and protect the sensor wires, sheets of foam or similar material are generally used between either side of the specimen and the test plates. The alternative of machining grooves in the specimen to carry the sense wires may be feasible, but is often impractical, and introduces other errors. In any case, specimens of this type are potentially heavy, friable, abrasive and of uncertain thickness uniformity. So the foam sheets also protect both the apparatus and the specimen. (Corsan and Williams, 1980) have studied the potential errors with this technique. More recently, Campbell and Rose (Campbell and Rose, 2013) describe its use with concrete test specimens in a Netzsch Application Note. We have employed this technique for many years with test materials such as rammed earth and brickwork walling weighing as much as 500 kg ((Zsembery et al., 1996)). Our older C 518 rigs use in-house data acquisition, including four precision thermocouples on each side of the test specimen as an integrated software-selectable option. EN-12664 refers to “contact sheets”. The term “interface material” is also used, at the risk of confusion with heat transfer pastes used for semiconductor cooling and similar applications. We use the term “buffer” sheets, or materials, to describe the foam material used in this way. These buffer sheets have significant thermal resistance, and they buffer the specimen both physically and thermally in the test apparatus.

With careful setup and uniform specimens, external thermocouples may be used quite successfully in conjunction with buffer sheets. Plate and specimen surface temperatures are consistent and effectively define the thermal resistance of each buffer as well as the test specimen, in proportion to the temperature differences. Interface resistance appears considerably reduced, as might be expected from contact with a soft buffer material. This consistent behavior suggests that the external thermocouples might actually be dispensed with. The difference between two measurements – buffers in conjunction with test specimen and buffers alone – represents the test specimen resistance, plus some smaller contact

resistance terms. These two measurements are more straightforward that using external thermocouples. This option is described in C 518, proposing the use of a "thin sheet of suitable homogeneous material", measured separately.

Brzezinski and Tleoubaev (Brzezinski and Tleoubaev, 2002) and Tleoubaev and Brzezinski (Tleoubaev and Brzezinski, 2007) have further developed an alternative dual-measurement technique originally suggested by Filla and Slifka (Filla and Slifka, 1997). With two test specimens identical except in thickness, a pair of measurements provides sufficient data to factor out the interface resistances, assuming these are constant. Whilst novel and effective, the technique requires a pair of uniform materials, available in different thickness having identical conductivities.

We have also observed that for specimens with significant non-uniformity in thickness, external temperature readings can be quite variable, raising concerns about how representative any chosen sensor locations might be. Corsan and Williams confirm these large variations in temperature by computation. In comparison to a determination of thermal resistance based temperature readings at a few chosen locations, a determination based on subtracting the thermal resistance of buffer sheets would seem to have some immunity from local effects, since all components are intrinsically spatially-averaged.

Buffer sheets also offer plate protection with heavy or abrasive specimens, even if interface resistance is not an issue. Polyurethane panels faced with granite chips are a notable example.

2.2.2 Theoretical Considerations

A heat flow meter (or guarded hot plate) apparatus is a means of applying Fourier's heat conduction equation in a constrained way. Ideally there will be uniform, (usually rectilinear) geometry, uniform plate temperatures, unidirectional heat flux and a uniform test specimen. Under these conditions, the temperature difference divided by the heat flux over the metered area is a direct measure of the total thermal resistance (R_t) between the points of temperature measurement. Figure 3.1 is a sketch of one of the alternative geometries which uses two heat flow meters, one imbedded in each plate. To illustrate the types of resistance term, a buffer material is shown only on top of the test specimen in this example.

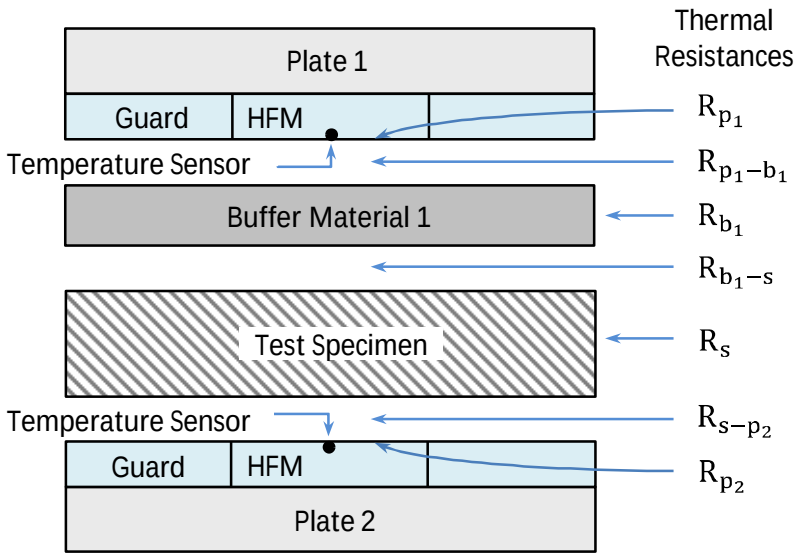

Figure 2.1. Heat flow meter apparatus with specimen and one buffer material present.

For a direct measurement where no buffer material is used, the test specimen is in contact with both plates and there is a simple series combination of thermal resistances.

The relationship can be expressed as

$$R_t = R_{p_1} + R_{p_1-s} + R_s + R_{s-p_2} + R_{p_2} \quad (1)$$

where

R_t is the total thermal resistance between the plate temperature sensors;

R_{p_1} is the internal thermal resistance of plate 1;

R_{p_1-s} is the interface thermal resistance between plate 1 and the specimen;

R_s is the specimen thermal resistance;

R_{s-p_2} is the interface thermal resistance between plate 2 and the specimen; and

R_{p_2} is the internal thermal resistance of plate 2

R_t, as measured, is a good approximation for R_s only if the other four terms in equation (1) are small. Commercial apparatus relying on embedded plate temperature sensors almost invariably measure R_t. The other four terms are absent if external temperature sensors are used at the specimen surfaces. However this is difficult to do without introducing other errors, especially since the temperature difference across the specimen may be relatively small.

Values for R_{p_1} and R_{p_2} are not generally published in equipment specifications. There is evidence that they are indeed quite small, especially for modern equipment which generally

employs metal plate facings. In any case, they are extremely difficult separate from the interface resistances R_{p_1-s} and R_{s-p_2} and for most purposes can be lumped together. These terms are widely ignored and are insignificant in many cases. Where test specimens have surface characteristics similar to calibration specimens, the interface resistance is already factored into the calibration. However this is really only valid for cases where the test and calibration specimens have similar thermal (and interfacial) properties.

The interface resistances are intended here to include classical "contact resistance" as might be measured between flat mating surfaces of a certain roughness with a certain contact pressure. However they also encompass gross effects arising with real-world specimens where imperfect flatness leads to voids, airspaces and generally-uneven contact. The literature provides very little guidance as to values for interface resistance that might apply for a typical thermal conductivity measurement. The range may be very broad even though insulation test apparatus use a relatively narrow range of contact pressures, generally around 2 kPa. Tleoubaev and Brzezinski report a value of 0.003 m^2.K/W as the total of the interface and internal terms in equation (1) for highly-flat Pyroceram. Values much higher than this are conceivable. At a 0.3 mm void, the local thermal resistance will be approximately 0.01 m^2.K/W.

Extending the components of Figure 2.1 to the case where a lower buffer sheet is also present, the total thermal resistance, R_{t_i}, is composed of a long chain of series components as follows:

$$R_{t_i} = R_{p_1} + R_{p_1-b_1} + R_{b_1} + R_{b_1-s} + R_s + R_{s-b_2} + R_{b_2} + R_{b_2-p_2} + R_{p_2} \quad (2)$$

When the buffer sheets are measured alone, the total thermal resistance $R_{t_{ii}}$ is

$$R_{t_{ii}} = R_{p_1} + R_{p_1-b_1} + R_{b_1} + R_{b_1-b_2} + R_{b_2} + R_{b_2-p_2} + R_{p_2} \quad (3)$$

The difference is therefore

$$R_{diff} = R_{t_i} - R_{t_{ii}} = R_{b_1-s} + R_s + R_{s-b_2} - R_{b_1-b_2} \quad (4)$$

R_{diff} has only three interface terms, all involving a soft-material interface. $R_{b_1-b_2}$, is subtractive although expected to be the smallest term, since it is for a soft-soft interface. The key question is therefore whether R_{diff} (by calculation) is a better approximation for the specimen thermal resistance, R_s than R_t (by direct measurement). This study compares measurements of R_t and R_{diff}, under the assumption that both will lead to an overestimate of R_s since the some interface terms are present in both cases. However the soft-material interface terms should be quite small and R_{diff} should be much closer to R_s.

A buffer material must have carefully-considered stiffness and resiliency. It needs to be soft enough to afford low interface resistance, and to accommodate test specimens with uneven surfaces. This requires there to be some compression at the high points, where the local contact pressure will be significantly higher, in proportion to the spatial extent of these areas. This however also means that the material will be sufficiently soft for there to be some residual compression even when contact is uniform, since as a first approximation, deformation will be proportional to pressure (in accordance with Hooke's law). For difference measurements with uniform specimens, the same thickness reduction occurs for the specimen-present and the specimen-absent measurements, so any compression cancels out. Compression will however be spatially-irregular when any sample non-uniformity is present, making this cancellation somewhat inexact. Further considerations are the consistency (repeatability) of apparatus-loading pressure and the potential for hysteresis and creep in the buffer material.

We have observed greater variance when buffer materials are used, beyond what would be expected due to the uncertainty implications of subtracting two numbers. The experimental program incorporated repeat measurements in order to study the extent of this variance. The sources of uncertainty appear to be complex and are addressed empirically at this stage.

2.3 Selection Of Test Specimens

Table 2.1 summarizes the twelve specimens chosen for study. All were 600 mm square. Specimens 1 and 2 were aluminum sheet, which is so conductive that thermal measurement is overwhelmed by interface resistance. Specimen 1 was flat whilst specimen 2 had a bow of approximately 3 mm in one plane. The instrument plates flattened the bow out almost completely but it was of interest to see what differences remained between the two sheets. The resistance of the HDPE and phenolic paper specimens was two orders of magnitude higher than the aluminum although still so low that interface effects predominate. Both had smooth flat faces, offering good surface contact at least. All other specimens were resistive enough for C 518 measurement to be conceivable. Specimen 5 was composed of fused rubber and cork granules, predominantly rubber. Although uniform and flexible, it was quite rough on both sides. Specimen 6, the MgO board, was smooth on one side, rough on the other. It also had a 1 mm bow at the midpoint which was largely eliminated by plate pressure. Specimens 7 and 8 were PMMA (acrylic) specimens from different sources with a slight thickness difference. Specimen 9 was a commercial flexible PVC flooring material. It was used as a pair of 1.5 mm sheets back to back with the softer base surfaces outermost and the

decorative upper surfaces in contact. It was a composite material with four or more layers, one with glass-fiber reinforcing, and had limited compressibility associated only with the bottom foam layer.

Table 2.1. The twelve test specimens. Thermal resistance is derived from generic thermal conductivity where this is known, otherwise from direct measurement.

Specimen number	Description	Thickness (mm)	Density (kg/m^3)	Thermal resistance ($m^2.K/W$)	Generic thermal conductivity (W/m.K)
1	Flat aluminum sheet	2.5	2720	0.00001	220
2	Bowed aluminum sheet	3.0	2680	0.00001	220
3	HDPE clear sheet	1.5	960	0.003	0.50
4	Phenolic paper board	1.6	1430	0.006	0.27
5	Granulated rubber & cork underlay	3.2	650	0.028	--
6	MgO board	15.9	1440	0.028	--
7	PMMA (acrylic) A	5.8	1190	0.031	0.19
8	PMMA (acrylic) B	6.1	1130	0.032	0.19
9	Flexible PVC flooring (pair of sheets)	3.0	760	0.033	--
10	“Masonite” hardwood	5.4	950	0.038	0.14
11	Corrugated polypropylene (“fluteboard”) A	3.3	170	0.062	--
12	Corrugated polypropylene (“fluteboard”) B	5.0	180	0.081	--

Specimen 10 was a typical board of Masonite material with one very smooth and one rough-textured surface. Specimens 11 and 12 were examples of corrugated polypropylene “twin-wall” sheet. Specimen 11 was a thinner, light-duty material, as used in signage, with thinner walls and closer flutes. Both were sealed at the ends to prevent air movement through the flutes.

2.4 Evaluation of Buffer Materials

Details of the buffers are given in Table 2.2. All were evaluated as pairs with one on either side of the test specimen. The PVC flooring material used as a buffer was identical to that used as a test specimen, with a back-to-back pair giving a total thickness of 3 mm. The silicone sponge was a grade described as “medium-soft” and “low compression set”. The EVA and nitrile foams were both of much lower density but product specifications were not available.

During the measurement program it became apparent that the buffers differed not just in terms of consistency in results but also in terms of the specimen thermal resistances they suggested, presumably as a result of differing contact resistance. Differences in compressibility and resilience of the foams were thought to be relevant and worthy of investigation. ASTM D 1056 (ASTM, 2007) provides guidance for making such assessments on rubber foams.

Compressibility, is measured as the force required for 25% compression and "compression set" is evaluated as the rate of recovery after 22 hours of compression. A test protocol was devised to adapt the intention of these tests to a deflection and time-frame that is more appropriate for buffer materials. A 50 mm steel disk resting on a sample of buffer material was loaded progressively up to about 3 kPa, followed by a 60-minute hold and progressive unloading in order to form a set of hysteresis results. Results are shown in Figure 2.2. The lower curves show the progressive initial loading and deflection, expressed as a percentage of thickness. The upper curves show the deflection as the load was progressively removed 60 minutes later. There are large differences in hysteresis, the implications of which are considered later.

2.5 Thermal Resistance Measurement Results

Each specimen was measured three times directly (with no buffer material present) and three times with a pair of each of the buffers. Each pair of buffers was also measured three times by itself. A 6 K temperature difference was used for all direct measurements in order to reduce the very high heat flows. Measurements involving the PVC buffers were performed at 10 K, the silicone sponge at 14 K and the EVA and nitrile buffers at 20K temperature difference.

A buffered result is obtained by subtracting a buffers measurement from a specimen-plus-buffers measurement, as described in Equation (4). Since three values were obtained for each of these measurements, the subtraction can be performed in nine different ways to obtain nine thermal resistance values. It might be statistically more rigorous to perform eighteen individual measurements for the construction of nine difference pairs but the difference measurements as calculated do represent a complete set of possible outcomes from the measurements performed.

Table 2.2. The four buffer materials. Properties apply for a single buffer (on either side of test specimen).

Buffer number	Description	Thickness (mm)	Density (kg/m^3)	Thermal resistance ($m^2.K/W$)	Thermal conductivity (W/m.K)
1	Flexible PVC flooring (pair of sheets)	3.0	760	0.035	0.087
2	Silicone sponge	6.5	440	0.081	0.080
3	EVA foam	4.2	31	0.12	0.035
4	Nitrile foam	7.3	71	0.21	0.035

Results are presented in Figure 2.3 showing nine calculated results for each buffer material. The first sketch shows thermal resistance results for the two aluminum sheets. The directly-measured value was consistently just above 0.008 $m^2.K/W$ for both, unaffected by the flatness difference between them. It is apparent that this resistance is almost entirely composed of interface components since the sheets themselves account for only 0.00001 $m^2.K/W$, effectively zero on the scale used. The scale is fine enough however to reveal considerable disparity in results for difference measurement with buffers. It also shows a correlation between the consistency of results with any particular buffer and the degree of hysteresis in the material as indicated in Figure 2.2. Specifically, the silicone provides the least variability, followed closely by the EVA. The PVC is significantly worse and the nitrile is worse still.

This trend is apparent throughout. For the aluminum sheets, measurements with the silicone buffers at least provide some consistency and suggest a thermal resistance of around 0.003 $m^2.K/W$, less than half the value by direct-measurement and therefore much closer to the correct value. Also evident in the figure is another recurrent characteristic of the nitrile buffers – a lower indicated thermal resistance.

Although the range for nitrile is very large, i.e. from 0.004 $m^2.K/W$ to the impossible negative value of -0.004, the mean is reasonably close to the correct (near-zero) value. Nitrile has the highest compressibility of all the buffer materials but only by a small margin. It appears likely that the very “accommodating” nature of the foam, manifest as its high hysteresis, may be accompanied by the potential for very-low contact resistance.

Initial results for EVA foam with specimens 1 and 2 were not consistent with the other ten. Since these were the only low-emittance specimens, radiation transparency was suspected. Consistency for the EVA returned, as in Figure 2.3, after the aluminum was sprayed flat black.

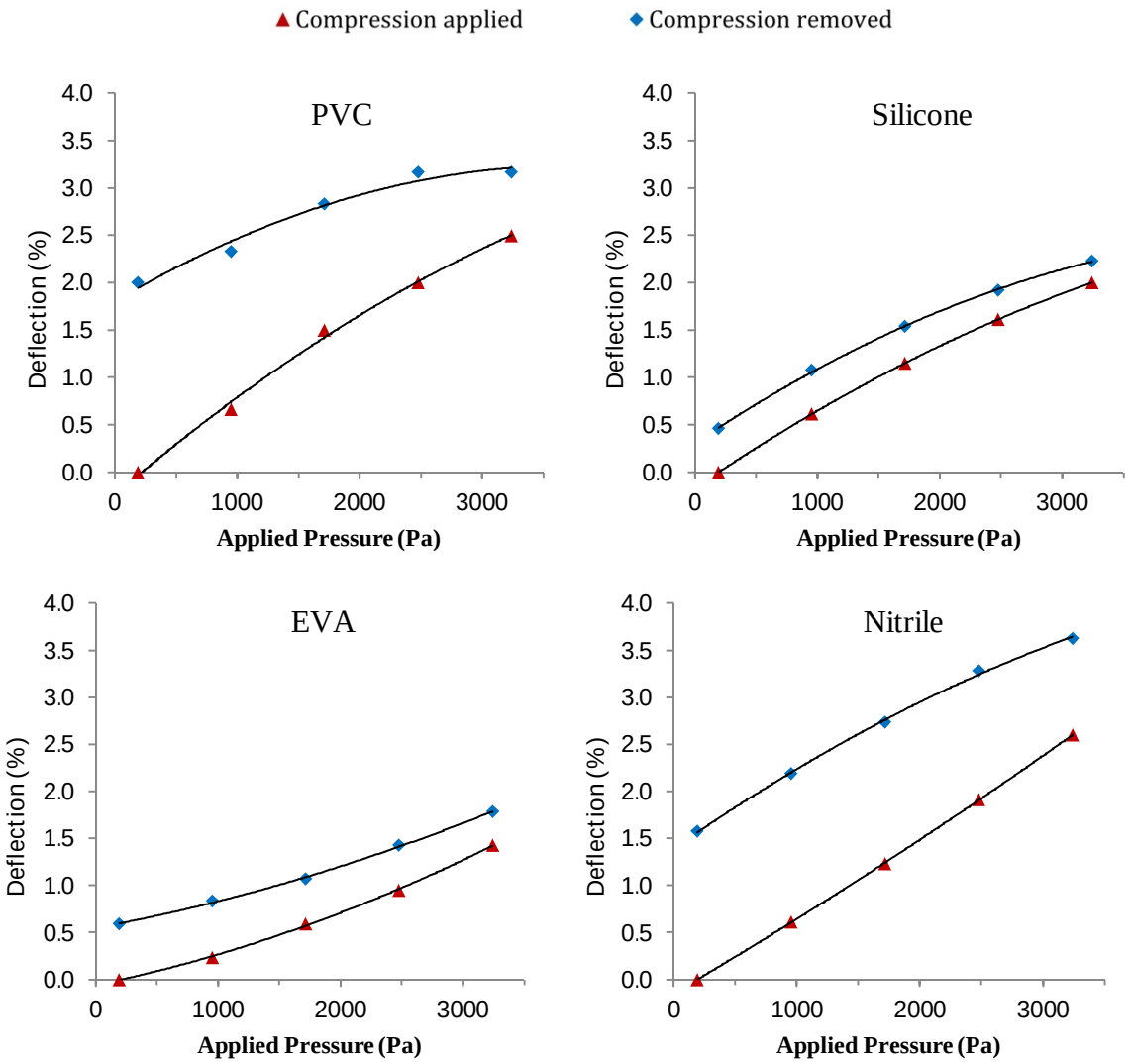

Figure 2.2. Compression performance of the four buffer materials. Lower curve shows deflection when compression applied, upper curve when load removed after 60 minutes.

Although specimens 3 and 4 had considerably higher thermal resistances than specimens 1 and 2, they were clearly still too low for C 518 measurement, even via difference measurement with buffer materials. The expected values were 0.003 m^2.K/W for the HDPE and 0.006 m^2.K/W for the phenolic paper. Measured values were either too high or too great in variance, as the figure shows. As with the aluminum sheets, results for these materials using the silicone buffers were at least reasonably consistent and much closer to the correct value.

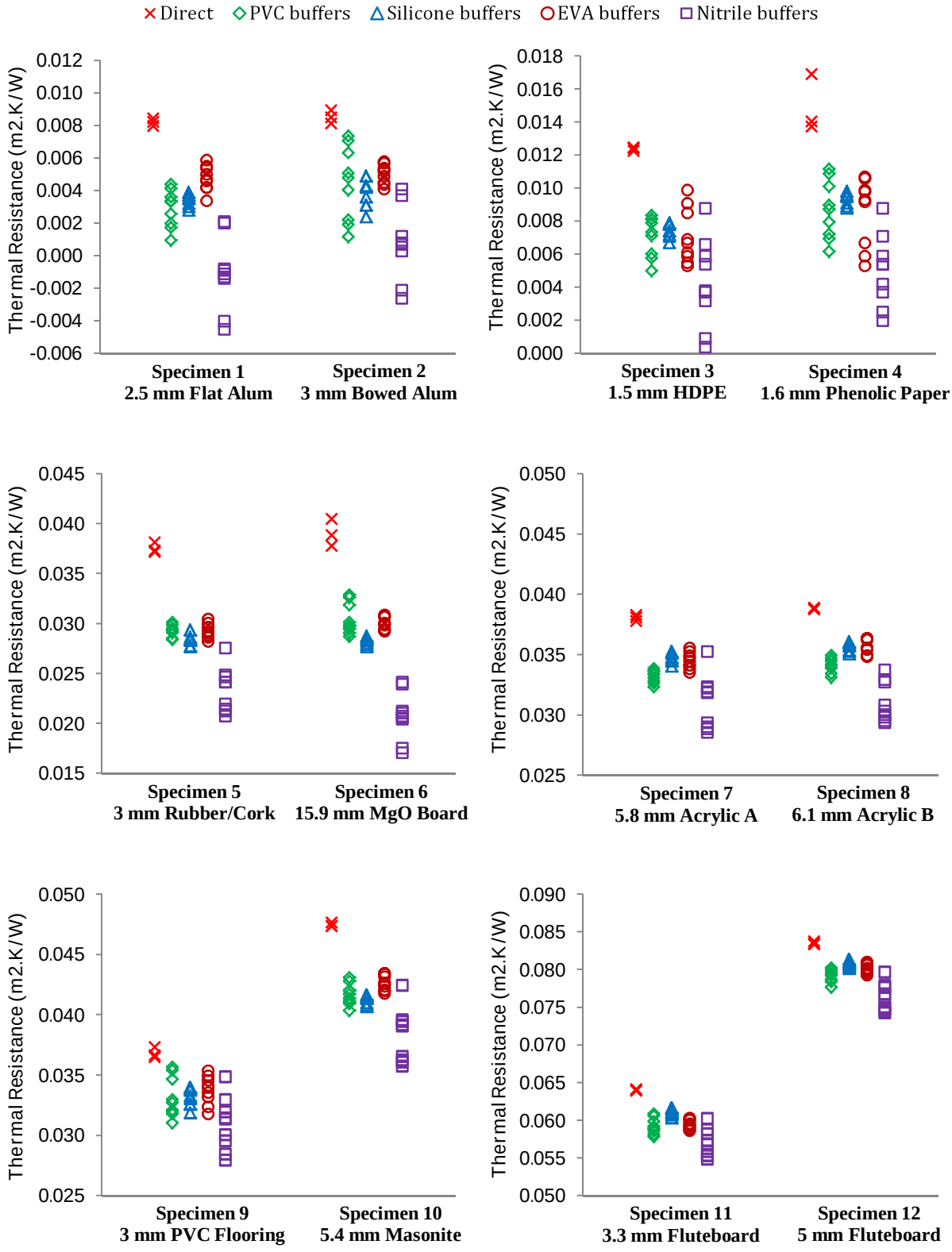

Figure 2.3. Thermal resistance of specimens 1 to 12 by direct measurement and with 4 buffer materials.

The other eight specimens had a thermal resistance of 0.03 m^2.K/W or greater, high enough for measurement by C 518 to be considered. The plots of Figure 2.3 display results in order of increasing thermal resistance and show a trend towards increasing consistency as interface resistance become a smaller proportion of the total. There are some important similarities, and differences, through the series. Accepting the ever-present high variance for all measurements involving the nitrile foam, quite consistent results are evident for the two samples of acrylic, including the relative performance of the four buffers. Results for the two fluted plastics are similarly consistent, although the relativities seem to be slightly different. In this case there appears to be a slightly higher thermal resistance with the silicone buffers. The results are consistent enough to suggest that the interface resistances depend to some extent on interaction between the surface characteristics of both the hard and the soft materials in contact.

Specimens 5 and 6 provide further indication of the variability in interface resistance. For these materials, the gap between direct and difference measurement is particularly high. In the case of the underlay material, both surfaces of the bonded rubber and cork granules were quite coarse. Presumably there was a particularly high interface resistance when this surface was in contact with the apparatus plates. In contact with the buffer materials able to mold to this roughness, it is understandable that the interface resistance was reduced by a greater amount than with flat-surfaced materials. Additional support to this notion is provided by the results for the nitrile foam buffers. With these, the suggested thermal resistance was particularly low relative to the other buffers. This would be quite consistent with the notion of a highly-compliant nitrile surface adapting to a coarse specimen. Results in the case of the MgO board are perhaps more dramatic but also less clear. It was not possible to measure the extent to which the bow in the sample was flattened out within the apparatus, where the loading pressure would have adopted a complex profile across the specimen related to compressibility of the buffer material. Whether by flattening of the specimen or compression of the buffer, results suggest that there may have been some residual airspace (or perhaps very low contact pressure) with three of the buffers, which was not present with the more-compliant nitrile. This is suggested by the dramatically lower thermal resistance obtained with the nitrile buffers for this particular specimen. For these two samples, measurement by difference using the three more-consistent buffers has produced a thermal resistance that is approximately 0.01 m^2.K/W lower, a reduction of the order of 30% for these two materials. Beyond this, results for nitrile buffers suggest that even these thermal resistance values are an overestimate. Unfortunately the ubiquitous variability of the nitrile measurements precludes

any real confidence in a quantifying the effect. Accurate thermal conductivity data is not available for either material to provide corroboration.

Specimens 9 and 10 provide further insight into the way surface characteristics are likely to affect the interface resistance. In the case of specimen 9, the PVC flooring, direct and difference measurement produced the closest agreement of any of the specimens, with the difference measurement producing only slightly-lower thermal resistance values for all buffers. This is consistent with the fact that, of the twelve specimens, only the PVC flooring material had soft surfaces. There is likely to be a lower contact resistance in all measurements cases, whether the contact is with the hard apparatus plates for direct measurement or with other soft buffer materials for difference measurement. One might expect the soft-soft interface between PVC flooring and a buffer to produce a slightly-lower contact resistance, which is what the data suggests. However it must be remembered that precise information on the scale of these effects is not apparent since direct measurement also includes unknown terms for apparatus internal resistance on both plates. Results for specimen 10 are for a material with one smooth and one rough surface. The relative performance of the buffers follows a similar pattern to the other materials. The reduction in thermal resistance achieved by difference measurement is consistent in that it is roughly intermediate between the rough-surface and smooth-surface values observed for the other materials.

2.6 Discussion

The difference-measurement technique has shown that it is not without difficulties. Buffer materials must have qualities that sit between excessively soft, leading to significant and variable compression and excessively hard, in which case they may not offer useful reduction in interface resistance. The choice of thickness is similarly balanced between too much thermal resistance and too little thickness in which to accommodate the hard and possibly uneven specimen surface. Only four materials have been tried; there are many other possibilities. Measurements with nitrile material have suggested that softer and more compliant materials might afford very-low interface resistance but the high variability would need to be overcome. Composite materials (of which PVC flooring is an example) might provide better overall performance than simple compositions. Foams loaded with high-conductivity fillers may perform better.

For the technique to provide reproducible results, the apparatus plates must provide reproducible pressure on specimens. This also applies for direct measurements but is even

more important with the difference technique due to the need to subtract the results from two measurements which must be made under conditions as close to identical as possible.

No attempt was made to allow the buffer materials to rest in an unloaded state between measurements. The hysteresis issue only became apparent after the test program had well progressed. Undoubtedly some buffers would have been reused before they had fully recovered and would have recompressed further than previously, with thermal resistance commensurately lower. Table 2.3 suggests that this effect would have been most significant for the nitrile where high thickness, low conductivity and large hysteresis all combine unfavorably.

A recent round robin of 27 laboratories (APLAC, 2010) considered samples of 25 mm glass fiber and 15 mm solid acrylic, the latter having a nominal thermal resistance of 0.09 m^2.K/W, lower than the official ASTM C 518 minimum. The laboratories reported uncertainties of up to 2.9% for the glass fiber and 4% for the acrylic. For the glass fiber, at 20 ºC mean, most laboratories achieved results within their stated uncertainty limits. However, for the acrylic, the range of results was 94% of the median and the interquartile range was 11.8%.

Table 2.3. Change in thermal resistance due to change in thickness equivalent to measured hysteresis at 2 kPa loading for each pair of buffer materials.

Buffer material	Thermal resistance (m^2.K/W)	Change in thickness (%)	Change in thermal resistance (m^2.K/W)
Flexible PVC flooring (pair of sheets)	0.070	1.27	0.0009
Silicone sponge	0.162	0.37	0.0006
EVA foam	0.24	0.49	0.0012
Nitrile foam	0.42	1.46	0.0061

Clearly, accurate measurement of the acrylic was more difficult than presumed, with the values from a few laboratories being distant outliers. It is notable that the generic thermal conductivity of acrylic is usually quoted at around 0.18-0.19 W/m.K but the median value for the round robin was 0.16 W/m.K. The difference might in part be explained by interface resistance. For the two 6 mm acrylic specimens of the current study, difference measurement using the silicone buffers suggested a mean thermal conductivity of approximately 0.17 W/m.K whilst for direct measurement the suggested value was closer to 0.15 W/m.K.

2.7 Conclusions

The thermal insulation test methods, developed with higher-performing materials in mind, are quite compromised at the low end of their measurement range by the presence of interface resistance. Alternative methods such as ASTM E 1530, appropriate for small uniform samples of much-higher conductivity, are not suitable for many building and industrial products. The use of conforming buffer materials at the interface between sample and apparatus plates provides a means of reducing interface resistance and extending the lower range of measurement. Although it introduces the requirement for measurement by difference, subtracting the thermal resistance of the buffer materials measured separately, the technique can clearly lead to improved measurement of specimens that have low to very-low thermal resistance. The method is also much simpler for most laboratories than the most-common alternative, which is to use external thermocouples requiring additional instrumentation.

The utility of the technique hinges on the fact that the interface terms are lower when there is at least one soft material at each interface. However it is not without difficulties. Variance is higher and the derived result is still an overestimate since some interface-resistance terms remain. Softer and more compliant buffer materials result in greater variance, so that the choice of buffer material is a compromise and may depend upon the specimen, especially if it has spatial irregularities and non-uniformities.

Amongst the four buffer materials studied, a silicone sponge produced the most consistent results, combining relatively high thermal conductivity and low hysteresis. Consistent performance as a thermal buffer was clearly associated with low hysteresis and the nitrile, with the highest hysteresis, produced unacceptable results. However high hysteresis is also associated with compliant surfaces and did appear to give nitrile the lowest interface resistance. These conflicting attributes might be resolved with alternative materials, perhaps composites, which offer the best features of both. In any case, the effects of hysteresis might be reduced by pre-conditioning buffer materials under zero load for an extended period before use.

Using the technique, measured thermal resistance is typically lower by an amount between 0.003 and 0.01 m^2.K/W. Interface resistance components of this size are large enough to be of consequence in many thermal measurements.

2.8 References

AIRAH. (2013) AIRAH Technical Handbook. Australian Institute of Refrigeration, Air-Conditioning and Heating Inc.

APLAC. (2010) APLAC TO53. Final Report, Thermal Insulation Proficiency Testing Program. Abbotsford, Vic, Australia: Asia Pacific Laboratory Accreditation Cooperation.

ASTM. (2007) ASTM D1056 - 07 "Specification for Flexible Cellular Materials--Sponge or Expanded Rubber.". *Annual Book of ASTM Standards, Vol. 08.01.* ASTM International, DOI: 10.1520/D1056-07

ASTM. (2010a) ASTM C177 - 10. "Test Method for Steady-State Heat Flux Measurements and Thermal Transmission Properties by Means of the Guarded-Hot-Plate Apparatus.". *Annual Book of ASTM Standards, Vol. 04.06.* ASTM International, DOI: 10.1520/c0177-10

ASTM. (2010b) ASTM C518 - 10. "Test Method for Steady-State Thermal Transmission Properties by Means of the Heat Flow Meter Apparatus.". *Annual Book of ASTM Standards, Vol. 04.06.* ASTM International, DOI: 10.1520/c0518-10

ASTM. (2011) ASTM E1530 - 11. "Test Method for Evaluating the Resistance to Thermal Transmission of Materials by the Guarded Heat Flow Meter Technique.". *Annual Book of ASTM Standards, Vol. 14.02.* ASTM International, DOI: 10.1520/E1530-06

ASTM. (2013c) ASTM E1461 - 13. "Test Method for Thermal Diffusivity by the Flash Method.". *Annual Book of ASTM Standards, Vol. 14.02.* ASTM International, DOI: 10.1520/E1461

Brzezinski A and Tleoubaev A. (2002) Effects of Interface Resistance on Measurements of Thermal Conductivity of Composites and Polymers *Proceedings of the 30th Annual Conference on Thermal Analysis and Applications (NATAS).* Pittsburgh: B&K Publishing

BSI. (2001) BS EN 12664:2001. "Thermal performance of building materials and products. Determination of thermal resistance by means of guarded hot plate and heat flow meter methods. Dry and moist products of medium and low thermal resistance". British Standards Institution

Campbell R and Rose M. (2013) Thermal Conductivity Measurements of Concrete Using the Heat Flow Meter (HFM) and Guarded Hot Plate (GHP) Methods. **http://www.netzsch-thermal-analysis.com:** NETZSCH Instruments North America.

Corsan JM and Williams I. (1980) Errors associated with imperfect surfaces in standard hot-plate thermal conductivity measurements. In: Metrology NPLDoQ (ed) *NPL Report QU57.* National Physical Laboratory, Teddington, Middlesex, TW11 OLW, UK.

Filla BJ and Slifka AJ. (1997) Thermal Conductivity Measurements of Pyroceram 9606 Using a High-Temperature Guarded-Hot-Plate *Thermal Conductivity 24 / Thermal Expansion 12, Proceedings of the 24th International Thermal Conductivity Conference and 12th International Thermal Expansion Symposium.* Pittsburgh, PA: Technomic

Standards Australia. (2006) AS/NZS 4859.1:2002 Materials for the thermal insulation of buildings - General criteria and technical provisions. Sydney: Standards Australia, Standards NZ

Tleoubaev A and Brzezinski A. (2007) Errors of the Heat Flow Meter Method Caused by Thermal Contact Resistance *Thermal Conductivity 29 / Thermal Expansion 17, Proceedings of the 29th International Thermal Conductivity Conference and 17th International Thermal Expansion Symposium.* Birmingham, Alabama: DEStech Publications

Zsembery S, Clarke RE and McNeilly T. (1996) Thermal transmission properties of Australian clay bricks. *Masonry International* 10: 30-34

3 A Difference Technique To Avoid Interface Errors in Measurement of High-Conductance Thermal Insulation

Journal Paper:

Clarke RE, Shabani B and Rosengarten G. (2016) A difference technique to avoid interface errors in measurement of high-conductance thermal insulation. *Journal of Building Physics*. Pre-published May 23 2016, DOI: 10.1177/1744259116637863

Additional Information for Chapter 3

The following pages of this chapter present, in the formatting style of this dissertation, a paper published in the Journal of Building Physics. The paper has been available electronically through the journal's "pre-publication" service since May 2016. Full publication is scheduled to occur in the next issue.

There are some minor formatting and editorial differences in the published version, including the positioning of figures and tables within the text.

In addition, there are minor changes to the text on pages 40, 41 and 45 in response to examiner's comments.

For inclusion in this dissertation, section numberings have been amended to incorporate the chapter number.

The journal has allowed Australian spellings.

A harmonized reference style based on Sage Harvard has been used in the presentation of this paper, as throughout this dissertation. Sage Harvard is also used by the Journal of Building Physics but there are small differences in the implementation. DOI numbers have been included where available.

A DIFFERENCE TECHNIQUE TO AVOID INTERFACE ERRORS IN MEASUREMENT OF HIGH-CONDUCTANCE THERMAL INSULATION

Robin E Clarke[1,2], Bahman Shabani[3] and Gary Rosengarten[1]

[1]School of Engineering, RMIT University, Melbourne, VIC, Australia

[2]CSIRO Australia, Clayton South, VIC, Australia

[3]School of Engineering, RMIT University, Bundoora, VIC, Australia

Corresponding author:

Robin E Clarke, CSIRO Australia, Private Bag 10, Clayton South, VIC 3169, Australia.

Email: Robin.Clarke@csiro.au

Keywords

thermal resistance, thermal test methods, contact resistance, interface resistance

Abstract

Lower limits of measurement are prescribed within all steady-state test methods for thermal insulation. These limits, typically 0.1 m^2.K/W, are largely required because of the increasing significance of interface resistance. We have previously proposed the use of a difference method, in conjunction with flexible buffer materials, to minimize the effects of interface resistance and facilitate measurement of rigid materials these limits. We have now studied this approach at higher thermal resistances and incorporated a refinement to include a known reference specimen in the difference measurement, which largely eliminates the residual resistance terms. Specimens of expanded polystyrene and cast acrylic were measured in a conventional heat flow meter apparatus using two alternative silicone buffer materials, one solid and the other a sponge. Analysis also included earlier measurements of twelve more highly-conducting specimens. Across all of these, thermal resistance values obtained by the difference method were lower by between 0.008 m^2.K/W and 0.016 m^2.K/W, attributable to removing the contribution of interface resistance.

3.1 Introduction

Test methods for thermal insulation arose with the need to characterize insulation materials for the building industry, especially for HVAC design. From its first iteration in 1946, ASTM C 177 (ASTM, 2013a) offered a standardized methodology for the guarded hotplate with a precision of ± 3% (Robinson and Watson, 1952). Limitations of early apparatus and the scope of interest at the time meant that specimen thermal resistance was generally below 1.0 m^2.K/W. The heat flow meter method, ASTM C 518 (ASTM, 2010b), became more prominent in the 1970s, offering faster and simpler measurement, an advantage for in-house quality testing as well as for commercial laboratories (Tye et al., 1987). Both methods have evolved so that a measurement capability up to 10 m^2.K/W is now available. Emphasis may have shifted from the lower values, but it remains important to be able to assess higher-conducting components for their role in overall building performance. Additionally, standard reference materials frequently have a thermal resistance below 1.0 m^2.K/W (Zarr et al., 2014) as do materials employed for inter-laboratory comparison (APLAC, 2010).

The lower limit of 0.1 m^2.K/W applies specifically for ASTM C 518, although those in other ASTM, ISO or European standards are effectively of this order. For some materials, the guarded heat flow meter method ASTM E 1530 (ASTM, 2011) is a potential alternative. It is however intended for use with more-conductive materials (non-insulations) and has a nominal upper limit of 0.04 m^2.K/W for full accuracy. It has an emphasis on minimizing interface resistance, through the use of small, highly-flat specimens and high contact pressure. A load of typically 200 kPa (100 times that of a typical heat flow meter apparatus) is applied through gimbal joints for even distribution. A heat-transfer compound is recommended for the contacting faces. Calculation is based on comparison with measurement of a known similar material, the process accounting for interface resistance, rather than eliminating it. These provisions highlight the effort needed to control interface resistance. However they would be problematic with larger-scale materials that are not well represented by a small, machined-flat specimen. Many insulations are compressible, or lack the required small-scale uniformity.

A number of transient methods exist, including laser flash, hot wire, line source, planar source and 3ω techniques. However the latter is restricted to very-small specimens in order to have an acceptably high excitation frequency whilst the precision and uncertainty of the other methods is unclear. Hust and Smith (1989) describe inter-laboratory variations with a standard deviation of 26% for needle probes and 17% for hot wire apparatus. Campbell et al. (2005) compared the sources of error for liquid, solid and granular materials with the line source method. Correlation with known materials was quite good but absolute errors as large

as 50% were observed for some materials. We have observed a standard deviation of 8% in repeated laser flash measurements of a 1.7 mm phenolic board. Tye and Salmon (2001) observed that stated values measured by transient methods were often well outside accepted limits for certain known materials. There are few standards for transient methods, none that give them applicability across a broad range of materials. The regulatory and commercial acceptance of the steady state test methods is linked to their ability to reliably achieve low uncertainties, typically around 3% under favourable conditions. At present, transient methods seem unable to deliver this, except in limited circumstances with careful calibration. There is ongoing development in heat conduction modelling with transient thermal devices (Kamai et al., 2015). Standard methods and apparatus with acceptable capabilities may arise in the future.

Steady state methods may also fail to achieve low uncertainty at low thermal resistance, due to interface resistance. The problem is fundamental to the methods since they aim to establish spatially-uniform heat flow through a full-thickness specimen. This requires a relatively large apparatus size, seldom less than 200 mm square with some exceeding 800 mm square (TA Instruments, 2016). For low interface resistance, good thermal contact must be maintained between specimen and plates over this large area. The standards address the issue by specifying flatness and parallelism requirements for both apparatus and specimen, 0.02% of the plate dimensions in the case of ASTM C 518. Although this is a challenging specification, it does not represent a high degree of absolute flatness for the plates of a larger apparatus and the standard acknowledges that it may not be sufficient for some measurements. Notwithstanding plate flatness, it would be very difficult to achieve this quality of flatness in the preparation of many rigid test specimens.

ASTM C 518 does not suggest contact pressures greater than 2.5 kPa, presumably because they would be difficult to achieve in practice. Higher pressures should significantly reduce interface resistance and are available on some newer commercial apparatus such as the Netzsch HFM 436 (Netzsch, 2015).

We have previously shown (Clarke *et al.*, 2014) how the difficulties with C 518 at low thermal resistance may be addressed by using a difference method and soft buffer sheets to provide enhanced specimen contact. A first measurement with the specimen present is followed by a second where it is absent. However, simple subtraction leads to an expression that includes the unknown resistance as well as some small but unknown interface-resistance terms. In this paper we describe an improvement to the technique wherein a known reference specimen is incorporated into the second measurement. With this approach, similar interface

terms are present in both measurements so that they are eliminated by subtraction, leaving just the unknown resistance.

Our previous study considered specimens below 0.1 m^2.K/W, technically outside the normal range for heat flow meter measurement. We have now studied two well-behaved materials, moulded expanded polystyrene beads (EPS) and cast acrylic resin (PMMA), at higher thermal resistances where significant interface-resistance errors might not have been anticipated. Additional analysis of the previous results is also presented.

3.2 Experimental Background

3.2.1 Measurement by Difference

Figure 3.1 is a schematic of an idealized heat flow meter apparatus with a test specimen in place. The test specimen resistance, R_s is the value of interest but what is measured by the heat flow meters and temperature sensors leads to a value of the total thermal resistance R_t. Assuming plate 1 is at the higher temperature, we have:

$$R_t = \frac{Q_x}{T_1 - T_2} = R_{p_1} + R_{p_1-s} + R_s + R_{s-p_2} + R_{p_2} \qquad (1)$$

where

Q_x is the heat flux;
T_1 is the hot plate temperature;
T_2 is the hot plate temperature;
R_t is the total thermal resistance between the plate temperature sensors;
R_{p_1} is the internal thermal resistance of plate 1;
R_{p_1-s} is the interface thermal resistance between plate 1 and the specimen;
R_s is the specimen thermal resistance;
R_{s-p_2} is the interface thermal resistance between plate 2 and the specimen; and
R_{p_2} is the internal thermal resistance of plate 2

The measured value of R_t is a good approximation for R_s only if the other four terms in equation (1) are small. The terms R_{p_1} and R_{p_2}, describing the resistance between the embedded temperature sensors (usually thermocouples) and the plate surface generally are quite small since the plates are designed to be highly conducting to maximize spatial temperature uniformity. However, for designs using temperature sensors embedded within (rather than on the surface of) the heat flow meter, they are measurably significant. In any case, they are extremely difficult to separate from the interface resistances R_{p_1-s} and R_{s-p_2}.

These terms embody the classical "contact resistance" as might be measured between flat mating surfaces of a certain roughness and contact pressure. However with hard, rigid specimens where imperfect flatness leads to contact at high points with adjacent voids and airspaces, these interface terms may be relatively large.

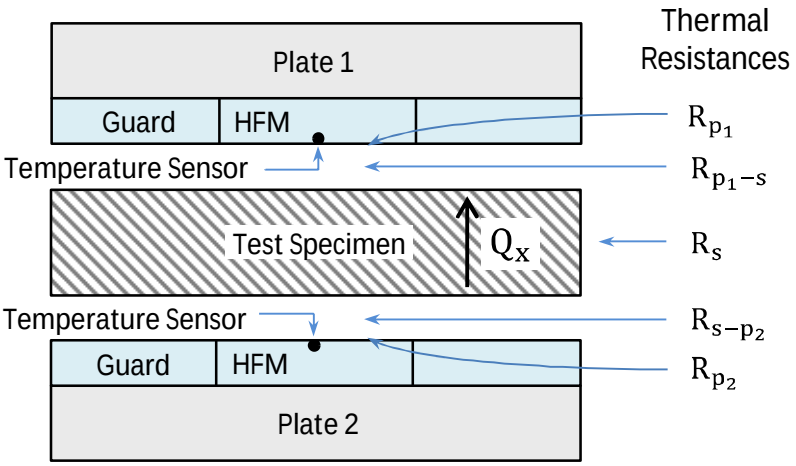

Figure 3.1. Heat flow meter apparatus showing thermal resistance components with specimen present.

Figure 3.2 shows the addition of buffer materials to a heat flow meter apparatus on either side of a test specimen. Their inclusion leads to a large number of thermal resistance components in series between the plates, as indicated in the sketch. The total thermal resistance R_t is:

$$R_t = \frac{Q_x}{T_1 - T_2}$$

$$= R_{p_1} + R_{p_1-b_1} + R_{b_1} + R_{b_1-s} + R_s + R_{s-b_2} + R_{b_2} + R_{b_2-p_2} + R_{p_2} \qquad (2)$$

where

R_t is the total thermal resistance between the plate temperature sensors;

R_{p_1} is the internal resistance of plate 1;

$R_{p_1-b_1}$ is the interface resistance between plate 1 and buffer 1;

R_{b_1} is the resistance of buffer 1;

R_{b_1-s} is the interface resistance between buffer 1 and specimen;

R_s is the specimen resistance;

R_{s-b_2} is the interface resistance between specimen and buffer 2;

R_{b_2} is the resistance of buffer 2;

$R_{b_2-p_2}$ is the interface resistance between buffer 2 and plate 2; and

R_{p_2} is the internal resistance of plate 2

Most of the resistance terms are unknown. However if a further measurement is performed with the specimen removed, many of these unknowns remain present and so may be eliminated by subtraction. Considering a first measurement R_t^1 and a second R_t^2, subtraction leads to:

$$R_{diff} = R_t^1 - R_t^2 = R_{b_1-s} + R_s + R_{s-b_2} - R_{b_1-b_2} \quad (3)$$

This option is described in C 518, proposing the use of a "thin sheet of suitable homogeneous material" measured separately, as the buffer. However, as with R_t, R_{diff} is a good approximation to R_s only if the interface terms are small. With the use of soft buffer materials there are good prospects for this to be the case since the interface terms in equation (3) all involve a soft-material interface, expected to have low thermal resistance. The $R_{b_1-b_2}$ term is subtractive although expected to be the smallest term, since it is actually at a soft-soft interface. We have previously confirmed that R_{diff} , established by a pair of measurements, may provide a significantly-lower estimate for R_s than a single measurement of R_t.

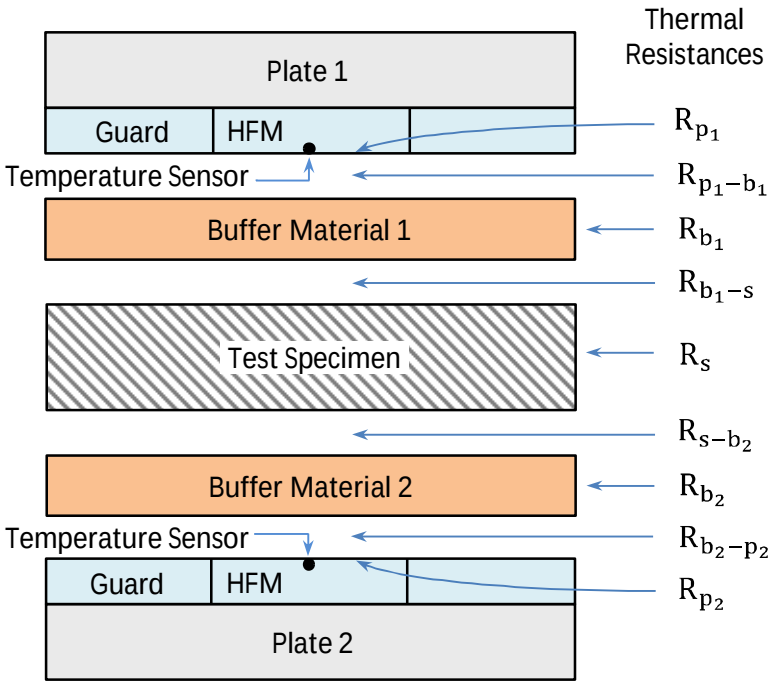

Figure 3.2. Heat flow meter apparatus showing thermal resistance components with specimen and two buffers present.

A further refinement of this technique is to perform the second measurement with a known specimen between the buffers, instead of with the specimen being simply absent. The expression for R_{diff} is then quite long when all terms are included but it may be assumed that the interface resistances between buffers and specimens are the same for both specimens, provided that roughness and flatness are reasonably similar based on visual inspection and assessment with a straight edge. If this is the case, R_{diff} reduces to:

$$R_{diff} = R_t^1 - R_t^2 = R_s^1 - R_s^2 \quad (4)$$

The value of principal interest, R_s^1, may therefore be obtained simply from a difference measurement with no consideration required for interface resistance beyond the assumption that buffer-specimen interface resistances are constant. Clearly there is the additional requirement for the resistance of reference specimen, R_s^2, to be known and the uncertainty in its value will impact directly upon the uncertainty in R_s^1. However the role of R_s^2 may be filled by a well-characterized reference material.

Another difference measurement of interest is that of stacking multiple examples of the same specimen. This technique is occasionally used to estimate the thermal resistance of very thin materials, such as fabric or paper. Whether buffers are used or not, for an initial stack of x+n specimens, followed by a further measurement after the removal of n specimens, most of the resistance components cancel out to leave the relationship:

$$R_{diff} = R_t^{x+n} - R_t^x = n(R_s + R_{s-s}) \quad (5)$$

where

R_s is the specimen resistance; and

R_{s-s} is the inter-specimen interface resistance (assumed to be constant).

Importantly, this relationship only holds when x is one or greater, i.e. when at least one specimen is present. When x becomes zero (removal of the final specimen), R_{diff} assumes the longer form of equation (3). It is reported (Lavrykov and Ramarao, 2012) that this method may be used to measure very large stacks of material such as paper and also that sensitive HFM apparatus are able to resolve the difference in R associated with the removal of a single sheet of paper, approximately 0.001 m^2.K/W. Under these circumstances with pliable sheets of paper lying together, interface resistance appears to be very low, although it may make up a significant proportion of this incremental resistance value. ASTM E 1530 would appear to be more suitable for such measurements.

ASTM C 518 does address interface resistance by proposing temperature sensors attached directly to the surface of the test specimen as the default, with plate-embedded sensors

allowable where specimen thermal resistance is sufficiently high. Temperature difference measured in this way leads directly to a value of R_s. However there are numerous difficulties with attached sensors (Corsan and Williams, 1980). Lead wires must either run in grooves machined in the specimen or be accommodated by a flexible buffer sheet. Even with correction factors, the alternative methods potentially give different values and are sensitive to the precise details of placement and attachment. Additionally, the measurement is reliant on the assumption that the heat flow conditions at the sensor locations are fully representative of the overall average. Even with four or more sensors, this may not be realistic for specimens that have significant non-uniformity, or have spatially-varying interface resistances. Furthermore commercial apparatus generally lack provision for temperature sensors external to the plates and would require an add-on system running separately to the main instrumentation. Finally, the work involved in fitting attached sensors, especially into machined grooves, is quite considerable.

3.2.2 Selection of Buffers and Specimens

The choice a buffer material involves compromise. The buffer must have sufficient compliance to conform at higher contact points, allowing contact to be spread over a larger area so that interface resistance is minimized. Less-uniform specimens will benefit from greater buffer compliance to ensure an adequate degree of contact. This might be achieved with a softer material or one of greater thickness. However a more-compliant or thicker buffer will have greater thickness uncertainty and greater variability in thermal resistance as a result of variation in specimen flatness or apparatus contact pressure.

High thermal conductivity is favourable since this will also minimize the variability in thermal resistance but many potential materials, including a broad range of foamed plastics, have quite low conductivity. Of the four prospective buffer materials we studied previously, a “medium-soft” grade of silicone sponge produced the most repeatable results for difference measurement. It was unclear to what extent this was due to the higher thermal conductivity (relative to less-dense foamed plastics) or to the higher resiliency and lower hysteresis.

We studied the hysteresis effects by comparing the thickness at 2.5 kPa of a buffer that had been under this amount of compression for at least an hour previously with one that had been under no compression. There was no discernable difference for any of the foamed plastics, even for very soft, high-hysteresis nitrile foam. These results suggest that the relatively-high conductivity of silicone sponge was the key benefit. We therefore elected to continue studies with the medium-soft grade of silicone sponge and to compare it to the most-conductive available grade, a solid (un-foamed) sheet in the thinnest practical thickness (1.7 mm,

nominally 1/16 inch). Whilst the compliance of this material was very low, it was thought to be possibly adequate for the very flat and uniform EPS and PMMA test specimens.

We also considered loss in resistance due to compression. The medium-soft silicone sponge compressed about 1.5% under a 2 kPa load, resulting in a similar change in thermal resistance, since the conductivity-density curve is relatively flat. For a pair of 4.2 mm thick buffers, the resistance change was slightly less than 0.002 m^2/K/W, measurably significant. With uniform test and reference specimens, buffer deflection should be the same and so should therefore be factored out. With irregular or non-flat surfaces, there is the potential for errors to arise due to inconsistent buffer compression. On the other hand, test specimens with poor surface uniformity or flatness are also likely to have erratic plate-specimen contact resistances, so that the presence of a buffer is likely to remain beneficial.

Solid silicone rubber is much less compliant. A load of 280 kPa was required to produce 5% compression. Being also thinner, total compliance was 40 times lower than the silicone sponge whilst conductance was 5 times higher. These attributes combined to ensure there would be negligible change to its resistance under 2 kPa loading. However the low compliance offers very little accommodation of thickness irregularities and leaves the potential for voids or areas of marginal contact, where the softer, thicker buffer would have maintained contact over a wider area.

Table 3.1 gives generic characteristics of the two chosen buffer materials, hereafter referred to as “sponge” and “solid”, as well as the test and reference specimens. The test specimens, EPS and PMMA, were spatially uniform and stable materials, qualities that see these materials often used as thermal reference materials. The EPS was the densest available grade, wire-cut to uniform dimensions. The PMMA was a cast sheet with the original gloss surface finish on both faces. Images of the specimens and buffers appear in Figure 3.3.

Paper-reinforced phenolic board, 1.7 mm thick, was used for the reference specimen. This stiff, uniform material had a thermal conductivity of 0.38 W/m.K, about twice that of the PMMA. Whilst higher conductivity allows lower uncertainty in thermal resistance, materials of very-high conductivity such as aluminium sheet were avoided because of their potential to introduce systematic error by altering the 3-dimensional heat flow profile in the apparatus.

Phenolic board has a glossy flat surface similar to the natural surface of the PMMA but not the EPS which was somewhat rough as a result of being wire cut. Accordingly two types of phenolic sheet were investigated, one with the natural surface and one for which the surface was artificially roughened using very coarse sandpaper.

Table 3.1. Characteristics of the buffer materials, test specimens and reference specimen.

Material	Role	Density (kg/m^3)	Conductivity (W/m.K)	Thickness (mm)	Resistance (m^2.K/W)
Medium-soft silicone "sponge"	Buffer material	460	0.08	4.2	0.05
"Solid" silicone	Buffer material	1190	0.16	1.7	0.010
EPS	Test specimen	35	0.033	11.3	0.34
PMMA	Test specimen	1180	0.18	24.9	0.14
Phenolic-paper board	Reference specimen	1400	0.38	1.7	0.0045

Figure 3.3. Photographs of EPS specimen with silicone sponge buffers on the left and PMMA specimen with solid silicone buffers on right, located in heat flow meter apparatus.

3.3 Results

All measurements were performed in a Fox 600 apparatus (TA Instruments, 2016) with 600 mm square specimens at a mean temperature of 23 ºC. Temperature difference was 12 K with the sponge buffers, reduced to 6K with the solid buffers in order to moderate the higher heat flow. The apparatus applied a set loading of approximately 80 kg, equivalent to a clamping pressure of 2 kPa. Each series of measurements was repeated five times to assess repeatability, which was found to be within approximately 0.2% for every series.

High-conductance measurements, involving the reference specimen or buffers alone, were studied initially. Figure 3.4 shows these results, including measurements with either one or two (stacked) reference specimens. Vertical axes have the same sensitivity to aid comparison of the differences between values.

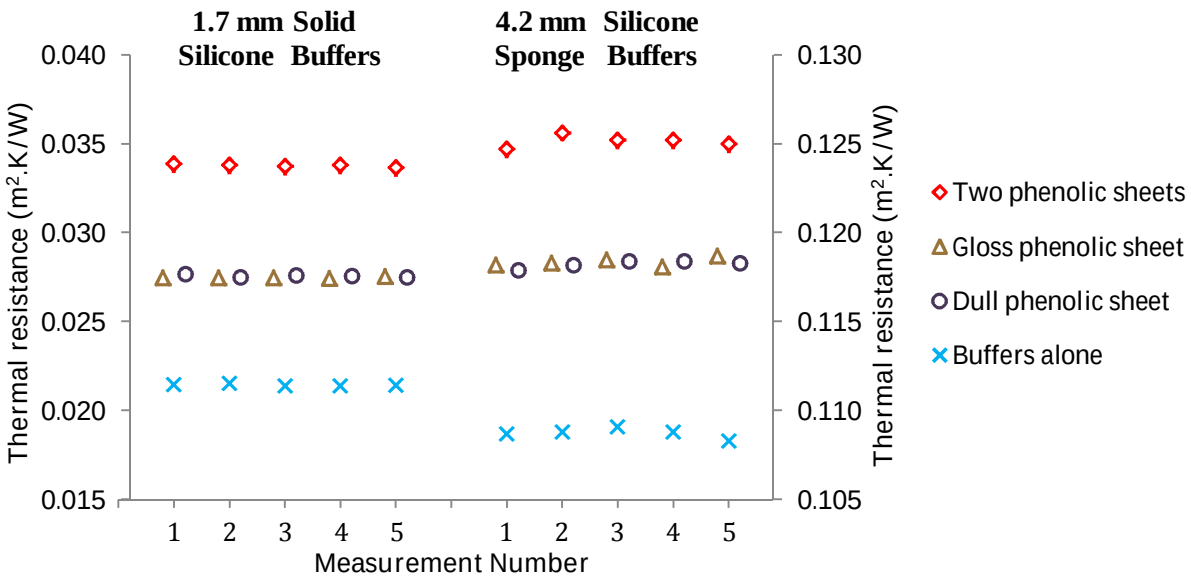

Figure 3.4. Heat flow meter measurement results for both types of buffer, alone or separated by one or two phenolic sheets.

It is apparent from the figure that roughening the phenolic surface to produce a "dull" finish had no measurable effect, suggesting there would be little purpose in attempting to match the surface roughness of reference and test specimens.

Results for the sponge buffers clearly demonstrate the earlier suggestion that stacking measurements require at least two specimens for linearity to be preserved in the general case, even if the particular values of interface resistance on this occasion have resulted in same-sized steps between the three sets of measurements with the solid buffers. Averaging each group of measurements and assuming that all similar types of interface have the same value (i.e. R_{b_1-s} is equal to R_{s-b_2}) leads to several simplified relationships when substituted into equation (3) for the case of a single sheet relative to buffers alone and equation (5) for the case of the pair of sheets relative to a single sheet. Additionally, since R_s is known on this occasion, values of the residual interface components may be calculated as shown in Table 3.2.

R_{s-s}, the calculated interface resistance between adjacent phenolic sheets, was slightly higher in the case of the softer buffer. This may reflect a slightly less-uniform contact. Although very uniform in thickness, the board was also very stiff so that slight undulations may have been less flattened out by the softer buffer.

Table 3.2. Calculated interface thermal resistance components.

Relevant equation	Interface resistance Term (for $\mathbf{R_s}$ = 0.0045 m^2.K/W)	1.7 mm solid silicone buffers (m^2.K/W)	4.2 mm silicone sponge buffers (m^2.K/W)
3	$2R_{b-s} + R_s - R_{b-b}$	0.0061	0.0096
	$2R_{b-s} - R_{b-b}$	0.0016	0.0051
5	$R_{s-s} + R_s$	0.0063	0.0068
	R_{s-s}	0.0018	0.0023

The greater difference between buffers in the values of $(2R_{b-s} - R_{b-b})$ are not easily explained, partly because the two component terms are not individually known. Certain assumptions are possible, for example, R_{b-b} should be very low in the case of the softer buffer since it represents the interface of two compliant materials. However, even if it approaches zero, the value for R_{b-s} must be 0.0026 or above. The higher value for $(2R_{b-s} - R_{b-b})$ in the case of the harder buffers allows for a greater range of possibilities. It is satisfied if both R_{b-s} and R_{b-b} have a value of 0.0016. R_{b-b} might be lower than this although the solid buffers were very hard and might have a significant buffer-buffer interface resistance.

Despite the uncertainties, these preliminary measurements collectively suggest that where buffers are involved, the interface resistance terms are all relatively low in comparison to specimen resistances of interest, around and below 0.1 m^2.K/W.

Figure 3.5 presents results for measurement of the two selected specimens, comparing direct measurement with measurement by difference. For both specimens, the direct measurement values represent five single repeated measurements incorporating just the test specimen, as in Figure 3.1. All other data are calculated difference values incorporating buffers, following the procedure of Figure 3.2 and equations (3) and (4). The two plots therefore summarize the apparent thermal resistance of the specimens by direct measurement and by difference measurement (with buffers) using either no reference specimen ("buffers alone") or with a phenolic sheet reference specimen ("buffers + ref"). The presentation format shows each of five first-measurement values associated with all five alternative second measurements, in order to represent the full range of 25 possible difference values. As the figure shows, the groupings for each measurement arrangement are closely clustered because of the high uniformity in the second measurements, particularly for the case of the solid buffers. As with Figure 3.4, vertical axes have the same sensitivity to allow direct comparison of difference values.

Interpretation of Figure 3.5 is simplified in recognizing an underlying pattern. The two alternative calculations for each buffer (the cases with and without the reference specimen) are closely correlated and have a consistent separation for each buffer type. This is to be expected, since the difference between them is effectively the value of $(2R_{b-s} - R_{b-b})$, which we have already observed to consistently have values of 0.0016 and 0.0051 with solid and sponge buffers respectively. These differences may be regarded as the degree to which the simpler difference measurement, without using a reference specimen, provides an overestimate of the actual specimen resistance. Measurement of the 25 mm PMMA appears to be more affected by the choice of buffer material, with a larger average difference between values derived from the alternative buffers.

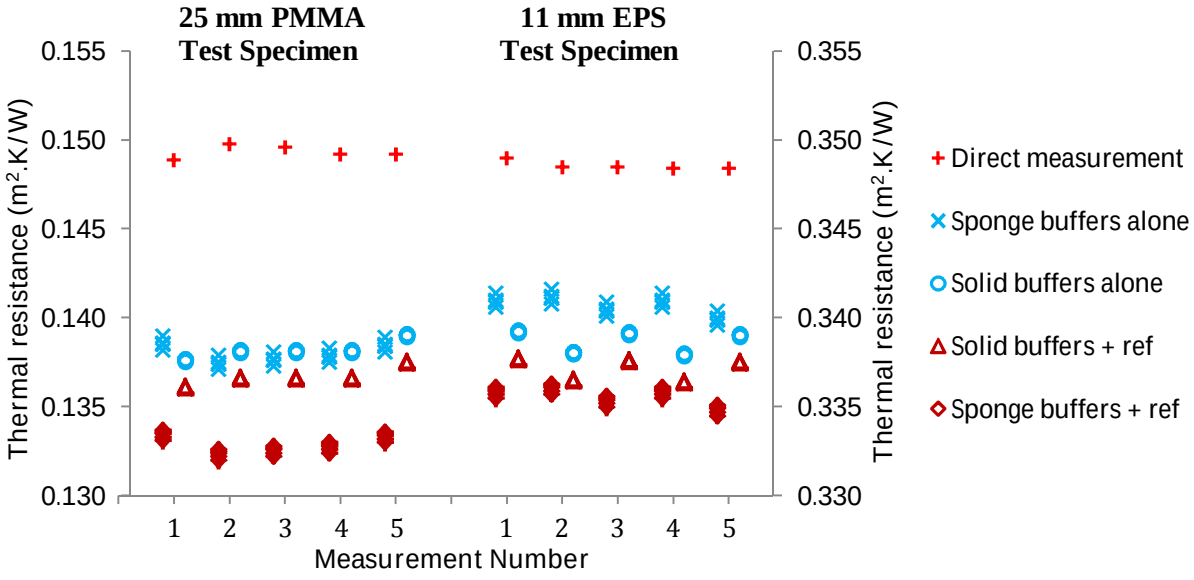

Figure 3.5. Heat flow meter measurement results for direct measurement of both specimens and as calculated by difference measurement, for both buffer types, with and without the inclusion of a reference specimen.

Considering just the reference-specimen method, overall results for the data appearing in Figure 3.5 are summarized in Table 3.3. Interface resistance values across all measurements ranged from 0.011 to 0.016 m^2.K/W.

Table 3.3. Overall summary of heat flow meter results comparing direct and difference measurement of specimen thermal resistance, R_s (m^2.K/W).

Buffer type	Mean results	25 mm PMMA	11 mm EPS
None	R_s by direct measurement	0.1493	0.3486
1.7 mm Solid silicone	R_s by difference measurement	0.1367	0.3372
	Absolute difference in R_s	0.0126	0.0114
	% overestimate in R_s	9.2	3.4
4.2 mm Silicone sponge	R_s by difference measurement	0.1329	0.3356
	Absolute difference in R_s	0.0164	0.0130
	% overestimate in R_s	12.3	3.9

In a previous study (Clarke et al., 2014) we considered a larger sample of twelve highly-conductive specimens with four different buffers. Since only the buffers-alone configuration was used for the second measurement, residual uncertainty remained in the unknown value of $(2R_{b-s} - R_{b-b})$. However, one of the four buffer types was the same medium-soft silicone sponge for which a value of 0.0051 has now been determined for $(2R_{b-s} - R_{b-b})$. An improved calculation of the interface resistance values for these earlier measurements has therefore been possible. Table 3.4 combines results for the current and previous studies, listed in order of increasing thermal resistance. Despite the much larger range of specimen types and resistance values, the range of total interface resistance has expanded only slightly, now being from 0.008 to 0.016 m^2.K/W. As previously observed, the higher values are associated with either bowed specimens (25 mm PMMA and the MgO building board) or those with very-rough surfaces (the granulated underlay and, to a lesser extent, the EPS board). Table 3.4 also lists the percentage error associated with the calculated value of interface resistance for a simple direct measurement and the overall uncertainty offered by difference measurement, using a reference specimen, at a 95% confidence level (coverage factor of 2). This uncertainty has been calculated in accordance with ISO GUM (ISO, 2008) and includes all relevant calibration and measurement uncertainties, including those propagated through the subtraction calculations that provide the difference values. Overall uncertainty could be reduced slightly if the reference specimen were to be independently measured with greater precision than the available figure of ±10%.

Table 3.4. Summary of measurements including results from previous study, showing interface resistance, the error it causes in direct measurement and calculated uncertainty for difference measurement.

Specimen	Thickness (mm)	Specimen resistance (m^2.K/W)	Interface resistance (m^2.K/W)	Direct measurement error (%)	Difference measurement uncertainty (%)
With 4.2 mm medium-soft silicone sponge buffers					
Flat aluminium sheet	2.5	0.00001	0.0100	*large*	*large*
Bowed aluminium sheet	3.0	0.00001	0.0098	*large*	*large*
Solid HDPE sheet	1.5	0.0025	0.0100	423.5	80.4
Phenolic paper board	1.7	0.0045	0.0106	246.9	59.2
Granulated rubber & cork underlay	3.2	0.025	0.0141	60.3	18.5
MgO building board	15.9	0.025	0.0158	67.8	18.4
Flexible composite PVC flooring	3.0	0.028	0.0087	30.9	15.6
PMMA (acrylic) A	5.8	0.030	0.0083	27.9	14.9
PMMA (acrylic) B	6.1	0.031	0.0082	26.9	14.8
“Masonite” hardwood	5.4	0.036	0.0113	31.1	12.6
Corrugated polypropylene board A	3.3	0.056	0.0080	14.2	8.8
Corrugated polypropylene board B	5.0	0.076	0.0077	10.2	6.8
PMMA (acrylic) C	24.9	0.133	0.0164	12.3	4.0
EPS board	11.3	0.336	0.0130	3.9	2.6
With 1.7 mm solid silicone buffers					
PMMA (acrylic) C	24.9	0.137	0.0126	9.2	3.0
EPS board	11.3	0.337	0.0114	3.4	2.2

3.4 Analysis & Discussion

3.4.1 Interface Resistance and Buffer Choice

Table 3.4 lists overall interface resistance values for a pair of interfaces. Individual values are therefore 0.004 m^2.K/W or greater. This is equivalent to the thermal resistance of an airspace 0.1 mm thick at the interfaces under these temperature conditions. It would require very close tolerances in both apparatus and specimen to achieve a mean separation of less than this over the 600 mm square area of a larger C 518 apparatus although such a uniform separation is improbable. The likely circumstance would be a complex combination of areas with different levels of contact. Considering the potential variability in such a situation, measured plate-to-specimen resistances have been relatively uniform.

In comparison, we have measured a consistent interface resistance of closer to 0.002 m^2.K/W between flat phenolic sheets. It does appear that when similar flat materials are stacked, interface resistances may be relatively low. As discussed earlier, Lavrykov and Ramarao (2012) reported an incremental thermal resistance of 0.001 m^2.K/W per added sheet of paper, so that the sheet to sheet interface resistance must be lower still, although it may make up a significant fraction of this value. It appears that broad uniform contact tends to occur in stacked thin materials, allowing quite low interface resistance in this situation.

The contact resistances achieved with flexible buffer materials have been broadly similar to those of stacked hard sheets, i.e. typically around 0.002 m^2.K/W. These are usefully lower than typical plate-to-specimen values although it would not be suggested that apparatus plates should be made with such materials. Instead, techniques using buffers allow interface resistances to be both low and consistent, so that they may be factored out by difference.

Indeed an important attribute of a buffer is the provision of invariant interface resistance since this is the principal assumption upon which equation (4) relies. The assumption of reproducible interface resistance is also implicit in the ASTM E 1530 methodology, which also relies on a comparative measurement in a somewhat similar way.

In the case of the EPS specimen, the alternative buffers produced quite similar results, tending to support the assumption of consistent interface resistances when either buffer is used. For the PMMA specimen, there was a small difference between results. Measurement of this specimen was hampered because PMMA has a relatively-high coefficient of thermal expansion, giving it a strong tendency to bow under the imposed temperature gradient at this thickness. This may have allowed for more-marginal interfacial contact with the thinner, harder buffers whereas the thicker softer buffers may have been able to retain good contact with the bowed specimen. Top and bottom-plate heat flows were very similar for all measurements, providing no inference of irregular heat flow patterns. As Table 3.5 shows, both results for the 25 mm PMMA suggested a slightly lower conductivity than the earlier results with 6 mm material. The sponge buffer provided a closer value but there may be real differences in conductivity related to manufacture, especially with such different thickness.

Considering the hardness of the solid buffers, their apparent effectiveness is surprising. There is the potential for intermediate materials, for example the harder silicone sponges, to have better properties than either of the buffers used in this study for certain classes of specimen. Similarly, there might be preferable reference materials such as the polyimides (typically Vespal) for which more precise thermal data is available. However they may have unexpected interface properties because of their greater flexibility. The paper-reinforced

phenolic board (equivalent to electronic circuit board material) was very stiff and expected to provide a contact characteristic similar to typical thicker, stiff test specimens.

A measurement result achieved by subtracting one thermal resistance from another brings a penalty of increased uncertainty, which may be minimized if both resistances are smaller, as may be seen in Figure 3.5 in the lower relative uncertainties for the two measurements involving the solid buffers. Using the reported measurements for the two specimens of 0.025 m^2.K/W as an example, the use of the solid buffers would have reduced the uncertainty from 18.5% down to 13% at a 95% confidence level. However such measurements do extend operation of the apparatus into a region of higher heat flows, remote from the conditions of calibration. We have observed unexpected effects such as a slight dependence in calibration on the cooling-water temperature at very high heat flows, suggesting some issues with plate temperature uniformity under such conditions.

There may also be a compliance advantage in using better-insulating buffers and ensuring that all measurements are above the ASTM C 518 minimum of 0.1 m^2.K/W. Whilst the difference calculation is outside the current scope of ASTM C 518, this is a lesser issue.

Table 3.5. Summary of PMMA (acrylic) measurements comparing apparent thermal conductivity derived by direct and difference measurement.

Buffer type	PMMA specimen	Thickness (mm)	Apparent thermal conductivity (W/m.K)	
			Direct	Difference
Sponge	A	5.8	0.152	0.195
Sponge	B	6.1	0.157	0.199
Sponge	C	24.9	0.167	0.187
Solid				0.183

3.4.2 Instrument Limitations

Standard deviations were calculated for all series of five measurements and all were less than 0.25%. Whilst this is typical for the Fox instrument over its usual range, capability clearly extends down to at least 0.02 m^2.K/W, as exemplified by results for the thinner buffers. For such low values, interface resistance is a significant fraction of the total, so this too must be relatively reproducible. For the Australasian building industry, a thermal resistance of 0.02 m^2.K/W lies at the lower limit of any significant interest. Our results therefore suggest that instrument resolution is not a limiting factor, rather that interface resistance is the main technical hurdle, due essentially to the low clamping pressure and large contact area that are inherent in the ASTM C 518 method. It also appears that even with high-

precision plates and uniformly-flat specimens, significant interface resistance remains. In any case, many specimens representative of real products are not intrinsically flat and are difficult, if not impossible, to make so.

3.4.3 Implications for Precision and Uncertainty

EPS board is a durable, stable material, often used for calibration specimens. Results for our 11 mm specimen suggest that a more-typical 25 mm EPS specimen would read high by about 1.5% with direct measurement due to interface resistance. If such a specimen was calibrated by primary measurement, in an apparatus that incorporated the same interface-resistance error, the indicated thermal resistance should remain correct. However, the rating of the specimen itself would be incorrect, as would be the apparent thermal conductivity. Stacking two such specimens would produce a result lower than expected. This could lead to misplaced concerns about edge effects or thickness effects when the cause lies simply with interface resistance. This study has made use of a single heat flow meter apparatus. Alternative designs may produce different values for the plate interface resistances. Even if they are characteristically lower in some other designs, the question of interface resistance is a potential confounding factor in calibrations and inter-comparisons between different instruments involving rigid specimens.

The 25 mm PMMA specimen was chosen in part to compare results with a 2010 Asia-Pacific (APLAC) round robin of 27 laboratories (APLAC, 2010) which included a specimen of 15mm cast PMMA, having a nominal thermal resistance slightly below 0.1 m^2.K/W. Twenty five laboratories reported results for the PMMA sheet at 20 ºC. Only 5 laboratories stated an uncertainty of greater than 4%. The spread in results was considerably wider than this with an interquartile range of 11.8%, although results from a few laboratories were distant outliers and might be regarded as skewing the data. Although cast PMMA has a generic thermal conductivity in the 0.18-0.19 W/m.K range, there were only 5 results above 0.18 W/m.K. In comparison, Table 3.5 summarizes the range of thermal conductivities that we measured for 6 mm and 25 mm PMMA, showing that difference measurement provided values more within the expected range. It is not known how many laboratories used special techniques (such as the attachment of external thermocouples). However there is evidence in the values reported that interface resistance has not been allowed for in a large percentage of cases. This might be no surprise if stated uncertainties had accommodated this error source, but they largely did not.

3.5 Conclusions

The nominal lower limit of 0.1 m^2.K/W for ASTM C 518 appears to be well justified in light of the potential introduction of error due to interface resistance in the measurement of rigid specimens. We have found that the total plate-to specimen interface resistance is typically around or above 0.01 m^2.K/W and so is a significant source of error at the nominal lower limit and even for test specimens of considerably higher thermal resistance. However, building on earlier work, we have demonstrated the utility of a difference measuring technique, in combination with buffer materials, to extend the measurement capability of ASTM C 518 to lower thermal resistance values for rigid specimens. The use of a reference specimen in the second of two measurements has meant the elimination of residual interface-resistance terms which were previously unresolved. The assumption that the test and reference specimens have similar interface resistances, required for the procedure to be numerically correct, appears justified from our experimental results and is consistent with the procedure of ASTM E 1530 which is targeted at measurement of much lower resistance values.

Two different silicone materials, a thin solid sheet and a thicker medium-soft sponge have both proved to be effective in the role of buffers. Optimum buffer characteristics may depend upon aspects of the specimen, particularly flatness and thickness uniformity. There is some evidence that a thicker, softer buffer is preferable for many specimens since it is better able to control interface resistance, despite the fact that uncertainties related to conductance and thickness are greater. Further work studying a range of buffer and specimen types would help to optimize future choices.

It would be particularly useful if ASTM C 518 was able to be used reliably for measurement of thermal resistance down to 0.02 m^2.K/W, since it would then provide coverage to the realistic lower limit of interest within the building industry in the performance of materials. The technique that we have described appears capable of reliable measurement down to this value using a standard heat flow meter apparatus, provided that attention is paid to the increasing uncertainty at lower resistances. The technique incorporates measurements that might individually be in accordance with ASTM C 518 but the additional step of deriving a net result by difference in the way suggested is not accommodated. Inclusion of this approach in a future revision of C 518 (and similar standards) would be beneficial.

3.6 References

APLAC. (2010) APLAC TO53. Final Report, Thermal Insulation Proficiency Testing Program. Abbotsford, Vic, Australia: Asia Pacific Laboratory Accreditation Cooperation.

ASTM. (2010b) ASTM C518 - 10. "Test Method for Steady-State Thermal Transmission Properties by Means of the Heat Flow Meter Apparatus.". *Annual Book of ASTM Standards, Vol. 04.06.* ASTM International, DOI: 10.1520/c0518-10

ASTM. (2011) ASTM E1530 - 11. "Test Method for Evaluating the Resistance to Thermal Transmission of Materials by the Guarded Heat Flow Meter Technique.". *Annual Book of ASTM Standards, Vol. 14.02.* ASTM International, DOI: 10.1520/E1530-06

ASTM. (2013a) ASTM C177 - 13. "Test Method for Steady-State Heat Flux Measurements and Thermal Transmission Properties by Means of the Guarded-Hot-Plate Apparatus.". *Annual Book of ASTM Standards, Vol. 04.06.* ASTM International, DOI: 10.1520/C0177

Campbell GS, Huffaker EM, Wacker BT, et al. (2005) Use of the line heat source method to measure thermal conductivity of insulation and other porous materials *Thermal Conductivity 27/ Thermal Expansion 15.* Knoxville, TN: DEStech Publications, Inc., Lancaster, PA, U.S.A.

Clarke RE, Rosengarten G and Shabani B. (2014) Flexible Buffer Materials to Reduce Contact Resistance in Thermal Insulation Measurements *Thermal Conductivity 32 / Thermal Expansion 20, Proceedings of the 32th International Thermal Conductivity Conference and 20th International Thermal Expansion Symposium.* West Lafayette, Indiana: Purdue University Scholarly Publishing Services, DOI: 10.5703/1288284315544

Corsan JM and Williams I. (1980) Errors associated with imperfect surfaces in standard hot-plate thermal conductivity measurements. In: Metrology NPLDoQ (ed) *NPL Report QU57.* National Physical Laboratory, Teddington, Middlesex, TW11 OLW, UK.

Hust JG and Smith DR. (1989) Interlaboratory Comparison of Two Types of Line-Source Thermal-Conductivity Apparatus Measuring Five Insulating Materials. Boulder, Colorado: NIST.

ISO. (2008) ISO/IEC Guide 98-3:2008 Uncertainty of measurement -- Part 3: Guide to the expression of uncertainty in measurement (GUM:1995). Geneva, Switzerland: International Organization for Standardization

Kamai T, Kluitenberg GJ and Hopmans JW. (2015) A Dual-Probe Heat-Pulse Sensor with Rigid Probes for Improved Soil Water Content Measurement. *Soil Science Society of America Journal* 79: 1059. DOI: 10.2136/sssaj2015.01.0025

Lavrykov SA and Ramarao BV. (2012) Thermal Properties of Copy Paper Sheets. *Drying Technology* 30: 297-311. DOI: 10.1080/07373937.2011.638148

Netzsch. (2015) *Netzsch Thermal Analysis.* Available at: https://**www.netzsch-thermal-analysis.com/**.

Robinson HE and Watson TW. (1952) Interlaboratory Comparison of Thermal Conductivity Determinations with Guarded Hot Plates *ASTM STP119 Symposium on Thermal Insulating Materials.* Cincinnati, Ohio, USA: ASTM International, DOI: 10.1520/stp119-eb

TA Instruments. (2016) *Thermal Conductivity Test Instruments.* Available at: **http://www.tainstruments.com/products/thermal-conductivity-meter/**.

Tye RP, Coumou KG, Desjarlais AO, et al. (1987) Historical Development of Large Heat Flow Meter Apparatus for Measurements of Thermal Resistance of Insulations *ASTM STP922 Thermal Insulation: Materials and Systems.* Dallas, Texas, USA: ASTM International, DOI: 10.1520/STP18510S

Tye RP and Salmon DR. (2001) Thermal Conductivity Certified reference Materials: Pyrex 7740 and Polymethlymethacrylate *Thermal Conductivity 26 / Thermal Expansion 14, Proceedings of the 26th International Thermal Conductivity Conference and 14th International Thermal Expansion Symposium.* Cambridge, Massachusetts: DEStech Publications

Zarr RR, Heckert NA and Leigh SD. (2014) Retrospective Analysis of NIST Standard Reference Material 1450, Fibrous Glass Board, for Thermal Insulation Measurements. *Journal of Research of the National Institute of Standards and Technology* 119: 296. DOI: 10.6028/jres.119.012

4 STEADY-STATE THERMAL MEASUREMENT OF MOIST GRANULAR EARTHEN MATERIALS

Journal Paper:

Clarke RE, Pianella A, Shabani B, et al. (2016) Steady-state thermal measurement of moist granular earthen materials. *Journal of Building Physics*. Pre-published May 23 2016, DOI: 10.1177/1744259116637864

Additional Information for Chapter 4

The following pages of this chapter present, in the formatting style of this dissertation, a paper published in the Journal of Building Physics. The paper has been available electronically through the journal's "pre-publication" service since May 2016. Full publication is scheduled to occur in the next issue.

There are some minor formatting and editorial differences in the published version, including the positioning of figures and tables within the text.

For inclusion in this dissertation, section numberings have been amended to incorporate the chapter number.

The journal has allowed Australian spellings.

A monochrome (black and white) version of Figure 4.2 appears in the published version. An improved colour version was prepared for this dissertation.

A harmonized reference style based on Sage Harvard has been used in the presentation of this paper, as throughout this dissertation. Sage Harvard is also used by the Journal of Building Physics but there are small differences in the implementation. DOI numbers have been included where available.

STEADY-STATE THERMAL MEASUREMENT OF MOIST GRANULAR EARTHEN MATERIALS

Robin E Clarke[1,2], Andrea Pianella[3], Bahman Shabani[4] and Gary Rosengarten[1]

[1]School of Engineering, RMIT University, Melbourne, VIC, Australia

[2]CSIRO Australia, Clayton South, VIC, Australia

[3]School of Ecosystem and Forest Sciences, Faculty of Science, The University of Melbourne, Melbourne, VIC, Australia

[4]School of Engineering, RMIT University, Bundoora, VIC, Australia

Corresponding author:

Robin E Clarke, CSIRO Australia, Private Bag 10, Clayton South, VIC 3169, Australia.

Email: Robin.Clarke@csiro.au

Keywords

heat flow meter; thermal test method; thermal conductivity measurement; green roof; granular loose fill

Abstract

A technique based on the heat flow meter method is proposed for measuring the thermal conductivity of moist earthen and granular loose fill materials. Although transient methods have become popular, this steady state approach offers an uncertainty that can be reliably estimated and a test method that is widely accepted for building certification purposes. Variations to the standard method are proposed, including the use of a rigid holding frame with stiff base and silicone sponge buffer sheets, in conjunction with difference measurement to factor out the contributions from base, buffers and contact resistance. Using this approach, results are presented for green-roof substrates based on scoria, terracotta and furnace-ash at different moisture contents. Thermal conductivity ranged from 0.13 to 0.80 W/m.K and fitted well to linear regression plots against moisture content. Further comparative measurements of a single specimen showed that direct measurement was less consistent than difference measurement, and that indicated thermal resistance was higher by 0.023 m^2.K/W, attributable to the presence of contact resistance.

4.1 Introduction

The thermal properties of earthen materials are of interest in many disciplines. These include geothermal energy, underground power transmission, ground-coupled heat pumps, ground-coupled buildings and finally the use of earth within structures including green roofs where earthen materials act as plant-growing media in addition to their thermal, environmental and architectural qualities (Farrell et al., 2012).

In any building-related context, the standard approach to thermal measurement is a steady-state method such the heat flow meter, ASTM C 518 ASTM (2015) or the guarded hot plate, ASTM C 177 (ASTM, 2013a). These two methods are similar in that they essentially measure the heat that flows through a uniform test specimen under a representative temperature gradient. Specimens are ideally of end-use thickness and of relatively greater length and width so that geometrically-uniform heat flow can be established through them. These methods have regulatory acceptance, linked to their ability to achieve low uncertainties, typically below 3% for standard insulation products, and are amongst the methods nominated in the Australian standard AS 4859.1, Materials for the thermal insulation of buildings (Standards Australia, 2006). However, they may be less optimal for higher-conducting materials (including granular earths) due to errors arising from contact resistance. ASTM C 518, for example, has a nominal lower limit of 0.1 m^2.K/W for thermal resistance.

There are alternatives, including a range of transient methods. However, as we discuss in the following section, the transient methods are unable to deliver reliably low uncertainty for many specimen types, including granular loose fills. With specimens of this nature, the steady-state methods would also struggle without particular care in technique and methodology. We have developed an approach, within the general ambit of ASTM C 518, which does offer standard uncertainties as low as 4% for the measurement of soils and highly-conducting loose fills. However, our methodology is not consistent with ASTM C 518 in certain ways, particularly in the use of rigid holding frames and in the technique of measurement by difference, which we have reported elsewhere (Clarke *et al*., 2014).

The work described herein arose from a study of four candidate substrates for green roofs, including the complication that they needed to be moist in order to support plant growth. Results are presented for a study of 30 green-roof substrates with a variety of moisture contents and for 10 further measurements on one specimen to study repeatability as well as to compare the difference method to simple direct measurement.

4.2 Alternative Methods

Alternative methods include the guarded heat flow meter method ASTM E 1530 (ASTM, 2011) and the laser flash technique but neither is suitable for loose fills, since a rigid specimen with a well-defined flat surface is required. Several transient methods are feasible, including hot wire, single and multiple line-source probe (Liu and Si, 2011), as well as planar source methods (Almanza et al., 2004). These offer rapid measurement and determination of additional characteristics such as thermal diffusivity. They require a relatively small amount of specimen material, since the only relevant properties are those in the vicinity of the heat source, a heated platinum wire, a thin heater probe (or probes) or a small heated square or disk, depending on the method. There are few applicable standards, most of which target a particular class of material such as refractories in the case of the hot wire standard, ASTM C 1113 (ASTM, 2013b) and plastics in the case of the transient line source standard, ASTM D 5930 (ASTM, 2009).

In the case of transient methods, the indications regarding precision and uncertainty are very mixed. Al-Ajlan (2006) reports consistent agreement with manufacturer's specifications for a range of building products using a commercial transient plane source apparatus. He does not discuss calibration. Similarly Rides et al. (2009) found what they described as good agreement between transient plane source, transient line source and the guarded heat flow meter. All measurements were within ±7% of the mean for cast PMMA. In contrast, Hust and Smith (1989) describe inter-laboratory variations with a standard deviation of 26% for needle probes and 17% for hot wire apparatus. Tye and Salmon (2001) observed that transiently-measured values, especially for thermal conductivity, are often well outside individual accepted levels for some known materials although in a later study involving a number of European laboratories, Salmon and Tye (2011) reported transient hot disk measurements on carefully-prepared masonry specimens that were generally within ±3% of guarded hotplate values. They suggested that considerable development had occurred over time to improve the accuracy of the technique.

More recently, Cha et al. (2012) performed direct comparisons between a heat flow meter and a transient plane instrument for several series of building materials. Within each series they achieved values for the coefficient of determination (the R^2 value) between 0.93 and 0.98. Whilst this indicates good correlation between the two instruments, the absolute values of the indicated thermal conductivities were vastly different for high density fibreboard series, whilst being closer for the other series. Almanza et al. (2004) also observed good correlation between steady state and transient results for conductivity although the actual values were not

close, with results for plastic foams being typically 20% higher whilst values for solid plastic sheets were 40-50% higher. They proposed that contact resistance, present in both forms of measurement, might be higher in the steady-state case, particularly with rigid specimens. However, interface resistance appears to be an issue with all methods. Campbell et al. (2005) studied and compared the sources of error for liquid, solid and granular materials with the line source method. Errors as large as 50% were observed for all materials although, as others have noted, correlation with known materials was quite good, allowing reasonable accuracy after calibration. Their analysis showed that measurements are very sensitive to ambient temperature stability and to probe diameter, which needed to be impractically small to correctly follow the radial heat flow equation. They found that contact resistance was an additional source of error with granular materials (sand and glass beads). Errors were greater with larger particles but the use of thermal grease on the probe to improve thermal contact reduced these to acceptable levels with all particle sizes.

An issue with probe methods and larger particles is the fact that the density of particles adjacent to the transient source may be significantly lower because its presence disrupts the particle packing arrangement. This effect is also present at the specimen faces with a steady-state measurement where it may contribute to a higher contact resistance. However the effect may be more pronounced with a transient method because of the higher significance of properties immediately adjacent to the heating source, even if contact resistance may be nominally accounted for by choosing the correct portion of the transient-heating temperature curve. In using the transient plane method, Bentz et al. (2011) observed significant errors due to lack of homogeneity in concrete specimens with mortar-finished surfaces that were of different composition to the core (which contained larger aggregate). Their solution was to slice the specimens so that a representative machined face was contacting the transient source. No such option exists for loose granular materials.

Another “local” issue with probe methods is that of moisture content. Using a transient plane instrument, Yu et al. (2009) reported very consistent measurements of sand that was either dry, or fairly wet, but very large variations (sometimes up to 30%) for repeat measurements of sands that were intermediately wet (less than 25%). Based on microscopic analysis, an explanation was offered in terms of the unpredictable dispersal of local water bridges between sand grains in the region of transient heating. A number of differing water-linked states of granular materials are recognized within soil mechanics (Dong et al., 2015) and the potential for them to have considerable influence on thermal conductivity is evident. Steady state methods avoid effects induced by local heating, instead imposing an overall temperature gradient to achieve a standardized test condition. As a result, both moisture

content and temperature throughout the specimen will re-equilibrate. Heat flow will eventually stabilize, at which time thermal resistance may be measured.

Certainly there is ongoing development in heat conduction modelling with transient thermal devices (Kamai et al., 2015), providing prospects for improved capability in future instruments. However, prediction of thermal conductivity remains problematic, as explained by Dong et al. (2015) in their review of competing models.

4.3 Steady-State Measurement of Moist Granular Materials

ASTM C 518 does not contain specific procedures for measurement of loose-fill materials, deferring instead to the standard for loose-fills, ASTM C 687 (ASTM, 2012). Despite the title, this standard is largely unsuitable for earthen loose fills. Vermiculite and perlite are included in the scope but moist materials are specifically excluded and the provisions are clearly directed at low-density attic insulations (such as glass fibre). In contrast, the ISO heat flow meter standard, ISO 8301 (ISO, 1991) does contain guidelines for loose-fills. However the coverage is fairly general with focus on preparation techniques to achieve uniform density and is also largely relevant only to low-density materials. Accepting their limitations, both standards contain useful advice and are considered in subsequent sections.

Where significant moisture is present in materials, heat and moisture movement are coupled and behaviour may be very complex. Moisture movement and phase change occurring as a result of the measurement-imposed temperature gradient may induce large heat fluxes. However if permeability is low and these effects are small, a quasi-steady state may be reached quickly, with thermal measurement providing results applying to the case of the initial (uniform) moisture distribution. Were the measurement to be continued, moisture distribution would slowly re-equilibrate with some (usually small) change to the final thermal resistance (Sandberg, 1995). Conversely, most granular formulations are characterized by high permeability to the extent that moisture equilibration is rapid and follows closely behind that of temperature, giving stabilization times of less than 24 hours, depending on composition and specimen thickness. Consequently, the final moisture-equilibrium condition is the only practical measurement option. In order to ensure this, the specimen must be vapour sealed to constitute a closed system, and the measurement duration must be sufficiently long.

4.4 Adaption of Measurement Apparatus

A commercial “k-Matic” apparatus has been adapted for high-conductance work including granular loose-fill measurement. The 305 mm square plate size is small for general use but optimal for granular and earth materials. At a typical measurement thickness of 60 mm, a manageable 5 litres of specimen material is required. The 100 mm square heat flow transducer in the bottom plate provides for an acceptable averaging volume for most aggregate sizes.

The k-Matic plate system incorporates a fixed upper plate and a moveable lower plate running on guide rods with self-aligning bearings. Although the original mechanical design allowed for only 1 kPa clamping force on a full-sized specimen, the height-setting mechanism was amenable to modification. With incorporation of heavier components, a calibrated closing force of up to 5 kPa was possible, helping to minimize interface resistance.

Stabilization times for dense, moist specimens may be some tens of hours. Automatic termination based on criteria such percentage change over an interval or absence of monotonicity is inadequate since long term changes may be invisible within short term noise. A data acquisition system was developed with emphasis on real-time statistical analysis of measurement progress and stability. Additionally, a log file of 30 key variables is continuously-updated and may be accessed for closer analysis at any time.

The k-Matic is optimized to operate the top plate hotter than the bottom. It may be reversed and the opposite is the default for many apparatus. However the standard configuration suppresses convection of both liquid and vapour as well as phase-change recirculation (heat pipe effect) in specimens.

4.5 Holding Frames

Steady-state measurement of loose fill materials requires holding frames with sides of low thermal conductivity in order to minimize edge heat flow. ASTM C 687 specifies that conductivity of the sides should be below 0.12 W/m.K whilst ISO 8301 is not specific. Both standards propose thin, thermally-insignificant membranes across the bottom to contain the loose fill material. ISO 8301 requires the same at the top to fully encase the specimen. ASTM C 687 does not have this requirement, suggesting in fact that the material should initially protrude six mm above the intended measurement thickness, so that a slight final compression is applied between the test-apparatus plates.

For practical handling and preparation of granular loose fills, which may need to be compacted in place to achieve a target density, a frame with rigid sides and a stiff base is required. The base cannot therefore be thermally insignificant and must be accounted for in the overall measurement. Figure 4.1 shows the frames made for the study. Height was set at 60 mm to balance the need for sufficient thickness for accurate thermal measurement against the relatively high weight of dense substrates. Sides were of radiata pine with a nominal thermal conductivity of 0.1 W/m.K. A 1.6 mm thick, paper-reinforced phenolic board, with a conductivity of 0.4 W/m.K, was used for the base. It was attached by closely-spaced brass screws and the completed assembly waterproofed using 3 coats of polyurethane lacquer to prevent moisture uptake or exchange with the contents. Timber-machining tolerances and shrinkage resulted in an eventual frame thickness of around 59 mm. Rigid foamed polyurethane might be a more-stable alternative.

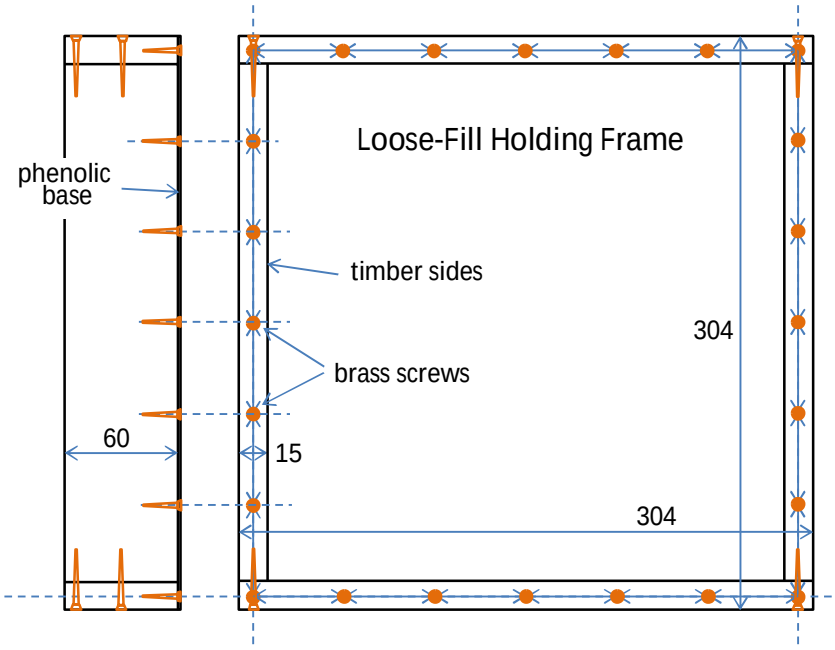

Figure 4.1. Loose fill holding frame, dimensions in mm.

4.6 Measurement Technique

The preparation of loose fill specimens may be challenging, particularly if a specific uniform thickness and density is required. ISO 8301 proposes thickness defined by the frame, possibly with accurate spacers set into the corners. This assumes a compressible specimen underneath the top membrane in order to assure contact at the top surface and possibly a

compressible frame. ASTM C 687 proposes an open slightly-high top, setting thickness according to the apparatus, also assuming a compressible specimen.

In the case of highly-conducting granular materials, an arrangement is required that provides good contact without the convenience of specimen compressibility. As we have shown (Clarke *et al*., 2014), interface resistance may become the largest source of error for specimens with thermal resistance significantly below 1.0 m^2.K/W when interfacial contact is compromised. The arrangement shown in Figure 4.2 is proposed. A buffer sheet of silicone sponge sits on the top surface, set in slightly from the sides, so that all contact pressure is transferred to the loose fill. The buffer sheet is slightly compressible and greatly improves the quality of contact with the potentially-uneven top surface of the loose fill, resulting in a low and predictable interface resistance. A buffer sheet is also used below the frame to minimize interface resistance at the bottom plate. Determination of overall thermal resistance therefore requires subtraction of the resistance of these buffers from the overall result, in addition to the contribution from the phenolic base. These three components may be combined and measured together, as shown in the bottom sketch of Figure 4.2. This reference measurement should occur at the same contact pressure to ensure no change in buffer resistance and for completeness it should include the layers of cling wrap typically used to seal the specimen. The film is very thin with negligible thermal resistance, but its presence ensures a closer match of the interface materials.

In performing a subtraction of one set of measured resistances from another, all of the components involved must be recognized. The simple difference may not represent a numerically-correct value of the specimen resistance because certain interface-resistance components are not present or are not identical in both measurements. This is unavoidably the case with loose-fills in a holding frame. For the measurement of specimen and frame, the total thermal resistance is:

$$R_t^1 = R_{p_1} + R_{p_1-b_1} + R_{b_1} + R_{b_1-s} + R_s + R_{s-x} + R_x + R_{x-b_2} + R_{b_2} + R_{b_2-p_2} + R_{p_2} \qquad (1)$$

where

R_t^1 is the total thermal resistance between the upper and lower plate;

R_{p_1} is the internal resistance of the upper plate (temperature sensor – surface);

$R_{p_1-b_1}$ is the interface resistance between upper plate and upper buffer;

R_{b_1} is the resistance of the upper buffer;

R_{b_1-s} is the interface resistance between upper buffer and loose-fill upper surface;

R_s is the resistance of the loose fill specimen;

R_{s-x} is the interface resistance between loose-fill lower surface and base;

R_x is the resistance of the base;

R_{x-b_2} is the interface resistance between the base and the lower buffer;

R_{b_2} is the resistance of the lower buffer;

$R_{b_2-p_2}$ is the interface resistance between lower buffer and lower plate; and

R_{p_2} is the internal resistance of the lower plate

The reference measurement, R_t^2, contains the following terms, including the new term R_{b_1-x} arising from contact between upper buffer and base:

$$R_t^2 = R_{p_1} + R_{p_1-b_1} + R_{b_1} + R_{b_1-x} + R_x + R_{x-b_2} + R_{b_2} + R_{b_2-p_2} + R_{p_2} \quad (2)$$

Therefore the difference is

$$R_{diff} = R_t^1 - R_t^2 = R_{b_1-s} + R_s + R_{s-x} - R_{b_1-x} \quad (3)$$

The three interface terms of equation (3) are all assumed to be small. R_{b_1-s} is the resistance at the interface between the bottom of the top buffer and the top surface of the loose fill, mediated by layers of plastic film. R_{b_1-x} is the analogous resistance between the bottom of the top buffer and the phenolic sheet, also mediated by the plastic film. These two resistances tend to cancel except that R_{b_1-s} is likely to be larger due to roughness and irregularity of the loose fill top surface. The remaining interface component, R_{s-x} is the interface resistance between loose-fill and base. This should be very small since the loose fill will make uniform contact with the base, especially since the fines will settle there too. A 4.3 mm thick silicone sponge was used for the lower buffer but a thicker 6.5 mm sheet was used at the top to better accommodate variability and non-uniformity in specimen thickness.

An alternative option is direct measurement without buffer sheets, along with subsequent subtraction of the small thermal resistance of the phenolic board, which must therefore be known. Defining the component terms based on the above nomenclature, the total thermal resistance is then:

$$R_t = R_{p_1} + R_{p_1-s} + R_s + R_{s-x} + R_x + R_{x-p_2} + R_{p_2} \quad (4)$$

As suggested above, R_{s-x} should be small. The internal resistances of the plates R_{p_1} and R_{p_2} should also be small and R_x, the resistance of the phenolic board, should be known. However the other two interface terms involving the plates, R_{p_1-s} at the top and R_{x-p_2} at the bottom, may be quite significant, based on experience with rigid specimens. R_{p_1-s} in particular has the potential to be large if the loose-fill top surface is not smooth and flat. At the very least, this surface must project above the level of the frame to allow measurement.

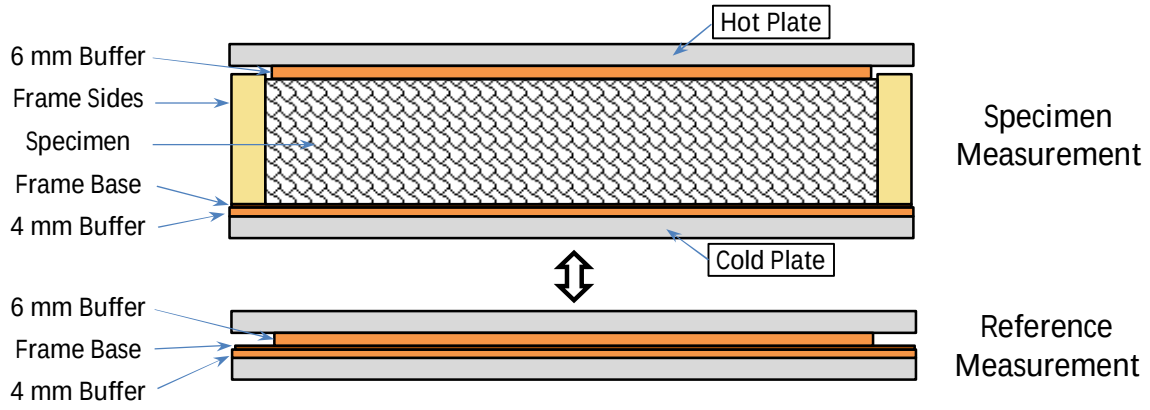

Figure 4.2. Configurations for specimen measurement and reference measurement.

For highly-conducting specimens, ASTM C 518 and ISO 8301 both propose the use of thermocouples attached directly to specimen surfaces for measurement of overall temperature difference in order to bypass the interface resistances between specimen and plates. More comprehensive advice on this approach is given in the European standard for measurement of products of medium and low thermal resistance, EN 12664 (BSI, 2001). Some form of buffer material, termed a "contact sheet" is generally required to allow passage of the thermocouple wires. It is acknowledged that corrections are required for the assumed effect of the buffers on thermocouple temperature. EN 12664 discusses further concerns, such as the effects of local non-homogeneity on temperature measurement but does not consider certain other potential sources of error, such as the interface resistance between the contact sheet and the specimen. Corsan and Williams (1980) discuss the difficulties with this approach, including the potentially large spatial variation in temperature due to variable contact with uneven surfaces. In any case, attaching thermocouples to a granular loose fill surface would be very challenging.

4.7 Specimen Selection and Preparation

Three green roof substrates were nominated, each based on a single primary material, together with a standardized fraction of organic matter in the form of composted coir (coconut husk), useful for plant nutrition and stabilizing moisture content. The three substrate formulations were very similar to those studied by Farrell et al. (2012) for the growth of succulent species:

1. Scoria mix composed of 60% of scoria with 8 mm screening, 20% scoria with 7 mm screening and 20% coir.
2. Terracotta mix composed of 80% crushed terracotta roof-tiles with 8 mm screening and 20% coir.
3. Power-station furnace ash mix composed of 60% bottom ash screened for particles below 2 mm, 20% bottom ash screened for particles 2-10 mm and 20% composted coir.

For each substrate, three levels of moisture content were defined; dry, moist and saturated. The dry condition was achieved by oven drying at 105-110°C for 48-72 hours. The moist condition was defined as 20% moisture content by volume, regarded as a typical in-service value, (i.e. not following heavy rain or a long dry period). A calculated amount of water was added at the mixing stage, with some fine tuning by wetting or drying the prepared specimen in its frame. The third condition, saturation, was achieved by fully wetting the mix then allowing it to drain and cease dripping before placing it in the holding frames. This was an inexact process so that the final moisture-content values for the same substrate composition varied slightly. Between different substrate types, saturation moisture content varied considerably.

For comparison, a commercial substrate was also measured only in the dry condition. This product was a mix of Hydrocell (a commercial soil improver), scoria, recycled concrete, horticultural ash and composted organics.

A small concrete mixer was used to mix the substrate constituents which were then poured into a wooden filling frame attached to the top of the holding frames. They were filled to a level of about 100 mm, giving a total material height of 160 mm including the holding frame underneath. As suggested in the Australian potting mix standard, AS 3743-2003 (Standards Australia, 2003), the assembly of frames was lifted 50 mm and dropped five times, in order to produce a standardized settlement. The filling frame was then removed and the material levelled off to the top of the holding frame using a metal ruler. Finally the specimen was sealed with plastic cling wrap to stabilize the moisture content. Figure 4.3 shows two prepared specimens.

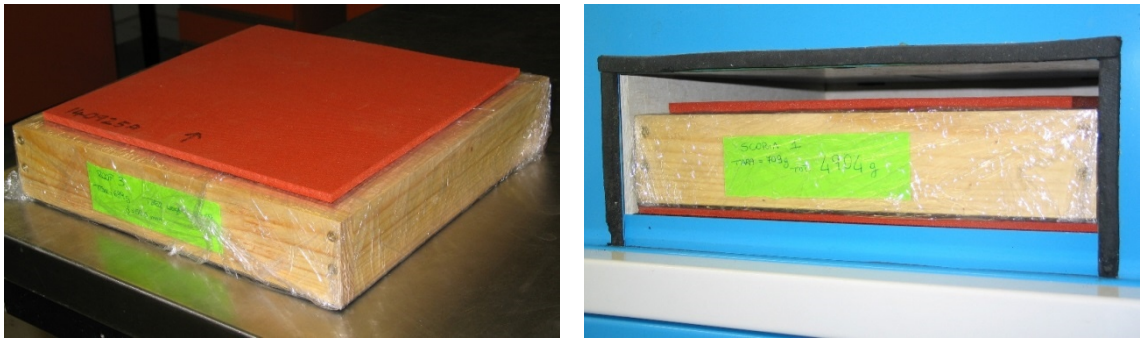

Figure 4.3. Specimens prepared for measurement, on the left with top buffer in place and on the right as located in heat flow meter apparatus.

4.8 Results and Analysis

Results of the 30 thermal measurements are shown in Table 4.1. Specimen thickness is stated to the nearest 0.5 mm, the highest meaningful precision given the top surface irregularities. The apparatus was left to run for approximately 24 hours with the top plate nominally at 33 ºC, the bottom at 13 ºC and the clamping pressure at 5 kPa. Weight change during measurement was very low, never exceeding 1 g (0.02 Vol%). Tabulated thermal resistance values have been derived by difference calculation, as described earlier, using the reference measurement value of 0.1428 m^2.K/W.

Thermal conductivity has been calculated from measured heat flow and thickness. Strictly it is the "apparent" value since there will be some stratification of moisture content and thermal conductivity as a result of the applied temperature gradient, with the calculated value being the effective average.

Data from Table 4.1 have been used to create Figure 4.4 which combines plots of thermal conductivity against volumetric moisture content for the three main substrates.

A linear regression fit has been applied to the data in Figure 4.4. A second-order polynomial gave insignificant improvement. Others including Sailor and Hagos (2011) have proposed a complex exponential relationship between conductivity and moisture content for substrates that include a significant percentage of sand, consistent with theoretical models.

Measurement uncertainty has been calculated in accordance with accepted principles (ISO, 2008) and includes contributions from thickness measurement, apparatus calibration, the individual uncertainties of measurements and the subtraction calculations that are the basis of difference measurement. Standard uncertainties in thermal conductivity are presented as error bars in the figure and range from ±7% for the highly-conducting wet terracotta to ±4% for the

dry substrates. Formal measurement reports would apply a coverage factor of two, which would double these uncertainty values.

Table 4.1. Measurement results for 30 green-roof substrates of varying moisture content.

Specimen name	Weight of substrate (g)	Thermal resistance (m2.K/W)	Thickness (mm)	Thermal conductivity (W/m.K)	Moisture % Vol
Scoria 1	4222	0.4286	57.5	0.1342	0.0
Scoria 2	4108	0.4252	58.0	0.1364	0.0
Scoria 3	4201	0.4166	57.5	0.1380	0.0
Scoria 4	4526	0.1631	56.5	0.3464	19.8
Scoria 5	4530	0.1678	57.0	0.3397	20.4
Scoria 6	4541	0.1731	57.5	0.3322	19.2
Scoria 7	5059	0.1387	59.5	0.4290	30.3
Scoria 8	5122	0.1386	59.5	0.4293	29.6
Scoria 9	5074	0.1438	59.5	0.4138	28.0
Terracotta 1	5956	0.2647	58.0	0.2191	0.0
Terracotta 2	5901	0.2871	59.0	0.2055	0.0
Terracotta 3	5891	0.2806	59.5	0.2120	0.0
Terracotta 4	5817	0.1189	59.0	0.4962	22.1
Terracotta 5	5826	0.1209	59.0	0.4880	22.4
Terracotta 6	5768	0.1066	59.0	0.5535	21.5
Terracotta 7	6522	0.0792	59.5	0.7513	35.5
Terracotta 8	6577	0.0770	59.5	0.7727	36.7
Terracotta 9	6508	0.0737	59.0	0.8005	34.9
Ash 1	3520	0.4048	59.0	0.1458	0.0
Ash 2	3575	0.4166	59.0	0.1416	0.0
Ash 3	3535	0.4019	59.0	0.1468	0.0
Ash 4	3490	0.1968	58.0	0.2947	17.3
Ash 5	3527	0.1913	58.0	0.3032	18.0
Ash 6	3528	0.1961	58.0	0.2958	18.1
Ash 7	5226	0.1073	59.5	0.5545	48.4
Ash 8	5149	0.1164	59.5	0.5112	46.6
Ash 9	4998	0.1179	59.5	0.5047	45.5
Commercial 1	3777	0.4586	58.5	0.1276	0.0
Commercial 2	3809	0.4693	58.0	0.1236	0.0
Commercial 3	3864	0.4627	59.0	0.1275	0.0

Figure 4.5 shows heat flow over the measurement term for a one example of each specimen type and moisture content. Whilst no heat flows fully stabilized in less than 6 hours, all of the dry specimens had done so by 8 hours and all had stabilized to within 1% of

their final value by 12 hours. However, monitoring beyond 12 hours would generally have been required in order to establish this fact.

The final specimen, "Commercial 3", was the subject of an additional study to assess measurement repeatability and compare the difference-measurement approach to direct measurement. A sequence of ten measurements was performed, alternating these two techniques. Direct measurement unavoidably included the phenolic sheet base, which was separately measured to have a thermal resistance of 0.0045 m^2.K/W. This value, equivalent to the R_{b_2} term in equation (4), was therefore subtracted from the measured thermal resistance.

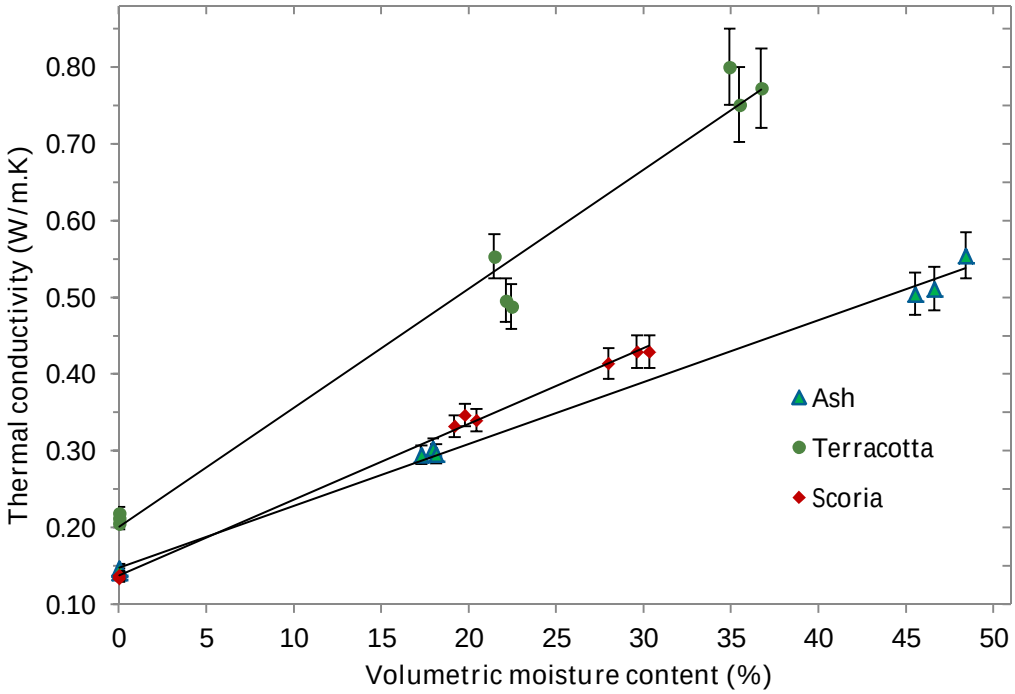

Figure 4.4. Measured thermal conductivity of scoria, terracotta and ash-based substrates as a function of moisture content with simple linear regression fit and error bars based on an uncertainty analysis.

The alternately repeated measurements occurred mostly on successive days. Figure 4.6 gives results for the two sets of thermal resistance values as well as the associated thickness values. Thickness, as measured by the apparatus, is plotted against the right-hand axis and was about 10 mm higher in the case of difference measurement due to the presence of the buffers.

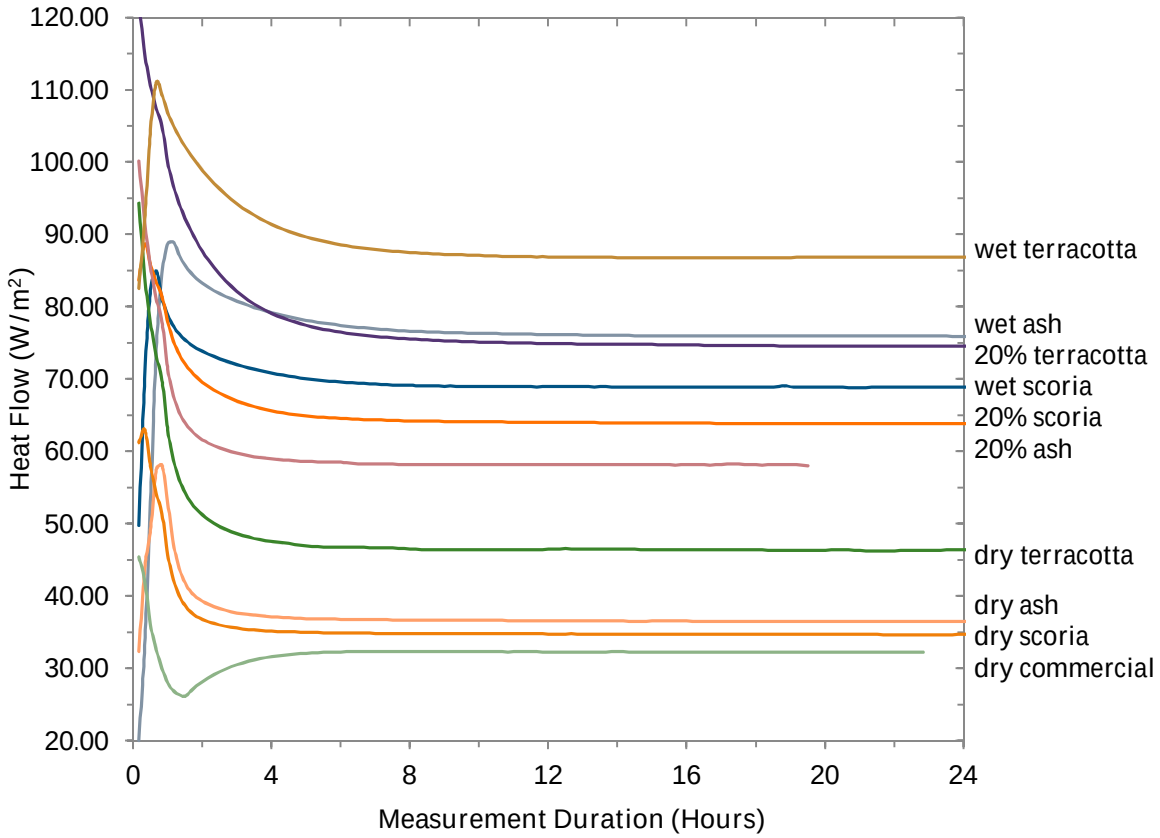

Figure 4.5. Stabilization times for one example of each specimen type in wet, 20% moisture and dry condition. Heat flows are moderated by the presence of top and bottom buffers.

Figure 4.6 reveals a downward overall trend in all values which was unexpected. The k-Matic thickness sensor is not highly accurate and operates at only one point on the perimeter but is sufficiently repeatable with measurement of the same specimen at the same orientation to confirm a pattern of steady settlement, clearly continuing beyond the initial standardized compaction (as per AS 3743), despite careful handling between measurements which involved little more than transfer to and from the weighing scales. In terms of repeatability, data are therefore more-appropriately assessed relative to curves of reducing thickness and thermal resistance over time, rather than constant values. Logarithmic decay curves gave a very good fit to the thickness data, as the Figure 4.6 shows, and have therefore been adopted. Repeatability of the repeated resistance measurements relative to these curves may then be compared to the repeatability of the individual specimen measurements as fitted to their moisture-content curves. This comparison is summarized in Table 4.2.

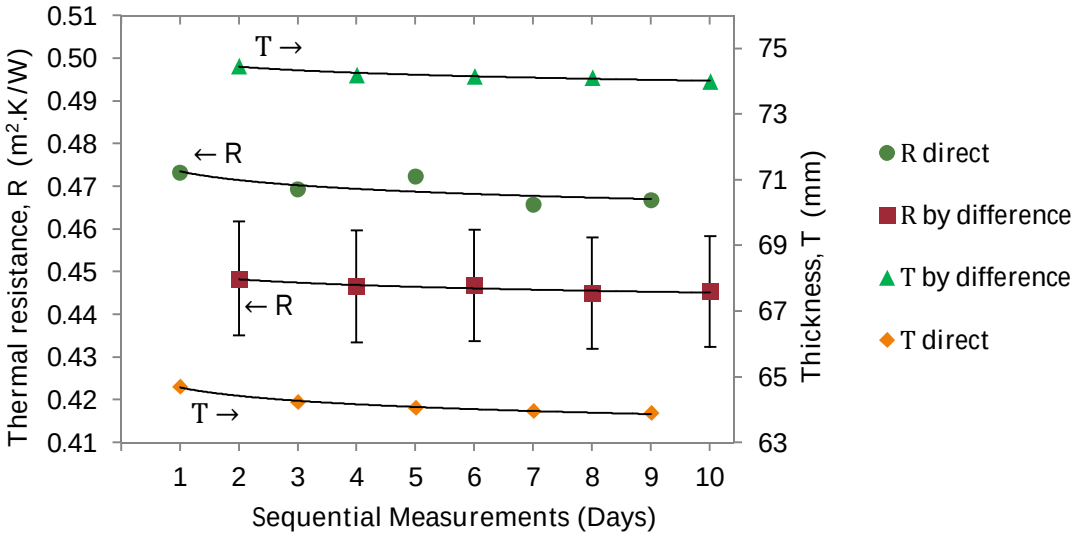

Figure 4.6. Repeated measurements of thermal resistance and thickness of Commercial 3 specimen with alternating direct and difference techniques.

Table 4.2. Summary of variability in thermal conductivity for all measurements.

Substrate	Number of specimens	Number of repeated measurements	Measurement technique	Mean deviation from trend (%)	Maximum deviation from trend (%)
Scoria	9	1	Difference	1.4	3.6
Terracotta	9	1	Difference	5.4	12.5
Ash	9	1	Difference	2.3	4.7
Commercial	3	1	Difference	1.4	2.1
Commercial 3	1	5	Direct	0.3	0.8
Commercial 3	1	5	Difference	0.1	0.1

In the case of the five measurements of the Commercial 3 specimen by difference, results were all within 0.1% of the trend line. This is typical of the repeatability achievable with a heat flow meter apparatus. The considerably greater variability amongst the other three substrates, measured only once, may therefore be largely associated with actual differences between specimens. Part of this will be due to thickness variation between specimens, since thickness could not be measured with an uncertainty of less than about 1%. There was some visible non-uniformity with granules of certain sizes tending to cluster together but this may have been insignificant when averaged over the 100 mm square metering area. On the other hand, total mass and density did vary slightly, as Table 4.1 shows. Moisture content also

varied. Although this has been accommodated as a variable in the plots, uncertainties arising in its measurement do remain. Significantly, the lowest variability is evident with the dry specimens, including the three specimens of commercial material which were measured only in the dry state.

Averaged over all moisture contents, mean variability was 1.4% for an ash-based substrate, 2.3% for scoria and 5.4%, for a terracotta-based formulation. Reasons for the higher variability of the terracotta specimens are not apparent. More tightly-controlled preparation techniques are conceivable but the results demonstrate the consistency achievable using techniques that are practical for large-scale substrate preparation. In any case, with the possible exception of the terracotta, uniformity was quite high considering the many sources of variation associated with specimen preparation.

Figure 4.6, in combination with Table 4.2, illustrates the principal advantages of difference measurement. Indicated thermal resistance tracked consistently lower by an average of 0.023 m^2.K/W and, although the data set is small, variance appears to be significantly lower. These results are both indicative of the presence of an interface resistance of approximately 0.023 m^2.K/W in the direct-measurement case. A large interface resistance is likely to be associated with large variability in its value. The much better repeatability of difference measurement, even though it requires subtraction of two measurements, would seem to confirm that interface resistances are consistently low when mediated by a soft buffer material.

The proposed value of interface resistance amounts to only 5% of the Commercial 3 specimen resistance but would be approximately 25% in the case of the wet terracotta. Standard uncertainty in thermal resistance for the difference measurements is indicated by the error bars and was approximately 3%. An uncertainty value for direct measurement is not shown since it would only be calculable if a value for interface resistance had been independently available.

It is also apparent from Figure 4.6 that, for this specimen, the systematic error arising from failing to account for interface resistance in direct measurement is greater than the total uncertainty associated with difference measurement.

4.9 Discussion

In Clarke et al. (2014), we describe measurements similar to those presented in Figure 4.6 to compare difference and direct measurement with 12 rigid specimens and in later studies (report in preparation) we looked at a further two material types. Results consistently suggested that the difference technique yielded a lower thermal resistance by between 0.008

m^2.K/W and 0.016 m^2.K/W. These values are significantly lower than the 0.023 m^2.K/W value for the Commercial 3 loose-fill specimen. As discussed, this value may be regarded as the difference between R_t (equation (4)) and R_{diff} (equation (3)). Both expressions contain a number of terms that are sufficiently small to be disregarded. It is likely that the higher value of R_t can be largely attributed to just the two sources that cannot be dismissed, the interfaces between the top plate and the loose-fill top surface and between the base of the holding frame and the bottom plate. The majority contribution is probably due to the former, a rigid flat plate achieving irregular contact with the high parts of an uneven granular surface, where contact against any hard surface is dominated by a relatively small number of larger protruding granules.

In other studies, we have observed the effect of increasing pressure on the same grade of silicone sponge (medium-soft) over a 1 kPa to 5 kPa range. As expected, interface resistance between the sponge and the contacting surface continued to fall as pressure was increased. Repeatability appeared to be slightly improved at higher pressures but results were consistent with flat surfaces as long as pressure exceeded about 1 kPa. For the uneven loose-fill surfaces and potentially more serious contact issues expected in this study, a pressure of 5 kPa was regarded as highly desirable.

Some contribution to the higher variance in the direct-measurement case for the repeated measurement of the Commercial 3 specimen may be associated with repeated disturbance of the granules and therefore of the contact points on the top surface. A significant advantage of the use of buffers is their ability to absorb local height variations, allowing more uniform contact so that heat flow is also potentially more uniform with less thermal field distortion.

The unexpected incremental settlement of the Commercial 3 specimen highlights the difficulty in controlling all of the measurement variables with loose fill specimens. At the same time, it illustrates the precision of the heat flow meter method in being able to clearly illuminate a subtle effect.

4.10 Conclusions

The ASTM and ISO steady-state test methods for building insulations do not adequately address the issues arising with dense, high-conductivity loose fills such as earths and green-roof substrates. However a review of transient methods suggests they are currently unable to achieve the low uncertainties required for test methods acceptable to regulatory authorities. It has been possible to develop certain variations to the heat flow meter method to achieve this whilst preserving the intent and core provisions. Chief variations have been the use of strong

and waterproof holding frames with stiff bases, accepting that the base contributes significant thermal resistance, and the use of buffer sheets above and below the test frame to ensure good specimen contact, but which also contribute additional thermal resistance in series with the loose-fill specimen. Measurement by difference has been effective in eliminating the contribution of these additional resistance components, as well as that of interface resistance between specimen and apparatus plates. At the same time, the use of external thermocouples has been avoided, greatly streamlining the measurement process.

A modified k-Matic apparatus has proved useful for the work, taking advantage of the small, 305 mm square size. Improvements to the plate assembly have allowed greater clamping pressure whilst a computerized data acquisition system has enabled monitoring for measurements of typically 24 hours duration, confirming well-behaved stabilization. Waterproof measurement frames and simple sealing with cling film has been effective, allowing measurement of specimens that were close to saturation. The combination of optimized apparatus, practical holding frames and use of the difference technique has meant that a program to measure 30 green-roof specimens has been very straightforward. However, steady state measurement of these materials is time consuming, with an allocation of up to 24 hours per measurement being required.

Repeated measurements of a single specimen have provided a demonstration of the value of difference measurement, suggesting a thermal resistance that was both more consistent and lower in this case by approximately 0.023 m^2.K/W, attributable to the avoidance of interface resistance.

Further work might establish improved guidelines for selection of buffer materials, clamping pressure, holding frames, and other aspects of the technique we have described. Development of a standard applicable to the measurement of earthen granular materials would be useful.

4.11 References

Al-Ajlan SA. (2006) Measurements of thermal properties of insulation materials by using transient plane source technique. *Applied Thermal Engineering* 26: 2184-2191. DOI: 10.1016/j.applthermaleng.2006.04.006

Almanza O, Rodríguez-Pérez MA and De Saja JA. (2004) Applicability of the transient plane source method to measure the thermal conductivity of low-density polyethylene foams. *Journal of Polymer Science Part B: Polymer Physics* 42: 1226-1234. DOI: 10.1002/polb.20005

ASTM. (2009) ASTM D5930 - 09 "Test Method for Thermal Conductivity of Plastics by Means of a Transient Line-Source Technique.". *Annual Book of ASTM Standards, Vol. 08.03*. ASTM International, DOI: 10.1520/d5930-09

ASTM. (2011) ASTM E1530 - 11. "Test Method for Evaluating the Resistance to Thermal Transmission of Materials by the Guarded Heat Flow Meter Technique.". *Annual Book of ASTM Standards, Vol. 14.02*. ASTM International, DOI: 10.1520/E1530-06

ASTM. (2012) ASTM C687 - 12. "Standard Practice for Determination of Thermal Resistance of Loose-Fill Building Insulation.". *Annual Book of ASTM Standards, Vol. 04.06*. ASTM International, DOI: 10.1520/c0687-12

ASTM. (2013a) ASTM C177 - 13. "Test Method for Steady-State Heat Flux Measurements and Thermal Transmission Properties by Means of the Guarded-Hot-Plate Apparatus.". *Annual Book of ASTM Standards, Vol. 04.06*. ASTM International, DOI: 10.1520/C0177

ASTM. (2013b) ASTM C1113 / C1113M - 09 (2013) "Standard Test Method for Thermal Conductivity of Refractories by Hot Wire (Platinum Resistance Thermometer Technique).". *Annual Book of ASTM Standards, Vol. 15.01*. ASTM International, DOI: 10.1520/c1113_c1113m

ASTM. (2015) ASTM C518 - 15. "Test Method for Steady-State Thermal Transmission Properties by Means of the Heat Flow Meter Apparatus.". *Annual Book of ASTM Standards, Vol. 04.06*. ASTM International, DOI: 10.1520/C0518-15

Bentz DP, Peltz MA, Durán-Herrera A, et al. (2011) Thermal properties of high-volume fly ash mortars and concretes. *Journal of Building Physics* 34: 263-275. DOI: 10.1177/1744259110376613

BSI. (2001) BS EN 12664:2001. "Thermal performance of building materials and products. Determination of thermal resistance by means of guarded hot plate and heat flow meter methods. Dry and moist products of medium and low thermal resistance". British Standards Institution

Campbell GS, Huffaker EM, Wacker BT, et al. (2005) Use of the line heat source method to measure thermal conductivity of insulation and other porous materials *Thermal Conductivity 27/ Thermal Expansion 15*. Knoxville, TN: DEStech Publications, Inc., Lancaster, PA, U.S.A.

Cha J, Seo J and Kim S. (2012) Building materials thermal conductivity measurement and correlation with heat flow meter, laser flash analysis and TCi. *Journal of Thermal Analysis and Calorimetry* 109: 295-300.

Clarke RE, Rosengarten G and Shabani B. (2014) Flexible Buffer Materials to Reduce Contact Resistance in Thermal Insulation Measurements *Thermal Conductivity 32 / Thermal Expansion 20, Proceedings of the 32th International Thermal Conductivity Conference and 20th International Thermal Expansion Symposium*. West Lafayette, Indiana: Purdue University Scholarly Publishing Services, DOI: 10.5703/1288284315544

Corsan JM and Williams I. (1980) Errors associated with imperfect surfaces in standard hot-plate thermal conductivity measurements. In: Metrology NPLDoQ (ed) *NPL Report QU57*. National Physical Laboratory, Teddington, Middlesex, TW11 OLW, UK.

Dong Y, McCartney JS and Lu N. (2015) Critical Review of Thermal Conductivity Models for Unsaturated Soils. *Geotechnical and Geological Engineering* 33: 207-221. DOI: 10.1007/s10706-015-9843-2

Farrell C, Mitchell RE, Szota C, et al. (2012) Green roofs for hot and dry climates: Interacting effects of plant water use, succulence and substrate. *Ecological Engineering* 49: 270-276. DOI: 10.1016/j.ecoleng.2012.08.036

Hust JG and Smith DR. (1989) Interlaboratory Comparison of Two Types of Line-Source Thermal-Conductivity Apparatus Measuring Five Insulating Materials. Boulder, Colorado: NIST.

ISO. (1991) ISO 8301:1991 Ed 1 Thermal insulation. Determination of steady-state thermal resistance and related properties. Heat flow meter apparatus. Geneva, Switzerland: International Organization for Standardization

ISO. (2008) ISO/IEC Guide 98-3:2008 Uncertainty of measurement -- Part 3: Guide to the expression of uncertainty in measurement (GUM:1995). Geneva, Switzerland: International Organization for Standardization

Kamai T, Kluitenberg GJ and Hopmans JW. (2015) A Dual-Probe Heat-Pulse Sensor with Rigid Probes for Improved Soil Water Content Measurement. *Soil Science Society of America Journal* 79: 1059. DOI: 10.2136/sssaj2015.01.0025

Liu G and Si BC. (2011) Single- and Dual-Probe Heat Pulse Probe for Determining Thermal Properties of Dry Soils. *Soil Science Society of America Journal* 75: 787. DOI: 10.2136/sssaj2010.0241

Rides M, Morikawa J, Halldahl L, et al. (2009) Intercomparison of thermal conductivity and thermal diffusivity methods for plastics. *Polymer Testing* 28: 480-489. DOI: 10.1016/j.polymertesting.2009.03.002

Sailor DJ and Hagos M. (2011) An updated and expanded set of thermal property data for green roof growing media. *Energy and buildings* 43: 2298-2303. DOI: 10.1016/j.enbuild.2011.05.014

Salmon DR and Tye RP. (2011) An inter-comparison of a steady-state and transient methods for measuring the thermal conductivity of thin specimens of masonry materials. *Journal of Building Physics* 34: 247-261. DOI: 10.1177/1744259109360060

Sandberg PI. (1995) Thermal Conductivity of Moist Masonry Materials. *Journal of Building Physics* 18: 276-288. DOI: 10.1177/109719639501800307

Standards Australia. (2003) AS 3743:2003 Potting Mixes. Sydney: Standards Australia

Standards Australia. (2006) AS/NZS 4859.1:2002 Materials for the thermal insulation of buildings - General criteria and technical provisions. Sydney: Standards Australia, Standards NZ

Tye RP and Salmon DR. (2001) Thermal Conductivity Certified reference Materials: Pyrex 7740 and Polymethlymethacrylate *Thermal Conductivity 26 / Thermal Expansion 14, Proceedings of the 26th International Thermal Conductivity Conference and 14th International Thermal Expansion Symposium.* Cambridge, Massachusetts: DEStech Publications

Yu M, Sui X, Peng X, et al. (2009) Influence of moisture content on measurement accuracy of porous media thermal conductivity. *Heat Transfer-Asian Research* 38: 492-500. DOI: 10.1002/htj.20272

5 Interface Resistance in Thermal Insulation Materials with Rough Surfaces

Journal Paper:

Clarke RE, Shabani B and Rosengarten G. (2017) Interface Resistance in Thermal Insulation Materials with Rough Surfaces.

Submitted to Energy and Buildings, 29 October 2016

Accepted subject to very minor revision, 14 January 2017

Additional Information for Chapter 5

The following pages of this chapter present, in the formatting style of this dissertation, a paper accepted for publication in Energy and Buildings. It incorporates revision based on reviewer comments, as returned to the publisher.

For inclusion in this dissertation, section numberings have been amended to incorporate the chapter number.

In addition, there are changes to the text on pages 110 and 110 to incorporate additional detail into the discussion in response to examiner's comments.

A harmonized reference style based on Sage Harvard has been used in the presentation of this paper, as throughout this dissertation. However this is not the style used by Energy and Buildings. DOI numbers have been included where available.

INTERFACE RESISTANCE IN THERMAL INSULATION MATERIALS WITH ROUGH SURFACES

Robin E Clarke[1,2], Bahman Shabani[3] and Gary Rosengarten[1]

[1]School of Engineering, RMIT University, Melbourne, VIC, Australia

[2]CSIRO Australia, Clayton, VIC, Australia

[3]School of Engineering, RMIT University, Bundoora, VIC, Australia

Corresponding author:

Robin E Clarke, CSIRO Australia, Private Bag 10, Clayton South, VIC 3169, Australia.

Email: Robin.Clarke@csiro.au

Keywords

thermal resistance measurement; rough surfaces; interface resistance; thermal insulation; heat flow meter

Abstract

We have previously shown how errors due to interface resistance arising in the measurement of highly-conducting insulation materials may be minimized by the use of flexible buffer sheets at the plate interface. We have found however that for materials with very rough surfaces, such as some building boards, thermal resistance and test thickness are both measured to be higher when harder buffers are used. This paper reports on an experimental study of nine materials and four buffer types to better quantify these effects. Thermal resistance was higher by up to 0.01 m^2.K/W and thickness by up to 0.5 mm using the hardest buffer relative to the softest. An analytical model has been developed, allowing measured roughness to be expressed as flat high and low areas of varying height and area fraction so that thermal resistance and height variations may be predicted as a function of roughness. These predictions have agreed reasonably well with optical roughness measurements. The model further predicts that interface-resistance errors are proportional to surface roughness and are always present with harder buffers, typically reaching 010 m^2.K/W for a mean roughness amplitude (S_a) of 200 μm. However with softer buffers these errors are absent below an onset level, typically at an S_a value of 60 μm.

5.1 Introduction

The presence of interface resistance is a recognized issue in the measurement of highly conducting building materials. The relevant measurement standards such as the heat flow meter method, ASTM C 518 (2015), accommodate large specimens with low contact pressure, making them better-suited to low-conductance materials such as building insulations. The guarded heat flow meter, ASTM E 1530 (2011), is an alternative method which is able to minimize interface-resistance errors through the use of very high contact pressure and small, highly-flat specimens. Improved apparatus and techniques are in development (Stacey et al., 2014).

To avoid interface resistance, ASTM C 518 suggests measurement of temperature at the specimen surface, rather than within the abutting apparatus plates. This requires provision for wiring to external temperature sensors, a feature not widely available on commercial test apparatus. In any event, Corsan and Williams (1980) found that the degree of imperfect contact tends to be spatially variable, so that it may be imprudent to rely on a small number of surface measurements. Compounding this is the difficulty in accurate measurement of surface temperature in the presence of thermal gradients, especially with potentially rough surfaces.

One measurement approach utilizes a number of similar specimens of differing thickness. The change in thermal resistance, R, with thickness, t (expressed as $\Delta t/\Delta R$), is taken as a measure of thermal conductivity independent of the influence of contact resistance (Hall et al., 1987; Brzezinski and Tleoubaev, 2002; Tleoubaev and Brzezinski, 2007). The method however requires two or more specimens having different thickness but equal and uniform conductivity (and therefore no significant surface roughness). In general, conductive materials are characterized using carefully prepared specimens, with smooth faces machined to close tolerances (Salmon and Tye, 2009; Salmon and Tye, 2011). Many building products cannot meet one or more of the requirements for size, surface flatness or clamping pressure.

We have previously described the use of sheets of compressible plastic foam located either side of a test specimen as an adjunct to the heat flow meter method (Clarke et al., 2014). The technique allowed hard, high-conductance specimens to be measured with levels of confidence and precision sufficiently high for commercial testing to be viable. Without these soft buffer materials, measurement would be impractical for two reasons. In the first place, the fragile hot and cold plates of the apparatus would be at risk of damage arising from contact with hard granular facings. In the worst case the full clamping force might be concentrated on a single hard grain to produce a damaging point load. Secondly, interface resistance between hard specimens and the hard apparatus plates is likely to be large enough

to produce unacceptable errors. Soft buffer materials allow for much better contact and lower interface resistances in the real-world situation where neither plates nor specimen are perfectly flat. We studied a number of buffer types but found that silicone sponge produced the most consistent thermal results. By separately measuring the buffers alone, the thermal properties of the test specimen could be derived by simple subtraction. We noted however that this procedure was numerically incorrect in that different interface-resistance terms were present in each measurement. Although the use of buffers ensured that all contact resistances involved at least one soft surface and were therefore likely to be small, the specimen-plus-buffers measurement uniquely included two buffer-specimen contact terms whilst the buffers-only measurement uniquely included a buffer-buffer contact term. It can be shown that this complication leads to a slight overestimate in thermal resistance from buffer-based measurements. Nevertheless results for 12 specimens were lower than those for direct measurement by 0.003 to 0.01 m^2.K/W, attributed to the reduction in interface resistance.

In further work (Clarke et al., 2016b), buffer hardness was also considered and results for a medium-soft silicone sponge and a solid silicone rubber were compared. The concept of comparison against a known reference specimen, measured with the same buffer configuration was also introduced. Assuming similar roughness (and presumably similar interface properties), the interface resistance terms cancel and the pair of measurements produces an algebraically-correct value of the thermal resistance of the test specimen by simple subtraction. This enabled correcting for the previously-unknown interface terms in earlier results. Across all specimens considered, measurements using buffers were lower by amounts ranging from 0.008 to 0.016 m^2.K/W.

Although unimportant for high-performance insulations, interface resistances of this order are quite significant for certain building components. Fire-resistant backing boards used behind cooktops are required by Australian building codes to have a thermal resistance exceeding 0.05 m^2.K/W. Interface resistance is clearly an issue at this thermal resistance, which incidentally occupies a niche that is outside the normal range of all ASTM test methods applicable to building materials. The nominal minimum of ASTM C 518 is 0.1 m^2.K/W whilst that of the guarded hotplate method ASTM C177 (2013a) is 0.06 m^2.K/W (stated in conductance terms). Conversely ASTM C 1530 targets materials of very low resistance with a nominal upper limit of 0.04 m^2.K/W. With care, any of these standards might easily stretch to cover 0.05 m^2.K/W. Our efforts with buffer materials have been aimed at ensuring that acceptable results are obtained when ASTM C 518 is applied to this task. This may include cases where manufacturers are unable to control thickness uniformity or surface roughness sufficiently to meet the challenging flatness requirements of measurement standards.

Limitations to the buffer-measurement approach became apparent with building boards having rough, textured surfaces. With smooth specimens, routine measurements were largely independent of buffer softness but with rough-surfaced specimens, harder buffers produced thermal resistance results that were higher (although still lower than with direct measurement). This is shown in Table 5.1, comparing results with a soft 4.2 mm silicone sponge and a 1.7 mm solid silicone sheet. The first two results for PMMA (acrylic) and EPS (polystyrene foam) were previously reported (Clarke et al., 2016b) and are cases where buffer-related dependence was too small to signify a significant trend. However the three following measurements were of low-resistance building boards where the thermal resistance measured with hard buffers was substantially higher in percentage terms.

Table 5.1. Measurements suggesting a dependency on buffer hardness.

Specimen	Thickness (mm)	Thermal resistance (m^2.K/W) by difference measurement		Difference in thermal resistance	
		4.2 mm soft buffers (both sides)	1.7 mm hard buffers (both sides)	(m^2.K/W)	(%)
PMMA	25	0.1329	0.1367	0.0038	2.9
EPS	11	0.3356	0.3372	0.0016	0.5
Building board C	9	0.0295	0.0391	0.0096	33
Building board P	12	0.0385	0.0449	0.0064	17
Building board W	9	0.0185	0.0250	0.0065	35

In contrast to the values in Table 5.1, thermal measurement of typical smooth materials has generally provided results with no significant dependence on buffer hardness. The inference is therefore that this dependence is associated with surface roughness although it is also apparent with the 25 mm PMMA material which has a very smooth finish on both sides. Our aim in this study has therefore been to understand and quantify the role of roughness in thermal measurements. We considered nine materials of very different roughness, each with four different buffers. Roughness was evaluated using confocal microscopy.

Whilst it might be expected that hard buffers would not fully accommodate the high and low points of an uneven specimen, no models of thermal contact resistance were available in order to explain and predict this effect. The study of contact resistance is most-widely associated with the electronics industry and deals with contact between smooth-faced metals or semiconductors, including the use of interface materials to maximize conductance (Narumanchi et al., 2008). Levels of contact pressure and heat flow may be orders of magnitude higher than those of interest for building materials with a dimensional scale of

roughness that is orders of magnitude lower. Not surprisingly, issues of scale are important even within this context, as discussed by Jackson et al. (2008) in relation to roughness, hardness, deformation, and even the governing equations for thermal resistance since phonon mean free path is involved at smaller scales. However assumptions that are appropriate on these scales would not be applicable for thermal insulation measurement, for example neglecting conductive and radiative heat flow through areas of non-contact (the airspaces).

Very little work on the influence of roughness (and other flatness imperfection) on interface resistance has been reported in the context of building insulation materials. It has however been studied by Corsan and Williams (1980) who developed an analytical model based on resistance networks to explain the large spatial differences in temperature observed during thermal measurement of masonry materials with uneven surfaces. They considered only very shallow depressions, less than 0.2 mm, which also allowed radiation terms to be neglected. The effect of surface depressions on local surface temperature was examined over a range of widths, the focus being on the use of this information to manage errors in direct measurement of temperature, bypassing the buffer materials.

In our case, the thermal properties of the buffer are fundamental whilst local temperatures are not even measured, so the approach must encompass the overall properties of the complete assembly, including the buffer. To this end we have developed an analytical model that defines roughness in terms of flat hills and flat valleys, with the valley depth and valley area fraction being independent variables specifying the degree of roughness. The assumption of only two surface heights is a simplification although even some very-complex contact-resistance models take a similar binary approach, allowing contact resistance to have only two discrete values, inside and outside of contact spots (Bobeth and Diener, 1982). The advantage of this approach is that determination of effective thermal resistance resolves to a simple two-zone bridging heat flow calculation. The disadvantage is that roughness is not expressed in the usual way, as the mean absolute amplitude of a continuously-variable surface height. However we have developed an additional geometric procedure to translate to the binary representation (characterized by valley depth and area fraction) from a generalized roughness following a sinusoidal or other profile, which may be characterized by a single amplitude parameter. Since roughness in terms of this parameter may be measured by a variety of techniques, it has been possible to directly compare predictions of the model with thermal and roughness measurement results from the experimental study. It has also been possible to develop a generalized prediction of the effect of specimen roughness on measurement results as a function of buffer hardness.

5.2 Development of an Analytical Model

5.2.1 Binary Roughness Model – Geometric Analysis

The basis of an analytical roughness model which considers a rough surface as composed of flat hills and adjacent flat valleys is illustrated in Figure 5.1. The model is scale-independent although valley depth, V, and the area fraction of valleys, Z_a, must both be specified. A buffer abutting the specimen surface undergoes compression where it is in contact with the hill areas, which is presumed to occur with zero contact resistance. The buffer is assumed to have a constant Young's Modulus for small compressions and to be sufficiently pliable to spring out to full thickness in the valleys. For decreasing area fraction of hills relative to valleys, the compression force will be concentrated over a smaller area so that these areas of the buffer will undergo increased compression, and the overall thickness of the buffer/specimen combination will decrease. The airspaces in the valleys therefore diminish in size, disappearing altogether when conditions are such that the uncompressed areas of the buffer touch the valley floor.

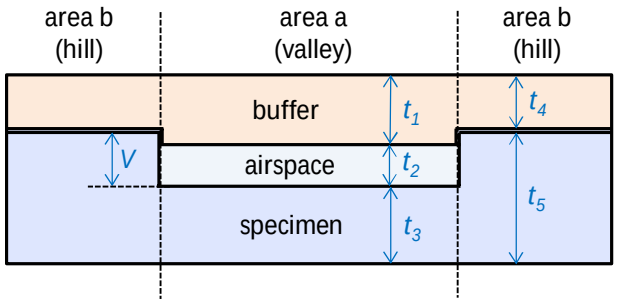

Figure 5.1. Representation of buffer compression at rough surfaces in analytical model.

The total clamping force of the plates is distributed across the buffers and specimen resulting in a pressure that is uniform when specimen and buffers are of uniform thickness. For a non-uniform specimen having high and low points, pressures will vary spatially with total force being the sum of the individual pressures and their associated areas. For a binary surface that has areas a and b of different heights, there will be two values of pressure. Therefore:

$$F = \sum_{x=1}^{n} P_x A_x = P_s A_s = P_a A_a + P_b A_b \quad (1)$$

where P_x and A_x are the pressure and area values for a surface of n different heights; P_s and A_s are the pressure and area values for the case of a single smooth flat surface; and P_a, A_a, P_b and A_b are the pressure and area values for the binary case of heights a and b only.

Equation (1) may be expressed in terms of area fractions as:

$$P_s = \frac{F}{A_s} = P_a \frac{A_a}{A_s} + P_b \frac{A_b}{A_s} = P_a Z_a + P_b Z_b \tag{2}$$

where Z_a and Z_b are the area fractions for areas a and b.

Since F and A_s are both easily measured, a value for P_s applying for uniform conditions is readily obtained. A value of Young's modulus for the buffer material may also be determined under these conditions since:

$$E_n = \frac{P_x}{\varepsilon_x} = \frac{P_x D_n}{d_x} = \frac{P_s}{\varepsilon_s} \tag{3}$$

where E_n is Young's Modulus for buffer n; P_x and ε_x are pressure and strain for the general multi-thickness case; D_n is the uncompressed thickness of the buffer; d_x is the reduction in thickness of the buffer under pressure P_x; and P_s and ε_s are measured values of pressure and strain for a smooth flat specimen.

Where the buffer is sufficiently stiff (i.e. Young's modulus is sufficiently high) and the area fraction Z_b is sufficiently large, the buffer is compressed only by the amount d_b insufficient to completely fill the valleys (area a). Therefore from (2), (3) and Figure 5.1:

$$P_s = P_b Z_b$$

$$t_4 = D_n - d_b = D_n \left(1 - \frac{\varepsilon_s}{Z_b}\right) \tag{4}$$

The value of t_4 indicates the degree to which the buffer has been compressed and allows calculation of t_2, the thickness of the airspace. Since t_1, t_3 and t_5 are known, calculation of overall thickness and overall thermal resistance may then proceed.

For an increasingly softer buffer or smaller value of Z_b, the point is reached where the airspace disappears and t_2 becomes zero so that the buffer has been compressed by the valley depth, V. From (3), at this point:

$$P_b = \frac{E_n d_b}{D_n} = \frac{E_n V}{D_n} \tag{5}$$

Beyond this point, the buffer will be compressed over both valley and hill areas, but to different degrees because of the height difference, V. Since strain is a linear function of

pressure, P_b will always exceed P_a by the value given in equation (5). Under these conditions, from (5):

$$P_b = P_a + \frac{E_n V}{D_n} \tag{6}$$

Combining (2), (3) and (6) into the expression for t_4 resolves to:

$$t_4 = D_n - d_b = D_n(1 - \varepsilon_s) - VZ_a \tag{7}$$

Equation (4) therefore provides the value of the apparent buffer thickness t_4 for the case of single contact of hills only ($d_b < V$) whilst equation (7) provides the value for when $d_b >$ V and there is contact at both hills and valleys. The two expressions simplify to agree when $d_b =$ V. The calculation procedure therefore checks for this condition. If $d_b = V$ then:

$$\left(\frac{D_n \varepsilon_s}{Z_b}\right) - V = 0 \tag{8}$$

If the expression on the left hand side has a value greater than zero then there is contact at both hills and valleys and equation (7) applies. Otherwise equation (4) applies.

Overall thickness is the value of $t_4 + t_5$.

5.2.2 Binary Roughness Model – Determination of Thermal Resistance

Thermal resistance is calculated as the area-weighted average of hill and valley contributions to conductance, with the latter potentially including an airspace. This is equivalent to the "Parallel Heat Flow Paths" calculation method which assumes that heat flows through areas a and b are separate and do not interact. The alternative "Isothermal Planes" method which assumes all planes transverse to the heat flow are at equal temperatures, is often preferred (Trethowen, 2000) but is difficult to apply for the geometry of Figure 5.1 since the hill and valley planes are not aligned.

Assumptions are made that the thermal conductivity of buffer materials is independent of their density (for the small compressions) and that heat transfer across airspaces is by conduction and radiation only. Convection heat transfer is an additional possibility at some scale of airspace dimension. However Robinson and Powlitch (1954) and ISO 6946 (2007) affirm that convection is negligible at the temperatures differences concerned, (less than 20K across the whole assembly) with airspaces no more than a few mm thick. This applies even for heat flow upwards which, although it is the standard mode for the Fox apparatus, is the direction most likely to support buoyancy-driven flows.

Applied to the geometry of Figure 5.1, the parallel paths calculation gives:

$$R_m = \frac{1}{C_m} = \frac{1}{C_a Z_a + C_b Z_b} = \frac{R_a R_b}{Z_a R_b + Z_b R_a} \tag{9}$$

where R_m and C_m are the mean overall thermal resistance and conductance and R_a, R_b ,C_a and C_b are the mean thermal resistances and conductances for areas a and b respectively.

R_a and R_b are each calculated as the series combination of the contributing resistances in the two paths. If an airspace exists in path a, its thermal resistance contribution is calculated as the parallel sum of conductive and radiative contributions. Radiation is modelled using the linearized approximation of the Stefan-Boltzmann law for an airspace with a pair of facing surfaces (Robinson and Powlitch, 1954):

$$h_r = 4\sigma E T_m^3 \tag{10}$$

where h_r is the radiation heat transfer coefficient; σ is the Stefan-Boltzmann coefficient; E is the total emittance of the pair of facing surfaces; and T_m is the mean absolute temperature of the pair of facing surfaces.

5.2.3 Geometric Adaption for Generalized Roughness

Surface roughness is commonly expressed as a mean absolute amplitude, representing a generalized profile (such as a sinusoid). Figure 5.2 suggests a geometric procedure for approximating such a shape in terms of the binary model, in order to calculate the interface thermal resistance. In this interpretation, the buffer is regarded as having a "sitting position" on the specimen roughness profile, contacting the higher points with the remaining area being a void (valley) with the buffer as its upper boundary. The contact area and voids are therefore analogous to the essential components of the binary model and although neither are flat planes, it may be reasonable to approximate them as such. We employ a spreadsheet to calculate total buffer force, mean airspace height and contact area fraction for a generalized roughness profile of normalized amplitude. A sinusoid and an expression based on $(\text{sine}+1)^2$ are shown. Local buffer force is calculated at 2 degree intervals and integrated over the area fraction of contact to obtain total force for 80 defined heights (buffer sitting positions) between normalized values of 1 (zero contact with the buffer) and -1 (full contact). Since the apparatus clamping pressure is a known constant value, the mean overall force on any buffer is constant, as is the mean overall deflection which is defined by the value of Young's modulus for that buffer. The spreadsheet therefore allows for the buffer sitting height that matches this mean overall buffer deflection to be identified for any amplitude of the roughness function. The corresponding mean contact area fraction (effectively Z_b), mean

buffer compression over the area of contact, and mean valley depth are then entered directly into the rectilinear model (Figure 5.1) for calculation of thermal resistance.

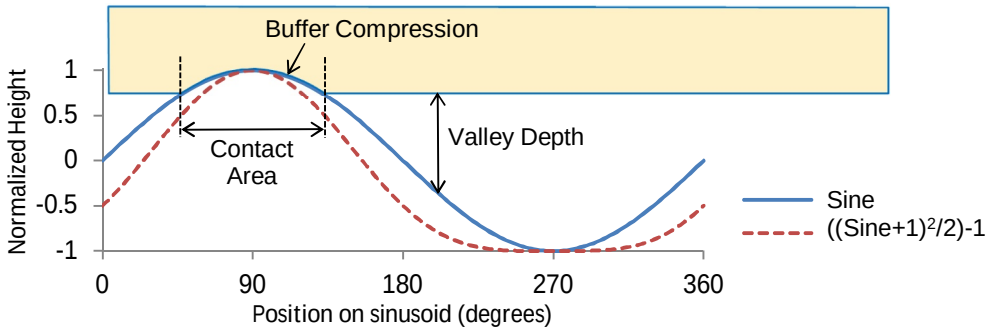

Figure 5.2. Interpretation of a generalized rough surface in contact with a buffer material in terms of the analytical model (with parameters of area-fraction and valley-depth).

5.3 Experimental Results

5.3.1 Thermal Resistance Measurement and Analysis

The experimental program involved nine specimen materials and four pairs of buffer materials. Thermal measurements were performed on each combination in a 610 mm square, Fox 600, heat flow meter apparatus in accordance with ASTM C 518, using a mean temperature of 23 ºC and a temperature difference of 10K. The buffers were selected from two material types, each at two thicknesses, as shown in Table 5.2. Shore A hardness was measured with a handheld durometer. The "soft" material was a soft-medium sponge which had sufficient compliance to compresses slightly under the 2.2 kPa apparatus plate loading. In contrast, compression was negligible for the "hard" solid material, which had a much higher Shore A hardness, higher density and higher thermal conductivity.

Table 5.2. Properties of studied silicone buffer materials.

Property	6.4 mm soft	4.2 mm soft	3.4 mm hard	1.7 mm hard
Density (kg/m^3)	450	450	1200	1200
Thickness (mm)	6.4	4.2	3.4	1.7
Thermal conductivity (W/m.K)	0.083	0.083	0.16	0.16
Compression under 2.2 kPa (%)	1.5	1.5	<0.1	<0.1
Compression under 260 kPa (%)	65	65	5	5
Shore A hardness	5	5	55	55

The nine test materials, which included the five materials described in Table 5.1, are listed in Table 5.3, which also gives the thermal measurement results. Additional rough-surfaced materials were a coarse mat made from granulated rubber and cork chips, and a sheet of "prismatic" polystyrene, manufactured as a lighting diffuser. Two smoother materials were included for comparison, a thinner (6 mm) PMMA sheet and a thin phenolic board. Images of the rougher surfaces are given in Figure 5.3.

The EPS, PMMA and rubber/cork mat, had the same surface characteristics on each side. Two of the building boards had faces with textures that were fairly different from each other but were all of intermediate roughness. Building Board C had one very rough surface and one that was relatively smooth. The prismatic polystyrene had a deep prismatic pattern on one face and was smooth on the other. All specimens were approximately 600 mm square. Each was measured once with each of the four silicone buffer types specified in Table 5.2. Instrument results for thermal resistance, R, and thickness, t, are given in Table 5.3, each being the total value for the specimen measured with a pair of similar buffers, therefore including interface resistance contributions from both faces of the specimen. Operating the apparatus in "auto thickness" mode, the plates applied the standard loading force on the specimen assembly, with thickness (plate separation), being registered by precision position sensors.

Table 5.3. Experimental results for nine specimens each measured with four buffer types. Specimens are numbered in approximate order of increasing surface roughness.

Specimen description, number, & thickness, t (mm)			Results for thermal resistance, R (m^2.K/W) and thickness, t (mm)							
			6.4 mm soft buffer		4.2 mm soft buffer		3.5 mm hard buffer		1.7 mm hard buffer	
Description	No.	t	R	t	R	t	R	t	R	t
PMMA	N/A	6	0.1975	18.99	0.1437	14.41	0.0671	12.78	0.0525	9.26
Phenolic board	1	1.7	0.1721	14.88	0.1175	10.31	0.0417	8.69	0.0275	5.23
EPS	2	11	0.5015	24.30	0.4483	19.89	0.3742	18.29	0.3589	14.77
Building board W	3	9	0.1862	22.02	0.1320	17.53	0.0617	16.03	0.0480	12.55
Building board P	4	12	0.2180	24.99	0.1652	20.54	0.0931	19.03	0.0781	15.55
PMMA	5	25	0.2987	37.82	0.2469	33.42	0.1764	31.92	0.1589	28.32
Rubber-cork	6	3	0.1894	16.16	0.1370	11.73	0.0655	10.22	0.0509	6.76
Building board C	7	9	0.2028	21.89	0.1500	17.50	0.0835	16.16	0.0667	12.66
Prismatic polystyrene	8	2.6	0.1870	15.63	0.1338	11.12	0.0685	9.87	0.0534	6.40

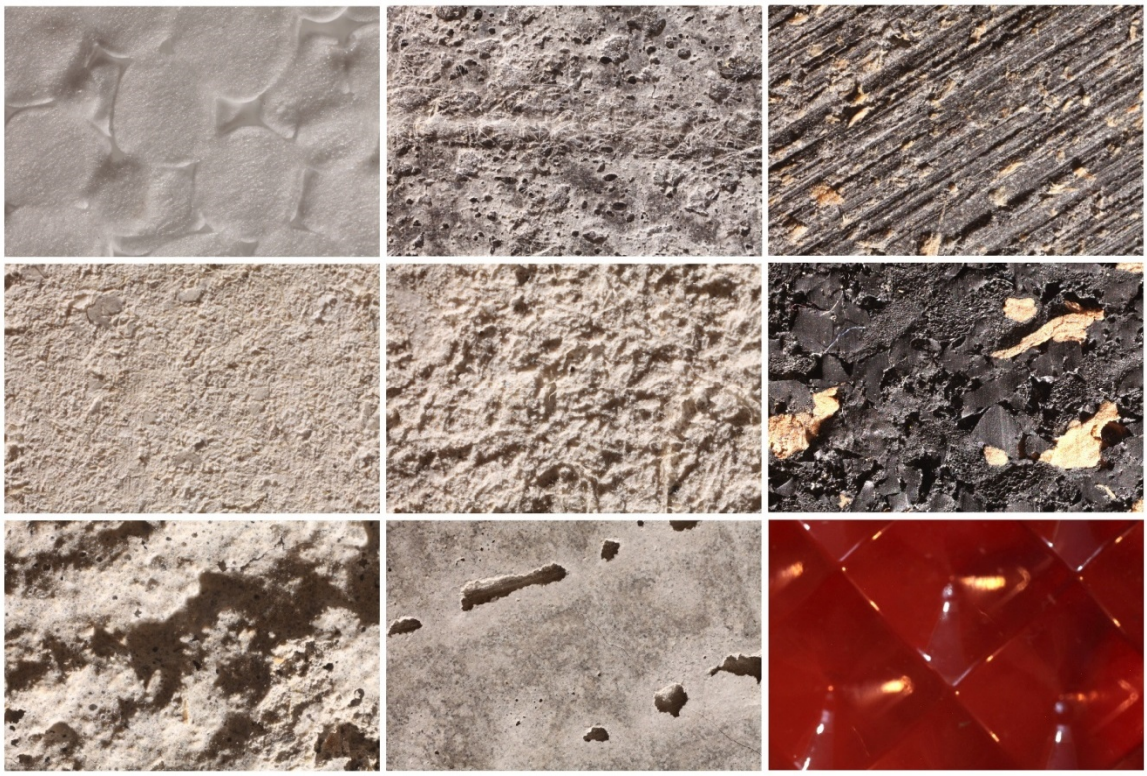

Figure 5.3. Images of the rougher surfaces of the Table 5.3 specimens. From top left to bottom right they are EPS, top and bottom of Building Board W, top and bottom of Building Board P, rubber/cork mat, top and bottom of Building Board C and prismatic polystyrene. Specimen width is 10 mm in all images.

Table 5.3 is not amenable to simple interpretation since both buffers and specimens are different for each measurement. Analysis could proceed via deriving a value for specimen thermal resistance of each specimen by difference calculation, as has been undertaken for Table 5.1. This involves subtraction of the reference measurement (with buffers) from the specimen measurement (also with buffers) then adding back the known thermal resistance of the reference specimen. Direct values for comparison would be derived, but unnecessary complication and measurement uncertainty would be introduced. Considering that the desired outcome is to compare overall results between one buffer and another, the most straightforward analysis is to compare the relativities between measurements. We have previously found that measurements are consistent and largely independent of buffer hardness with thin smooth materials such as the 6 mm PMMA and the 1.7 mm phenolic board (Clarke et al., 2016b). The analysis therefore uses the 6 mm PMMA, measured with the thicker (softest) sponge, as a baseline and compares the difference between readings of this and each rougher material for each other harder buffer type. Consideration of the four cases is illustrated in Figure 5.4. The excess values for thermal resistance, R_x and thickness, t_x are defined as:

$$R_x = (R_d - R_c) - (R_b - R_a) \tag{11}$$

$$t_x = (t_d - t_c) - (t_b - t_a) \tag{12}$$

where R_a and t_a are the total thermal resistance and thickness respectively of the reference smooth specimen measured with the reference soft buffer; R_b and t_b are the total thermal resistance and thickness respectively of the rougher specimen measured with the reference soft buffer; R_c and t_c are the total thermal resistance and thickness respectively of the reference smooth specimen measured with the harder buffer; and R_d and t_d are the total thermal resistance and thickness respectively of the rougher specimen measured with the reference hard buffer.

R_a, t_a, R_c and t_c may be regarded as normalizing parameters and would not be required if the buffers were identical in thickness and thermal resistance when measuring a smooth specimen. The thermal resistance excess expressed in this way is an indicator of the extent to which measurement of a rougher specimen with a harder buffer produces a thermal resistance result that is higher than that produced by a softer buffer. Similarly, the thickness excess indicates the extent to which thickness is measured to be higher with a harder buffer because it undergoes less compression when in contact with the high parts of a rough specimen.

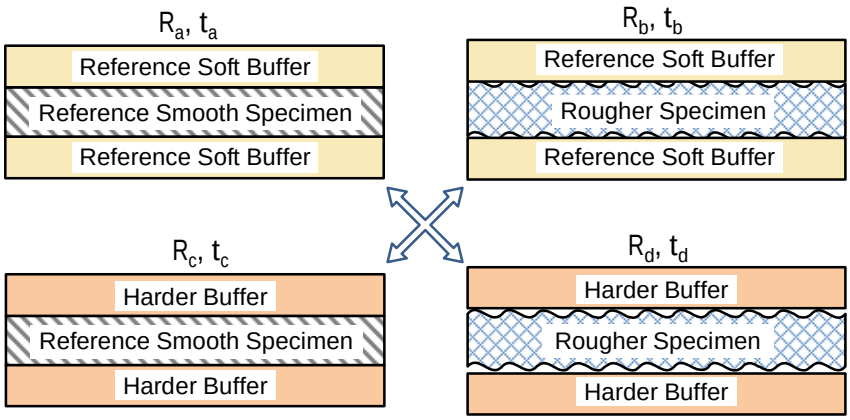

Figure 5.4. The set of four measurement cases used to determine excess values for thermal resistance and thickness for measurement of rougher surfaces with harder buffers.

Since R_x and t_x express thermal resistance and thickness relative to results with the 6.4 mm sponge and the 6 mm PMMA, the analysis reduces to consideration of the relative performance of the other eight specimens and the other three buffers. This data is shown in Figure 5.5-Figure 5.7 where excess thermal resistance and excess thickness are plotted for each of the eight rougher specimen types (identified in Table 5.3) and each of the three harder

buffers. Vertical scales of the three plots are similar to aid inter-comparison. As expected, the excess values are all positive or close to zero. In the case of the 4.2 mm sponge, the thickness excess tends to be 0.1- 0.2 mm and the thermal resistance excess around 0.001 m^2.K/W across all materials, except that both values are close to zero for the only smooth specimen, the phenolic board. Results for the two solid silicone buffers were quite similar to each other across all specimens, showing well-correlated increases in R_x and t_x, in association with increasing roughness. R_x reached 0.011m^2.K/W for the prismatic polystyrene which had one extremely-rough surface. For these surfaces, t_x reached almost 0.5 mm. As was the case with the 4.2 mm buffers, R_x and t_x were close to zero for the phenolic board. The 25mm thick PMMA (Specimen 5) was consistent with earlier indications. Despite appearing smooth, it behaved as though it had a surface of intermediate roughness.

The error bars shown for both R_x and t_x have been derived from an individual uncertainty analysis for each data point, using a coverage factor of 1, and with care to separate systematic and random contributions since subtraction of similar numbers is involved. Results for the two solid silicone buffers are reasonably well correlated, suggesting that random errors are well controlled.

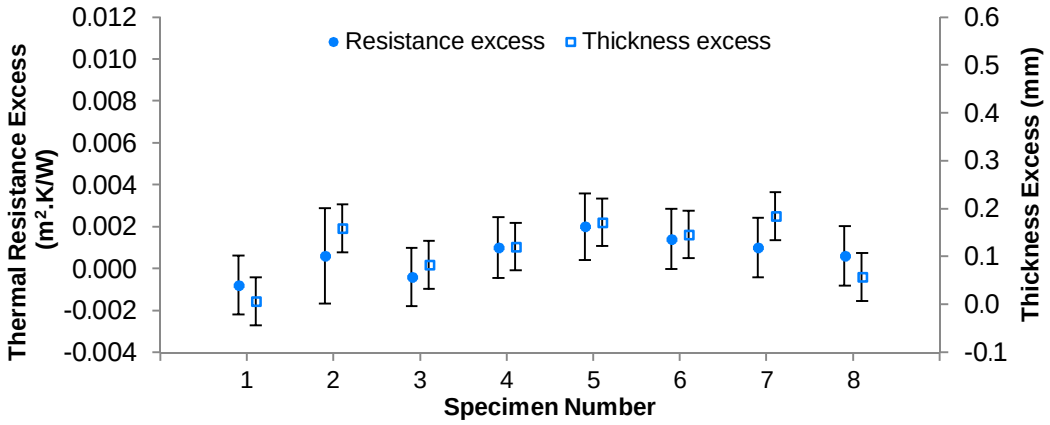

Figure 5.5. Measured thermal resistance excess (R_x) and thickness excess (t_x) for 8 rough-surfaced specimens (as described in Table 5.3) combined with 4.2 mm silicone sponge buffers.

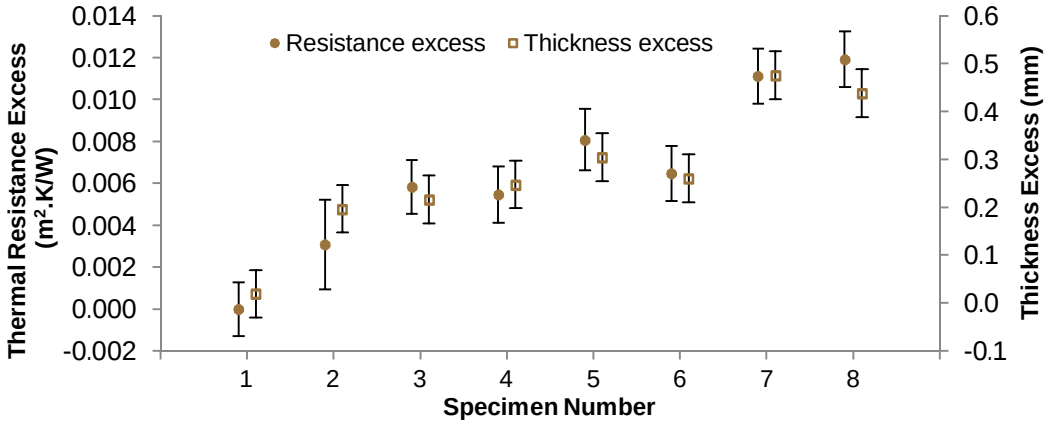

Figure 5.6. Measured thermal resistance excess (R_x) and thickness excess (t_x) for 8 rough-surfaced specimens (as described in Table 5.3) combined with 3.5 mm solid silicone buffers.

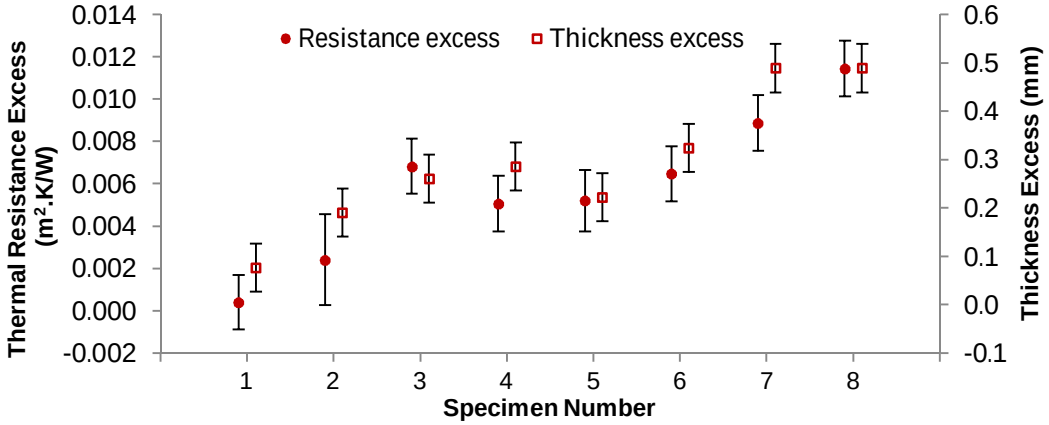

Figure 5.7. Measured thermal resistance excess (R_x) and thickness excess (t_x) for 8 rough-surfaced specimens (as described in Table 5.3) combined with 1.7 mm solid silicone buffers.

5.3.2 Surface Roughness Measurement and Analysis

Surface roughness was measured with an Olympus OLS4100 laser scanning confocal microscope. With associated software, this instrument provides automated measurement of two or three-dimensional (area based) roughness parameters. It is oriented towards fine scales of roughness but was able to provide results for most specimens using the lowest-magnification (5X) objective, which allows for a height amplitude of up to 1.9 mm over a 2.4 mm square field of view. The prismatic sheet was not measurable despite the fact that by physical measurement it had a peak roughness slightly below this limit. The PMMA sheets were not measured since their roughness was negligible relative to all other specimens. The microscope has a stitching facility which was used to provide a larger total working area for rougher specimens. Table 5.4 provides overall results including the working area, which

ranged up to 12 mm square (5 x 5 stitch). Both sides of the building boards were measured since these were visibly different. The other materials were measured on only one side.

Results are given in the table in terms (and units) of standard three-dimensional roughness parameters. In the case of the prismatic sheet, three-dimensional roughness was based on calculation. This was possible since it had a regular geometric pattern of pyramidal hills and valleys, with allowance for the inexact shape and rounded peaks. S_{sk} is a measure of skewness, with all results being zero or negative, suggesting a predominance of valleys rather than hills relative to the mean. The largest skew value was for the bottom of Board C which was relatively smooth but for a percentage of flat-bottomed valleys. This shape, evident in Figure 5.3, is redolent of the binary (two-height) analytical model.

The parameters S_p and S_v are the single maxima of hill height and valley depth readings respectively, relative to the mean. Overall, valleys were more prominent than hills. The values are consistent with the skewness parameter and with the appearance of most surfaces. The next column shows S_a, the most-commonly used three-dimensional index of roughness, defined as the mean absolute height (or depth) away from the average plane. It is much lower than S_p and S_v although to differing degrees depending on the specimen. Certainly it better represents the phenolic sheet which appeared to be reasonably smooth, suggesting that some of the high peaks indicated by S_p and S_v are due to data outliers. The outlier problem with optical roughness measurement is considered by Le Goic et al. (2013), along with filtering methods in the interpretation of S_p and S_v values.

Table 5.4. Summary of confocal microscope surface roughness measurements. Values for the 8th specimen were obtained by calculation.

Sp. No.	Specimen	Working area (mm x mm)	Standard roughness parameters				Combined roughness S_{2a} (µm)	1.7 mm hard buffer t_x (µm)	4.2 mm soft buffer t_x (µm)
			S_{sk}	S_p (µm)	S_v (µm)	S_a (µm)			
1	Phenolic board	4.8 x 4.8	-0.5	177	118	7	14	76	6
2	EPS	12.0 x 12.0	-2.4	309	979	39	78	191	159
3	Board W top	7.2 x 7.2	0.0	215	220	23	58	260	83
	Board W bottom	7.2 x 7.2	-2.5	265	630	36			
4	Board P top	7.2 x 7.2	-0.4	698	357	51	66	286	121
	Board P bottom	7.2 x 7.2	-1.7	279	250	15			
6	Rubber-cork	12.0 x 7.2	-2.6	449	1398	75	151	324	146
7	Board C top	12.0 x 12.0	-0.1	645	791	168	191	489	184
	Board C bottom	12.0 x 12.0	-9.6	323	1154	23			
8	Prismatic sheet	N/A	0.0	900	900	400	400	489	57

Table 5.4 also has a column for a combined value defined as S_{2a}, calculated by adding the S_a values for each pair of specimen interfaces. Values are therefore the sum for the two faces, either individually measured or assumed to be the same. The prismatic material is an exception since its smooth lower surface was assumed to make no contribution to S_{2a}. This term is not directly equivalent to a single value of S_a but as a measure of the overall roughness of a pair of interfaces, it may be compared to experimental results for t_x which also derive from a pair of interfaces. A mostly-consistent ordering of materials is apparent in measurements using hard buffers. EPS was a minor exception, ranking slightly higher in roughness with optical measurement. Its relative softness may have allowed it to flatten somewhat when pressed against a buffer.

The major exception to consistent ordering was the 25 mm PMMA specimen which ranked intermediate in roughness according to thermal measurement but was visibly very smooth. Lack of flatness was investigated as an alternative explanation. Micrometer readings were taken at the perimeter since accurate measurement well inside the edges was not practical. Thickness was found to be far from uniform, as Figure 5.8 shows. Average absolute deviation from the mean was 280 µm. This term is algebraically equivalent to the roughness term S_a, although in this case it is constructed from just 48 measurements, representative of the edges although not necessarily the whole specimen. More exactly it is effectively a total value for both sides of a specimen and so might be compared with the value of S_{2a}. For specimens 4 and 6, which ranked nearby in thermal measurement, the values of S_{2a} were 66 and 151 µm respectively. These are lower but of similar magnitude, considering that the horizontal scales differ by two orders of magnitude. The likely implication is that thickness non-uniformity occurring on a macroscopic scale and roughness occurring on a microscopic scale have similar effects on interface resistance.

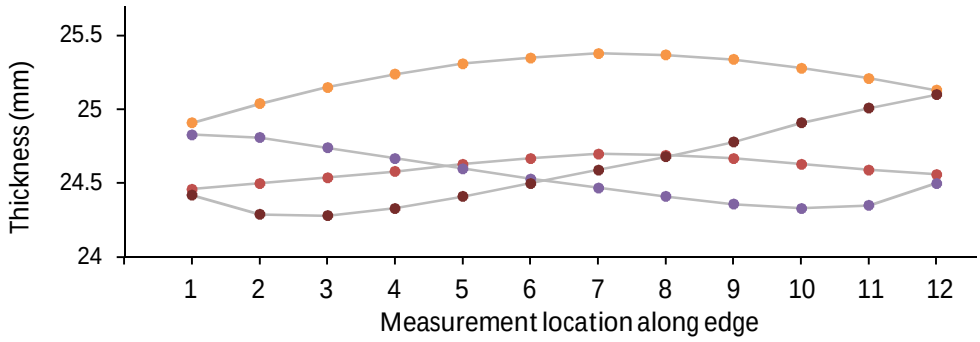

Figure 5.8. Thickness measurements along 4 edges of 25 mm PMMA specimen.

5.4 Modelling Results

5.4.1 Binary Model

Interpretation of the experimental results utilized the excess values, R_x and t_x, which the analytical model may readily calculate. However the model deals with a single interface. For comparison with experimental values of R_x and t_x, two sets of predictions for these terms may be summed for cases where both faces of a specimen are rough and are in contact with a buffer.

Modelling was performed for three valley depths, 0.2, 0.4 and 0.6 mm, these choices being physically consistent with the roughness qualities of the specimens and producing similar results, as given in Figure 5.9 and Figure 5.10. The area ratio of "valleys", Z_a, was varied between 0.05 (mostly hills) and 0.999 (almost entirely valleys). Buffer properties (thermal conductivity and compressibility) are as given in Table 5.2 whilst a single specimen thermal conductivity of 0.25 W/m.K and thickness of 10 mm have been assumed. Calculation of t_x and R_x was found to be relatively insensitive to these parameters. Even with EPS having a much lower thermal conductivity, variations were large as a percentage only for smaller values of Z_a, where t_x and R_x are also small. Specimen and buffer facing surfaces were assumed to have an emittance of 0.9.

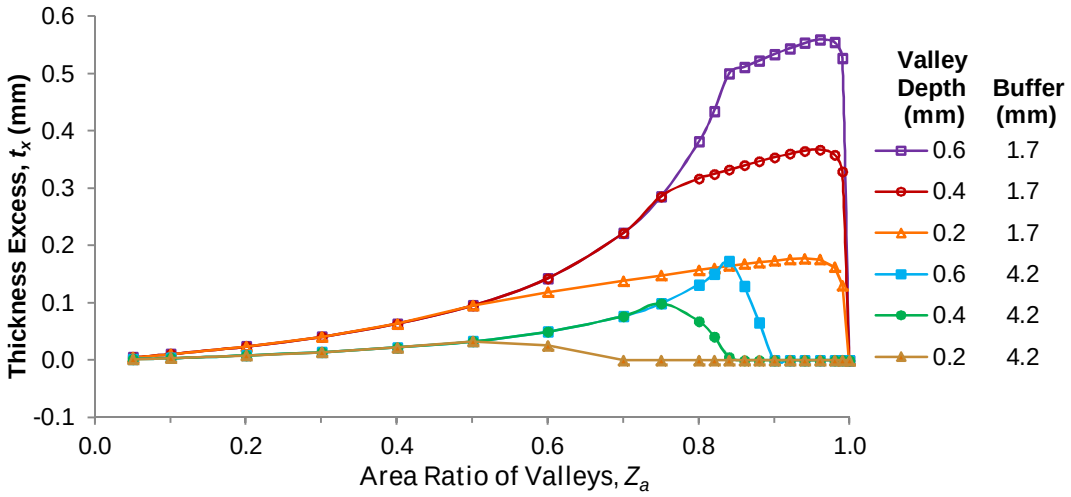

Figure 5.9. Thickness excess predicted by the analytical model for two buffer types and three roughness levels (as indicated by valley depth).

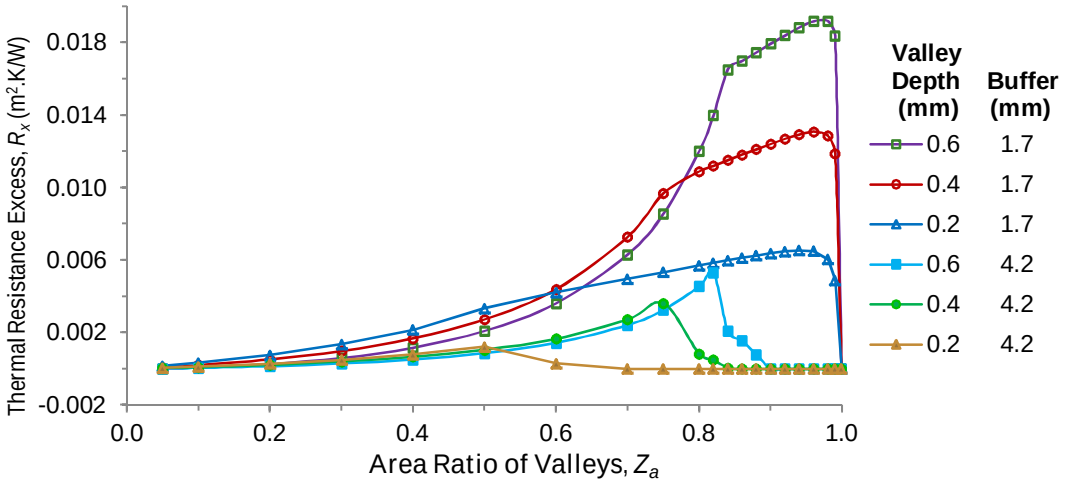

Figure 5.10. Thermal resistance excess predicted by the analytical model for two buffer types and three roughness levels (as indicated by valley depth).

R_x and t_x both increase with increasing Z_a. The curves are of similar shape since both terms are similarly affected by the interaction of surface roughness with the buffers. As Z_a increases, harder buffers are more able to be supported on the remaining hill areas, sitting relatively higher so that increased thickness and increased thermal resistance (due to the retained airspace) are both maintained. Depending on the buffer and the valley depth, a point is reached where the buffer is so compressed at the hills that it touches the valley floor. At this point both R_x and t_x fall to zero since neither buffer sits above the valley floor where it would contribute to higher thermal resistance or thickness. This point is reached at a Z_a value of 0.5 for the 4.2 mm soft buffer and 0.2 mm valley depth but not until about 0.95 for the harder buffer at any valley depth.

The plots show R_x and t_x as always positive. R_x may in fact be slightly negative for deeper valleys at lower area ratios (essentially a flat surface with few valleys) but R_x and t_x both remain small at lower area ratios. Intermediate data reveal that conductance is significantly lower through those heat flow paths that include the airspaces but the effect is similar for all buffer types so that there is little difference between the calculated values of R_x.

According to the model, the depth of valleys affects thermal resistance for the same buffer because of the differing airspace contributions but it does not affect thickness as long as the buffer has expanded freely into the valley regions without touching the bottom. This is apparent in the way the t_x curves for each valley depth lie directly on top of each other up to a certain area ratio. This is the point where the more shallow valleys become filled, so that results diverge from those of the deeper valleys and occurs at an area ratio of 0.75 in the 0.4

mm valley case. By this point both R_x and t_x have become significant, R_x reaching 0.010 m^2.K/W for the 1.7 mm buffer at 0.4 mm valley size and t_x reaching almost 0.3 mm These combinations of R_x and t_x are reasonably similar to those measured experimentally for the roughest specimens. Considering all buffers and all valley depths, it is possible to find simultaneous agreement with the combinations of R_x and t_x given in Figure 5.3 for all test materials within a range of Z_a broadly spanning 0.2 to 0.8.

The model may also provide values for the overall thermal resistance of a specimen in combination with a single rough interface. Figure 5.11 shows this for the same nominal specimen, 10 mm thick with a thermal conductivity of 0.25 W/m.K, which would therefore have a thermal resistance of 0.04 m^2.K/W assuming a smooth surface. Thermal resistance values are given for the same three roughness levels (valley depths) over a range of area ratios. Unlike Figure 5.9 and Figure 5.10, results are not relative to those with the softest 6.4 mm buffer, so that the figure includes results for this buffer as well as the thinner (4.2 mm) soft buffer and the 1.7 mm hard buffer.

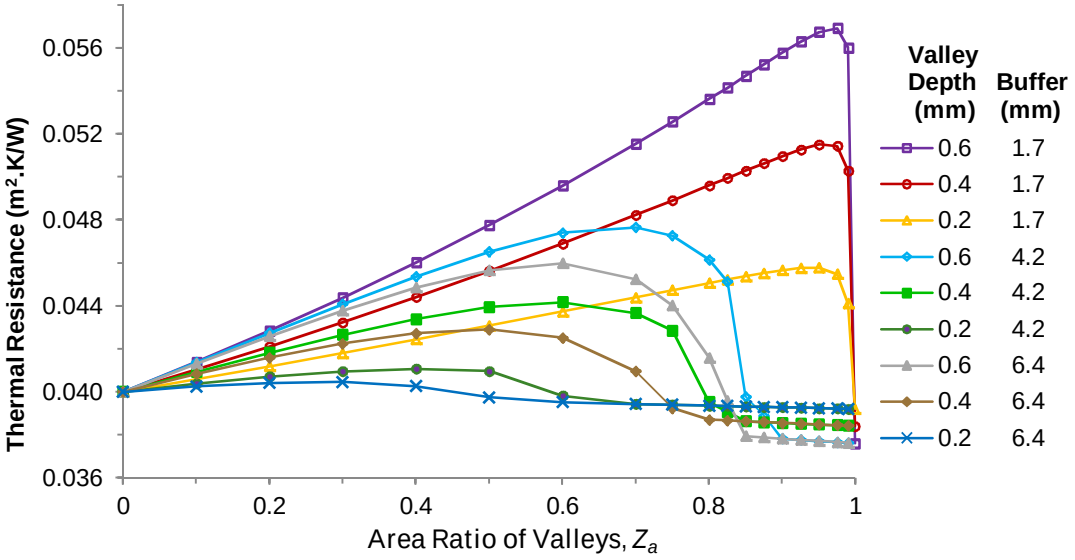

Figure 5.11. Thermal resistance for a specimen with a single adjacent interface as predicted by the analytical model for three roughness levels (as indicated by valley depth) and three buffer types.

Overall, the figure shows that thermal resistance is lower when softer buffers are used relative to hard, especially at higher area ratios. For each valley depth, thermal resistance reaches a maximum at some area ratio then falls away as the airspace begins to disappear and the space is filled with buffer material. In the case of the harder buffers, the increase in

thermal resistance is preserved for much higher area ratios and falls only when close to an area ratio of 1.0 in a similar fashion to R_x. Modelling was also performed for the case of direct measurement (with no buffer). The resultant curves (not shown) are very similar to those for the hard buffer, lying very slightly below at each valley depth except that they continue straight to the vertical axis as the area ratio approaches 1.0, rather than rolling over. This is because the hill areas are presumed to be capable of supporting the plate closing force, even when their area fraction approaches zero. Indicated thermal resistances for direct contact with 0.2 mm and 0.6 mm valleys were 0.047 and 0.058 m^2.K/W respectively at 0.999 area ratio.

The figure shows thermal resistance falling below the nominal value for the specimen at high area ratios. This is due to the method of specifying thickness which, in line with most methods of physical measurement, includes the roughness component of the specimen. The core is therefore thinner than the nominal thickness (10 mm in this case).

5.4.2 Generalized Roughness Model

The generalized roughness model was used derive estimates of R_x from the measured roughness parameters for comparison with measured values of R_x. Table 5.5 shows results for all ten surfaces studied. Buffer sitting level is also listed since it provides an insight into the contact geometry. In the case of the 4.2 mm soft buffer, this value was -1 for several of the less rough materials, meaning that for these materials the buffer was sufficiently compliant to absorb all roughness and provide complete contact with the specimen surface. Calculated R_x values were all very low as were the measured values. The 1.7 mm hard buffer behaved very differently. It rested high up on most materials, with a sitting level exceeding 0.9 for several. This suggests a very low degree of contact, little more than touching the tips of a sinusoidal roughness profile. Agreement between measured and predicted values was reasonably good with an R-squared value of 0.79. Several alternative functions for the roughness profile were examined, including the expression based on $(\text{sine}+1)^2$ shown in Figure 5.2. Relative to the sinusoid, it is characterized by sharper peaks and broader valleys and provided values of R_x that were about 15% lower. Either profile could be more representative of certain specimens.

Table 5.5. Calculated excess thermal resistance (R_x) for roughness measurements of individual surfaces, compared with measured total values combining the top and bottom interfaces of eight specimens. Table also gives buffer sitting level for various sinusoidal valley area fractions.

Sp. no.	Specimen	S_a (μm)	1.7 mm hard buffer				4.2 mm soft buffer			
			Calculated			Meas. R_x (m^2.K/W)	Calculated			Meas. R_x (m^2.K/W)
			Buffer sitting level	One side R_x (m^2.K/W)	Comb. R_x (m^2.K/W)		Buffer sitting level	One side R_x (m^2.K/W)	Comb. R_x (m^2.K/W)	
1	Phenolic	7	0.66	0.0001	0.0002	0.0004	-1	0	0	-0.0008
2	EPS	39	0.89	0.0011	0.0022	0.0024	-1	0	0	0.0006
3	W top	23	0.84	0.0011	0.0029	0.0068	-1	0	0	-0.0004
	W bottom	36	0.88	0.0018			-1	0		
4	P top	51	0.91	0.0027	0.0031	0.0051	-0.75	0	0	0.0010
	P bottom	15	0.80	0.0004			-1	0		
6	Rubber -cork	75	0.93	0.0040	0.0080	0.0065	-0.4	0.0005	0.0010	0.0014
7	C top	168	0.96	0.0066	0.0076	0.0089	0.12	0.0012	0.0012	0.0010
	C bottom	23	0.84	0.0010			-1	0		
8	Prismatic	400	0.98	0.0096	0.0096	0.0114	0.52	0.0017	0.0017	0.0006

Buffer sitting level	1.00	0.95	0.90	0.80	0.50	0.00	-0.50	-0.80	-0.90	-0.95	1.00
Valley area fraction, Z_a	1.00	0.89	0.85	0.79	0.67	0.50	0.33	0.20	0.15	0.10	0.00

The R_x term is useful mostly because it is directly measurable. It has enabled verification that the generalized procedure can successfully express typical roughness profiles in terms of Z_a and V. However R_x is limited in its ability to predict the extent of interface effects since it provides a value relative to the reference buffer case, which may itself suffer from interface effects. As already noted, the thermal resistance of a single interface is not directly measurable but the overall success of the model with R_x values suggests that it may also be applied in the single-interface case. This is effectively a re-expression of Figure 5.11, where Z_a and V have been intermediate values calculated by the generalized procedure. Again considering a sinusoid, Figure 5.12 presents results of these calculations for the same specimen with a nominal thermal resistance of 0.04 m^2.K/W. It shows that all buffers produce an interface resistance that is proportional to roughness above an onset value, below which it is essentially zero. For the 6.4 mm soft buffer, interface resistance was evident for S_a greater than 60 μm and reached 0.007 m^2.K/W at 300 μm. The 4.2 mm buffer was able to accommodate only 40 μm of roughness before interface resistance was introduced whilst the 1.7 mm hard buffer had no onset margin, with interface resistance commencing from zero roughness. For this buffer it reached 0.014 m^2.K/W for a roughness of 300 μm. The initial

downward trend in thermal resistance for soft buffers arises, as in Figure 5.11, because the thickness of the core reduces as surface roughness increases for the same overall specimen thickness.

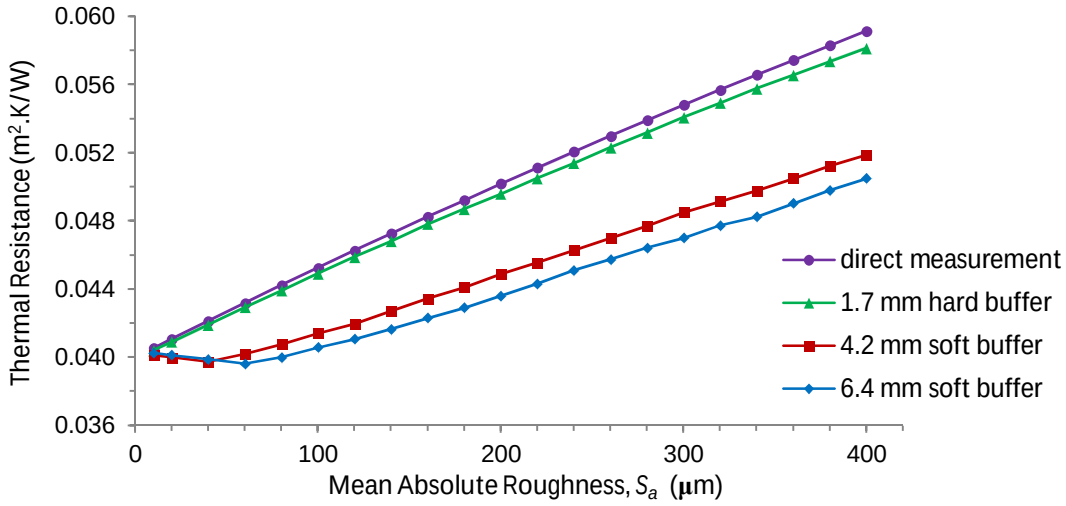

Figure 5.12. Thermal resistance for a specimen with a sinusoidal roughness profile and a single adjacent interface as predicted by the analytical model for direct measurement and with three buffer types.

5.5 Discussion

Lack of flatness appears very similar to roughness in its effect on thermal properties. The relationships between t_x and R_x evident from Table 5.3 are very similar for all materials and all buffer types. In particular, there was no indication that the 25 mm PMMA would have roughness of different character. It appears that the horizontal scale of height irregularities is relatively unimportant, which should not be unexpected since it is not even a relevant parameter in the analytical model, derived on theoretical grounds. It was opportune that the 25 mm PMMA specimen was very smooth, allowing roughness to be solely associated with large-scale non-flatness on this occasion. A combination of both short and long range non-uniformity might have obscured this indication and might partly explain the imperfect correlations between some results.

It appears that where roughness measurement is possible it might be of assistance in predicting the potential scale of interface error due to fine-scale roughness. In contrast, the value of t_x, measured as the excess thickness between different buffers, seems to be a useful predictor of the way thermal resistance measurement results will be affected by roughness or

lack of flatness at all scales, even up to the horizontal dimension of the whole specimen. Determining t_x requires measurement of the settled height of four separate buffer-specimen arrangements (equation(12)) but is straightforward in the heat flow meter apparatus. A low value of t_x would give confidence that interface resistance should not greatly affect thermal resistance measurement.

The interface resistance that contributes to a measurement result might be attributed to the test specimen, so that higher performance might be claimed. However it is not an intrinsic property as it depends also upon the characteristics of the contacting surface. In a building application, adjacent surfaces could range from hard concrete to wet render. The latter would substantially fill the voids of even a very rough board, resulting in an interface resistance of effectively zero. Specimen thermal resistance is therefore an ambiguous property unless the facing surfaces are specified. The same applies with thickness. It is effectively specified by the low points in a situation involving contact with soft materials or render whilst for direct measurement between hard apparatus plates, it is the higher contact points that determine the apparent thickness.

Rigid specimens may warp under the imposed temperature gradient during thermal testing. This is difficult to observe or measure within the apparatus and is more evident upon removal whilst one side is hot and the other cold. Hard buffers would more-strongly resist warping but be more likely to leave voids when they did warp. The evidence seems to suggest that these are not issues. For the strongly-warping 25 mm PMMA, the relative values of t_x and R_x were closely aligned with those of other specimens for all 3 buffer types, as evident from Figure 5.5-Figure 5.7. Since t_x is a parameter determined before measurement when the apparatus plate spacings are set, it can be inferred that subsequent thermal expansion has not affected the measured R_x values.

Figure 5.12 shows interface resistance approaching zero as roughness becomes negligible, for any buffer or even for direct measurement. This is a consequence of the airspace thickness approaching zero. With flat materials such as phenolic board (with a measured S_a value of only 8 μm) an extremely small interface resistance would therefore be expected with direct measurement. Our earlier study (Clarke et al.,2016b) has shown that this is not the case. The direct-measurement thermal resistance was higher by more than 0.01 m^2.K/W, compared with that measured using any buffer type. An explanation may lie in thickness non-uniformities in the plates of our particular apparatus. ASTM C 518 prescribes flatness tolerances for apparatus plates and rigid specimens, both as 0.02% of the plate dimension, equivalent to 0.12 mm for a 600 mm apparatus. Preliminary investigation has suggested that

the apparatus might not achieve this flatness everywhere. An airspace of this thickness has a thermal resistance of 0.005 m^2.K/W. Since both plates are involved, a compliant apparatus might still allow up to 0.01 m^2.K/W in airspace resistance, which is of the order of the observed values. The apparent inconsistency between the studies is a consequence of a different approach to definition. The earlier study provides experimental values for interface resistance, considered as the difference between direct and difference measurements (with buffers) and makes the case for using buffers. Our measurements suggested an interface resistance defined in this way as ranging from 0.010 m^2.K/W total (both plates), up to 0.016 m^2.K/W for the rougher or more uneven materials. Slightly lower difference values (up to 0.013 m^2.K/W) were calculated where harder buffers were used. This suggested that some interface resistance remained with harder buffers, highlighting a limitation in this approach to defining interface resistance. The present study presumes that buffers are always used to achieve minimal thermal resistance between plate and buffer, so that the interface between buffer and specimen can be considered in isolation in terms of the significance of buffer hardness and specimen roughness. Interface resistance is then defined relative to the case of a smooth specimen against a soft buffer, which inherently has minimal interface resistance.

Achieving flatness of the required order is difficult enough with apparatus plates but is impractical for many potential specimens (Rennex, 1985). Surface machining is sometimes an option but is often impossible, especially for a skinned or faced product. Corsan and Williams (1980) concluded that the softest possible buffers should be used in the measurement of hard specimens in order to minimize the effects of wide-area thickness non-uniformities. Our results suggest the same approach to deal with the small-scale uniformities that characterize surface roughness. Whilst they were concerned with direct measurement and surface temperature sensors, we have found the same principles to apply with indirect measurement using buffers.

Many approximations have been made in the foregoing analysis. Physical parameters such as the compressibility of buffer materials are difficult to measure exactly, and may vary spatially, with temperature and with loading. Resistance calculation relies on the parallel-paths method, which is inexact. The procedure of converting roughness into the binary analytical model parameters involves assuming a certain roughness profile (such as a sinusoid) and that contact and void areas may both be approximated as flat planes of contact. The view factors for radiation are significantly different for such non-planar geometry, although heat transfer for thin airspaces is dominated by conduction.

5.6 Conclusions

The technique of using buffer materials and difference measurement for thermal resistance measurement below the nominal apparatus minimum of 0.1 m^2.K/W has been generally effective in minimizing errors due to interface resistance. However it provides results that are dependent upon the hardness of the buffers when specimen surfaces are very rough or lacking in flatness.

Although harder buffers (typically 1.7 mm solid silicone sheet) may offer some advantages over softer buffers (typically 6.4 mm silicone sponge), they produce thermal resistance results with rough surfaced specimens, such as some building boards, that are higher by as much as 0.01 m^2.K/W. With hard buffers, the apparent thickness of the measurement assembly is also higher by as much as 0.5 mm and is well correlated with the thermal resistance increase. These excess values may be reliably measured and have been given the terms R_x and t_x.

An analytical model that considers roughness in a simplified binary way as a varying fraction of flat hills and flat valleys (forming airspaces) has been very effective in predicting values of R_x and t_x that are consistent with measurements, particularly in the way these values are correlated.

Confocal microscopy has provided roughness rankings that are in general accordance with measured values of t_x for a range of specimens. In quantifying roughness, microscope results have also facilitated an interpretation of roughness in terms of the sitting height of a buffer material against a rough surface, producing areas of contact and areas of void. This has in turn allowed for generalized roughness, considered as a sinusoid, to be interpreted in terms of the binary analytical model. Estimates for R_x derived in this way from optical roughness measurements have agreed well with measured values.

Applied to an individual measurement, the model predicts that soft buffers may allow contact with the test specimen to be substantially free of interface resistance up to a certain level of roughness, in our case an S_a value of 60 μm. Beyond this threshold, interface resistance will increase in direct proportion to roughness. Hard buffers exhibit the same proportionality but the onset threshold is at virtually zero roughness and interface resistance may exceed 0.010 m^2.K/W for an S_a value of 200 μm. The measurement uncertainty that this introduces will be largely determined by the overall thermal resistance of the test specimen and might generally be neglected only for specimens exceeding about 1 m^2.K/W.

Microscopic roughness measurement cannot identify large-area flatness imperfections and yet these appear to also contribute to higher R_x values. On the other hand t_x is well

correlated with R_x at all roughness scales, making it a useful predictor of potential roughness errors, especially since it can be easily measured. Recognizing this, laboratories might instigate a stepwise plan, including measurement of t_x as a prelude to thermal measurement.

Rough surfaces potentially confer additional thermal resistance on a material. Its value however depends upon the characteristics of the contacting surfaces, chiefly their compressibility. Measurement results would therefore be more consistent and useful if the characteristics of abutting surfaces were defined. Harder facing surfaces provide higher resistance results and may represent certain applications. However, measurements using the softest practical buffer as an interfacial material provide results that better represent the bulk properties of the specimen.

5.7 References

ASTM. (2011) ASTM E1530 - 11. "Test Method for Evaluating the Resistance to Thermal Transmission of Materials by the Guarded Heat Flow Meter Technique.". *Annual Book of ASTM Standards, Vol. 14.02*. ASTM International, DOI: 10.1520/E1530-06

ASTM. (2013a) ASTM C177 - 13. "Test Method for Steady-State Heat Flux Measurements and Thermal Transmission Properties by Means of the Guarded-Hot-Plate Apparatus.". *Annual Book of ASTM Standards, Vol. 04.06*. ASTM International, DOI: 10.1520/C0177

ASTM. (2015) ASTM C518 - 15. "Test Method for Steady-State Thermal Transmission Properties by Means of the Heat Flow Meter Apparatus.". *Annual Book of ASTM Standards, Vol. 04.06*. ASTM International, DOI: 10.1520/C0518-15

Bobeth M and Diener G. (1982) Upper bounds for the effective thermal contact resistance between bodies with rough surfaces. *International Journal of Heat and Mass Transfer* 25: 1231-1238. DOI: 10.1016/0017-9310(82)90217-4

Brzezinski A and Tleoubaev A. (2002) Effects of Interface Resistance on Measurements of Thermal Conductivity of Composites and Polymers *Proceedings of the 30th Annual Conference on Thermal Analysis and Applications (NATAS)*. Pittsburgh: B&K Publishing

Clarke RE, Rosengarten G and Shabani B. (2014) Flexible Buffer Materials to Reduce Contact Resistance in Thermal Insulation Measurements *Thermal Conductivity 32 / Thermal Expansion 20, Proceedings of the 32th International Thermal Conductivity Conference and 20th International Thermal Expansion Symposium*. West Lafayette, Indiana: Purdue University Scholarly Publishing Services, DOI: 10.5703/1288284315544

Clarke RE, Shabani B and Rosengarten G. (2016b) A difference technique to avoid interface errors in measurement of high-conductance thermal insulation. *Journal of Building Physics* Prepublished May 23 2016, DOI: 10.1177/1744259116637863

Corsan JM and Williams I. (1980) Errors associated with imperfect surfaces in standard hot-plate thermal conductivity measurements. In: Metrology NPLDoQ (ed) *NPL Report QU57*. National Physical Laboratory, Teddington, Middlesex, TW11 OLW, UK.

Hall JA, Ceckler WH and Thompson EV. (1987) Thermal properties of rigid polymers. I. Measurement of thermal conductivity and questions concerning contact resistance. *Journal of Applied Polymer Science* 33: 2029-2039. DOI: 10.1002/app.1987.070330615

ISO. (2007) ISO 6946:2007 Building components and building elements - Thermal resistance and thermal transmittance - Calculation method. *ISO 6946*. Geneva, Switzerland: International Organization for Standardization

Jackson RL, Bhavnani SH and Ferguson TP. (2008) A Multiscale Model of Thermal Contact Resistance Between Rough Surfaces. *Journal of Heat Transfer* 130: 081301-081301. DOI: 10.1115/1.2927403

Le Goic G, Brown CA, Favreliere H, et al. (2013) Outlier filtering: a new method for improving the quality of surface measurements. *Measurement Science and Technology* 24: 015001. DOI: 10.1088/0957-0233/24/1/015001

Narumanchi S, Mihalic M, Kelly K, et al. (2008) Thermal interface materials for power electronics applications *11th Intersociety Conference onThermal and Thermomechanical Phenomena in Electronic Systems, 2008. ITHERM 2008*. Orlando, Florida, DOI: 10.1109/ITHERM.2008.4544297

Rennex B. (1985) Summary of Error Analysis for the National Bureau of Standards 1016-mm Guarded Hot Plate and Considerations Regarding Systematic Error for the Heat Flow Meter Apparatus *ASTM STP879 Guarded Hot Plate and Heat Flow Meter Methodology*. ASTM International, DOI: 10.1520/stp32900s

Robinson HE and Powlitch FJ. (1954) The thermal insulating value of airspaces. Housing research paper no. 32. Washington, DC: US Government Printing Office.

Salmon DR and Tye RP. (2009) An Inter-Comparison of Two Methods for Measuring the Thermal Conductivity of Low-Density Masonry Materials *Thermal Conductivity 30: Thermal Expansion 18*. Pittsburgh, Pennsylvania, USA: DESTech Publications, Inc

Salmon DR and Tye RP. (2011) An inter-comparison of a steady-state and transient methods for measuring the thermal conductivity of thin specimens of masonry materials. *Journal of Building Physics* 34: 247-261. DOI: 10.1177/1744259109360060

Stacey C, Parfitt MJ, Simpkin AJ, et al. (2014) Design of a Guarded Hot Plate for Measuring Thin Specimens of Polymer and Composite Materials *Thermal Conductivity 32 / Thermal Expansion 20, Proceedings of the 32th International Thermal Conductivity Conference and 20th International Thermal Expansion Symposium*. West Lafayette, Indiana, DOI: 10.5703/1288284315551

Tleoubaev A and Brzezinski A. (2007) Errors of the Heat Flow Meter Method Caused by Thermal Contact Resistance *Thermal Conductivity 29 / Thermal Expansion 17, Proceedings of the 29th International Thermal Conductivity Conference and 17th International Thermal Expansion Symposium*. Birmingham, Alabama: DEStech Publications

Trethowen HA. (2000) Validating the isothermal planes method for R-value predictions. Porirua [N.Z.]: Building Research Association of New Zealand.

6 THERMAL ANALYSIS OF A NON-HOMOGENEOUS INSULATING PANEL

Journal Paper:

Clarke RE, Shabani B and Rosengarten G. (2017) Thermal Analysis of a Non-Homogeneous Insulating Panel.

Submitted to Journal of Building Physics, 6 January 2017

Current status: Accepted, Review Pending (7 January 2017)

Additional Information for Chapter 6

The following pages of this chapter present, in the formatting style of this dissertation, a paper submitted for publication in the Journal of Building Physics. The journal editor has indicated acceptance of the paper for publication, although review is currently pending.

For inclusion in this dissertation, section numberings have been amended to incorporate the chapter number.

Figures 6.6 and 6.7 have been stretched horizontally to improve visibility in this dissertation relative to the half-page width of these figures as submitted to the journal.

A harmonized reference style based on Sage Harvard has been used in the presentation of this paper, as throughout this dissertation. Sage Harvard is also used by the Journal of Building Physics although small differences in the implementation are expected. DOI numbers have been included where available.

THERMAL ANALYSIS OF A NON-HOMOGENEOUS INSULATING PANEL

Robin E Clarke[1,2], Bahman Shabani[3] and Gary Rosengarten[1]

[1]School of Engineering, RMIT University, Melbourne, VIC, Australia

[2]CSIRO Australia, Clayton, VIC, Australia

[3]School of Engineering, RMIT University, Bundoora, VIC, Australia

Corresponding author:

Robin E Clarke, CSIRO Australia, Private Bag 10, Clayton South, VIC 3169, Australia.

Email: Robin.Clarke@csiro.au

Keywords

Non-homogeneous insulating panel; Heat flow meter apparatus; Thermal modelling; Thermal insulation measurement

Abstract

This paper describes heat flow meter measurements and transient thermal modelling (using ANSYS) of a webbed, hollow-cored panel located between silicone sponge buffer materials chosen to provide boundary conditions comparable to standard surface coefficients. Panel surface temperatures were also measured at eight locations to record the thermal measurement as a temperature step function following isothermal stabilization. An uninsulated configuration was studied as well as cases with different levels of bulk insulation filling the panel cores. Measured and modelled temperature-time plots agreed well after corrections for web and airspace thermal conductivity. Modelled spatial variation in heat flow exceeded 200% for one insulated case but was only about 2% for the uninsulated panel. Modelled values for heat flux and overall thermal resistance agreed well with standard analytical calculations. However heat flows indicated by the apparatus were consistently higher than the modelled and calculated values by up to 8%, expected to be due at least partially to specimen non-homogeneity. Nevertheless results suggest a useful role for the apparatus in providing temperature measurement under controlled conditions, helping to validate thermal modelling as a potential alternative to hot box measurement for non-homogeneous assemblies.

6.1 Introduction

6.1.1 Measurement of Non-Homogeneous Specimens

Accurate thermal measurement of a non-standard specimen may provide challenges for a thermal testing laboratory. A preliminary challenge may lie in deciding whether or not a measurement is even practical. For products with an emphasis on structural, weatherproofing or fire performance, other properties that might be desirable to facilitate thermal measurement, such as flatness or compositional uniformity, might be of secondary design interest.

The most common methods for measurement of thermally-insulating materials are the guarded hot plate and the heat flow meter methods, represented by the standards ASTM C 177 (2013a) and ASTM C 518 (2015) respectively. However it is only the hot box methods described in ASTM C 1363 (2011) that accommodate specimens with significant non-homogeneity. The reason for this distinction relates to the fact that hot box methods have provision to measure the air temperature on either side of a large specimen, allowing a value of total (overall) thermal resistance, including surface heat transfer coefficients, to be determined. ASTM C 1363 allows for a variety of airflow regimes depending upon the intended application of the panel under test. Temperature probes (usually thermocouples) may be located within a baffle spaced away from the surface. The intent is that the air temperature measurements will provide an inherent spatial averaging. However, depending on air velocity, boundary layer development and other factors, temperature sensors may tend to provide an averaging that is weighted towards the upstream rather than the adjacent heat flow. Non-uniform heat flows will also result in non-uniform temperatures, making it much harder to measure temperature distribution with sufficient spatial precision to be confident that the average heat flow through the other five surfaces of the metering box is zero (Kosny and Childs, 2002). Such temperature differences are a primary source of systematic error.

In contrast, the guarded hot plate and heat flow meter methods operate with the test specimen in direct contact with isothermal plates. This configuration requires a uniform specimen. In the case of a guarded hot plate method, the arrangement of heating wires and cooling coils is aimed at providing isothermal conditions when there is a uniform heat flow distribution from plate to plate through the test specimens. As is noted in the standard, deviations from this ideal situation may be caused by specimen inhomogeneity. Constructions with very high lateral thermal conductivity (using metal-faced plates) may minimize the temperature non-uniformity that such specimens might cause. At the same time,

high lateral conductance means that there may be high lateral heat flows, and consequent errors, even with low spatial temperature variation. In a way analogous to the hot box, hot plate temperature non-uniformities make it harder to measure the temperature difference across the gap between metering and guard areas with sufficient precision to be confident that the mean value is zero (as required to avoid systematic error).

The heat flow meter apparatus has a different mode of operation, relying instead on the output of one or more calibrated heat flux transducers (HFTs), generally located within the central "metering" area of a pair of plates. Uniform location of thermopile elements within the transducer is not strictly required for measurement of a uniform specimen. Rather, there might be a variety of arrangements of small thermopile elements dispersed through the length and width to provide a representative signal, chosen for design and manufacturing reasons (Miyake and Eguchi, 1985). Therefore if heat flow is non-uniform, not only might the plates no longer be isothermal but in addition the HFT output might not represent a true average value, depending on the exact location of these sensing elements (Bomberg and Solvason, 1983).

There is very little discussion in the literature on the performance of HFTs under conditions of non-uniform heat flow. The standard presumption is that the devices are intended only for uniform heat flow although at the same time it is accepted that many thermal insulation materials have some inherent variability (De Ponte, 1985). The use of larger apparatus with larger HFTs is partly to achieve higher sensitivity and allow thicker specimens but it is also favoured because of the expectation that a larger HFT will "average" the readings over a larger area (Tye et al., 1987; Bomberg, 1994).

De Ponte and Maccato (1980) and Trethowen (1986) also note that certain thermopile designs are sensitive to lateral temperature gradients, adding an extra dimension to the potential errors arising from heat flow being non-uniform in the direction of interest. Graves and Yarbrough (1993) describe the use of an array of smaller HFTs in order to characterize inhomogeneous materials, such as those affected by aging which tends to be more significant closer to the edges. However each HFT is assumed to occupy a zone in which heat flow is at least approximately uniform.

6.1.2 Indications from a Webbed Panel

We undertook thermal measurements on a novel building panel attempting to combine strength, low cost, and ease of construction. The design was based on a pair of fibre-reinforced magnesium oxide (MgO) boards spaced 150 mm apart and joined by webs of

similar material at 124 mm spacing, leaving hollow cores. A heat flow meter apparatus was available to us. We proceeded on an exploratory basis, recognizing that as a non-uniform specimen, it would lie outside the normal scope of the heat flow meter method. However the regular 124 mm web spacing was of smaller dimension than the 254 mm square heat flux transducers, suggesting that non-uniformity might not be severe, especially since the webs and the open cores were not greatly different in estimated thermal resistance. It was also apparent that the simple repeating geometry of the panel (Figure 6.1) afforded the prospect of re-measurement after moving it laterally some set fraction of the web spacing. This could be expected to produce a varying HFT output if it was sensitive to spatial variation in heat flow. A set of three such measurements was performed, moving the panel one quarter of the web spacing (31 mm) between each. There was no apparent non-uniformity effect. The results were almost identical. An analysis of the panel aimed at explaining these results was initiated since they had implications for understanding the limitations of the heat flow meter method.

6.1.3 Specifying the Properties of a Partitioned Airspace

In a thermal analysis of the panel, the airspace cavities are the largest overall source of uncertainty. Determination through numerical methods is complex and it is usual to refer to tabulations and correlations in industry handbooks. These provide effective thermal resistance values for larger (un-partitioned) building airspaces and are most-commonly derived from the hot box measurements made by Robinson and Powlitch (1954). Tabulated values are available for single airspaces up to about 100 mm thick with certain configurations of orientation, temperature difference, surface emittance and thickness. Non-reflective materials are typically assumed to have an emittance of 0.9. For a horizontal airspace with heat flow upwards and typical temperature conditions, such an airspace is rated to have a thermal resistance of about 0.150 m^2.K/W. Yarbrough (1983) developed polynomial fits for this data with emphasis on a computation procedure that was efficient for multi-layered reflective insulation products (although it demonstrated that these products generally underperformed relative to predictions). Han et al. (1986) used two-dimensional finite difference modelling, which provided mixed agreement with experimental values and prediction for multiple airspaces that was no better. Desjarlais and Yarbrough (1991) developed an alternative data-fitting procedure which allowed some extrapolation of the Robinson & Powlitch data for greater thickness. They benchmarked their calculations against recent experimental work reported by Desjarlais and Tye (1990) which included multiple-airspace measurements. Agreement was excellent for single airspaces but multiple airspaces continued to be poorly predicted, not being simply additive. Fricker and Yarbrough (2011)

reported ongoing use of their software based on the Robinson and Powlitch data. This work all deals with cavities of large extent, not the closely-spaced webs of the test panel.

Several recent studies of heat transfer across smaller voids and airspaces have employed computational modelling. Pavlík et al. (2014) and Sambou et al. (2016) took this approach in considering sideways heat flow through hollow bricks. (Gossard et al., 2012) developed Nusselt number correlations for small rectangular cavities, as found in hollow blocks, also considering horizontal heat flow, under conditions where the Nusselt number remained under 4. In one of a series of publications, each devoted to a particular heat flow direction, Saber (2013) studied upwards heat flow through airspaces of different aspect ratio (equivalent to partitioned airspaces with different partition spacing) based on numerical simulation. His analysis considered specific cases of temperature, thickness and aspect ratio but also proposed correlation equations to cover a wider range of values. Although the highest thickness considered was 90 mm, results were insensitive to airspace thickness for heat flow upwards with non-reflective surfaces and thus can be extrapolated. There was a small increase in thermal resistance associated with reducing aspect ratio although at 200 mm minimum partition spacing for 90 mm thickness, the lowest aspect ratio was still considerably higher than the webbed panel. From Saber's plots summarizing his analysis, the airspace thermal resistance with this web spacing would be 0.162 m^2.K/W.

The appendix of ISO 6946 (ISO, 2007) provides a simplified calculation method for airspace thermal resistance which can accommodate closely-spaced webs. It uses a simple derivation of convective heat transfer coefficient according to temperature difference and employs the aspect ratio in the calculation of view factors for determining the radiative transfer. Using an estimated temperature difference across the airspace for typical testing conditions, the airspace thermal resistance according to ISO 6946 is calculated to be 0.174 m^2.K/W, with a Nusselt number of about 12. This value was adopted as a starting point for analysis.

6.2 Method

6.2.1 Overview

Studying the issues arising in measurement of the non-homogeneous panel requires an understanding of the temperature fields. The simple geometry of this particular panel meant that it could be considered as a two-dimensional problem. This is apparent from Figure 6.1 which is a schematic of the panel installed in a 610 mm square heat flow meter apparatus.

The panel segment supplied was 800 mm long so it is shown overhanging the apparatus on its long axis. Analysis of the panel was structured as a combined exercise in thermal modelling using ANSYS, supported by experimental measurements using thermocouples to determine temperatures at key locations on the panel. Since it is potentially more revealing, thermal measurement and modelling were both set up to be performed dynamically, considering the response of the panel to a temperature transient. After pre-conditioning to a uniform 23 ºC in the heat flow meter apparatus, the hot and cold faces were set to 33 º and 13 ºC respectively. This provided a step response that could be modelled using the transient thermal module within ANSYS 14.5. At the same time it effectively followed the path of a normal heat flow meter measurement, aside from the prescription of a specific isothermal starting temperature.

The proposed thermal measurement setup incorporated flexible buffer materials at the interface between specimen and apparatus plates. We have previously described the use of this procedure in order to minimize errors due to contact resistance and to protect the apparatus plates when measuring hard, uneven materials (Clarke et al., 2016b; Clarke et al., 2016a). Buffers can provide an additional facility in the case of non-uniform heat flow. In decoupling the test specimen from the isothermal plates, they alter the spatial heat flow profile. By choosing buffers that duplicate typical values of indoor and outdoor surface coefficients, they can create heat flow profiles similar to those that would be expected in service so that the plate to plate thermal resistance is analogous to the air to air (overall) thermal resistance measured in a hot box. The range of surface coefficient values commonly applied for indoor and outdoor wind speeds are commensurate with the thermal resistance of typically-used thicknesses of silicone sponge buffer material. The use of flexible buffers also provides accommodation for thermocouple wires, allowing straightforward attachment of thermocouples to the easily-accessible outer surface of the panel to facilitate comparison of measured and modelled temperatures at different locations.

Thermal modelling requires data for both the thermal properties of components and the geometry. The latter are easily derived for a panel of simple rectilinear geometry but two component data values were not precisely known, specifically the conductivity of the MgO boards and the effective thermal resistance of the uninsulated airspaces. Calibration of modelling results against temperature measurement was proposed as a means of obtaining improved estimates for these properties.

The design of the panel afforded the opportunity to add thermal insulation to greatly increase overall thermal resistance and also create greater disparity between the high-conductance and low-conductance heat flow paths. Two different levels of insulation were

proposed, along with the uninsulated case in which the open panel ends were covered with tape so as to create sealed airspaces.

Additionally the simple geometrical form of the panel meant that it was amenable to calculation of overall thermal performance using standard calculation procedures for steady-state bridging heat flow.

6.2.2 Setup for Thermal Measurements

A Fox 600 heat flow meter apparatus was used for the thermal measurements (TA Instruments, 2016). This instrument has a 610 mm square measurement area with HFTs in both the top and the bottom plate and provides automatic recording of measurement results upon heat flow reaching steady state. The criteria for stability and attainment of steady state may be adjusted to extend the measurement duration. A report file contains a log of plate temperatures (generally constant) and heat flows, top and bottom, at 6-minute intervals for the duration of the measurement. This information, and the thickness which is also measured by the apparatus, are used by the software to calculate the thermal resistance and conductivity.

The panel utilized a glued and stapled construction, providing a rigid assembly with good thermal contact between webs and faces. The webs were of slightly-thicker material than the faces. Voids were somewhat narrower than their height. The panel width of 600 mm fitted comfortably but the excess length required it to overhang the plates. The instrument can accommodate over-length specimens by leaving front and back doors open.

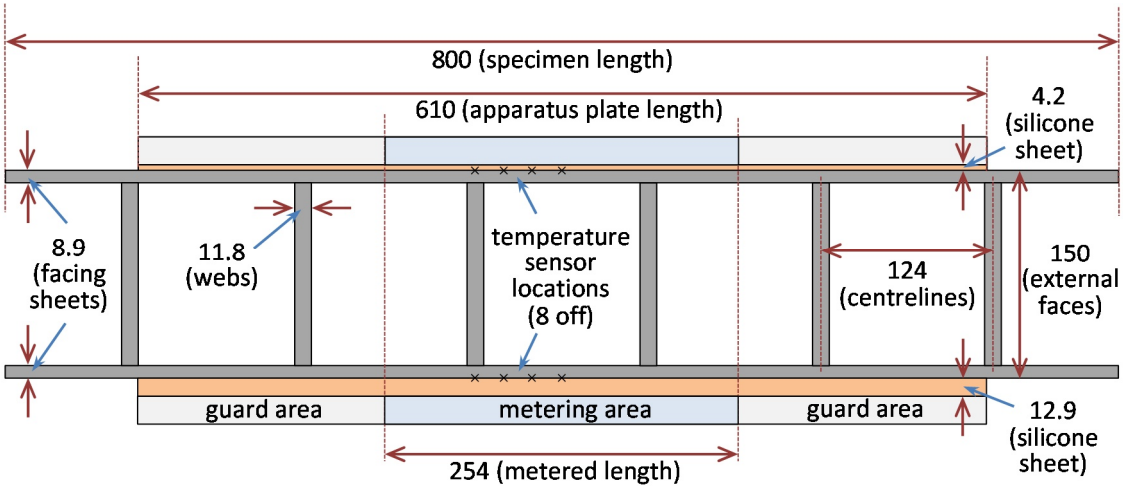

Figure 6.1. Webbed panel shown as set up for measurement in a 610 mm square test apparatus, with silicone sponge buffer sheets top and bottom. All dimensions are in mm.

Buffer characteristics were chosen to provide a pair of boundary conditions similar to the surface heat transfer coefficients that apply for exposure to indoor and outdoor air. These coefficients depend upon the panel orientation and the assumed air speed over the faces and thus are lower for outdoor conditions, assumed to be at the colder (upper) face. The chosen buffers were a medium-soft grade of silicone sponge with thermal resistances of about 0.05 and 0.16 m^2.K/W for cold and hot sides respectively. These are very close to the standard values for horizontal surfaces with 3 m/s outdoor air and still indoor air respectively. As an alternative strategy, buffers of higher thermal resistance could be used in order to create greater temperature difference and greater spatial variation in temperature.

Panel surface temperature was measured at eight points, shown more clearly in Figure 6.3. Webbed panel fitted with double layer of polyester insulation, with silicone sponge buffer resting on top.. The Fox-600 has no provision for such measurements so the more-extensive instrumentation system of an adjacent apparatus was used. The system accommodates up to eight external type T thermocouples. The default wiring uses 32 AWG Teflon-coated twisted pair wire, which is robust and flexible but not generally fine enough for precision measurement. It was therefore brought to junction boards on the edge of the panel, where it connected to 40 AWG (0.08 mm) wire running under glass fibre tape to the specified locations.

The overhanging ends of the panel were insulated in order to make them as close to adiabatic as practical. In the case of the uninsulated panel, the open sides (front and back) were sealed with paper tape, creating five individually-sealed airspaces. The uninsulated case was compared with two different levels of insulation. The first used a single piece of polyester fibre insulation, nominally 150 mm thick, cut to match the width of the voids. The second level used a double layer of the same material, achieving a lower thermal conductivity with compression to double the density (see Figure 6.3).

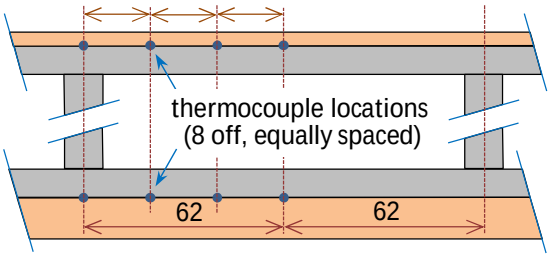

Figure 6.2. Locations of eight thermocouples adhered to the top and bottom faces of webbed panel. Dimensions are in mm.

Figure 6.3. Webbed panel fitted with double layer of polyester insulation, with silicone sponge buffer resting on top.

6.2.3 Setup for Modelling

The physical properties data required for modelling appear in Table 6.1. To obtain a thermal conductivity value for the magnesium oxide material, it was measured in the Fox 600 apparatus using the buffer technique previously described. Thermal conductivity was very high resulting in limited precision. The polyester fibre was measured at a thickness of 132.2 mm which involved slight compression, then measured again with compression to half this thickness for the dual-layer case. The values of specific heat are broad estimates since reliable values were not available. Measurement of the silicone buffer materials in the Fox apparatus was straightforward.

Table 6.1. Physical properties data as used for modelling. Uncertainty in R is at 95% confidence level.

Element	Heat flow path length (mm)	Width (mm)	k (W/m.K)	R (m^2.K/W)	Uncertainty in R (%)	Density (kg/m^3)	Specific heat (J/kg.K)
Panel faces	8.90	631.8	0.491	0.0181	20	1180	1000
Panel webs	132.2	11.80	0.491	0.275	20	1180	1000
Top silicone sheet	4.20	631.8	0.079	0.0543	3	450	2000
Bottom silicone sheet	12.9	631.8	0.079	0.162	3	450	2000
Uninsulated cavity	132.2	112.8	0.760	0.174	see text	1.2	1000
Single-layer polyester	132.2	112.8	0.0585	2.262	5	10.3	2000
Dual-layer polyester	132.2	112.8	0.0435	3.044	4	20.5	2000

The panel was modelled in two dimensions as a half-shape with a symmetrical boundary on the right side as shown in Figure 6.5. Isothermal surfaces were specified across the top and bottom. Since the outer webs were located just beyond the edges of the plate, the isothermal surfaces were extended slightly for the sake of simplicity so that these webs were

included, giving a full width of 632 mm. The cantilevered edges of the panel were also removed for simplicity, leaving a simple left hand edge which was set as an adiabatic surface.

Modelling was performed using the transient thermal analysis module in ANSYS 14.5. The eight temperature measurement locations were set up as defined locations within ANSYS to facilitate more-detailed analysis although their location was placed within the first full airspace away from the half space adjacent to the axis of symmetry (Figure 6.5). This was in order to allow asymmetric modelling within that airspace if later required. Results appeared to be mesh-independent for grid sizes below 2 mm. Across six heat flow measures, results for a 1 mm grid were different by an average of 0.1% compared with a 2 mm grid. The 1 mm grid, with 54,000 nodes, was computationally tractable and so was then used by default.

6.3 Thermal Measurement Results

Measurement of each insulation configuration began with an isothermal phase with both plates set at 23 ºC. It took up to 2 hours for all eight panel surface thermocouples to indicate this temperature, at which point temperatures were reset to 13 ºC at the top and 33 ºC at the bottom to initiate a measurement run. The plates took barely ten minutes to re-stabilize, providing a good approximation to a step function for modelling purposes. Equilibration of panel surface temperatures and heat flows then took many hours. The left hand side of Figure 6.4 is a plot of the eight surface temperatures for the uninsulated and the single-layer insulation cases. Upon stabilization of heat flow, a measurement was completed in terms of the Fox-600 management program so that data could be collected. The panel was immediately moved 31 mm to the next location and a new measurement started. Temperature logging continued through this process. A brief temperature spike is visible on the plots corresponding to the plates being briefly opened. Re-stabilization then took less than 30 minutes so that the second measurement was completed and measurement at the third location then started within a further two hours.

The equilibration curve for the uninsulated case contained an unexpected temperature overshoot of the bottom surface accompanying the initial transient, followed by slow fall in temperature approaching steady state. Anticipating some experimental problem, such as leakage around the sealing tape, the measurement was repeated. Results for this are shown on the right hand side of Figure 6.4, along with the equilibration curves for the dual-layer polyester insulation case. The temperature curves for the repeat measurement are of very similar shape, with the same overshoot. Measured temperatures are considered in more detail in the next section.

Thermal resistance results produced by the Fox-600 appear in Table 6.2, set out in groups of three corresponding to the three panel positions. Also included are the earlier uninsulated-case results, for which alternative buffers were used. Specimen thermal resistance has been calculated by removing the effect of the buffers, as well as their contact resistance, from the measured total (Clarke et al., 2016b). Results are averages of the top and bottom heat flows and show good agreement between the three sets of uninsulated-panel measurements, with the mean values being very close and the standard deviations all being below 1%, even if the extremely similar results for the set of three earlier measurements have not been replicated. Results for both insulation cases are also similar, with standard deviations well under 2%.

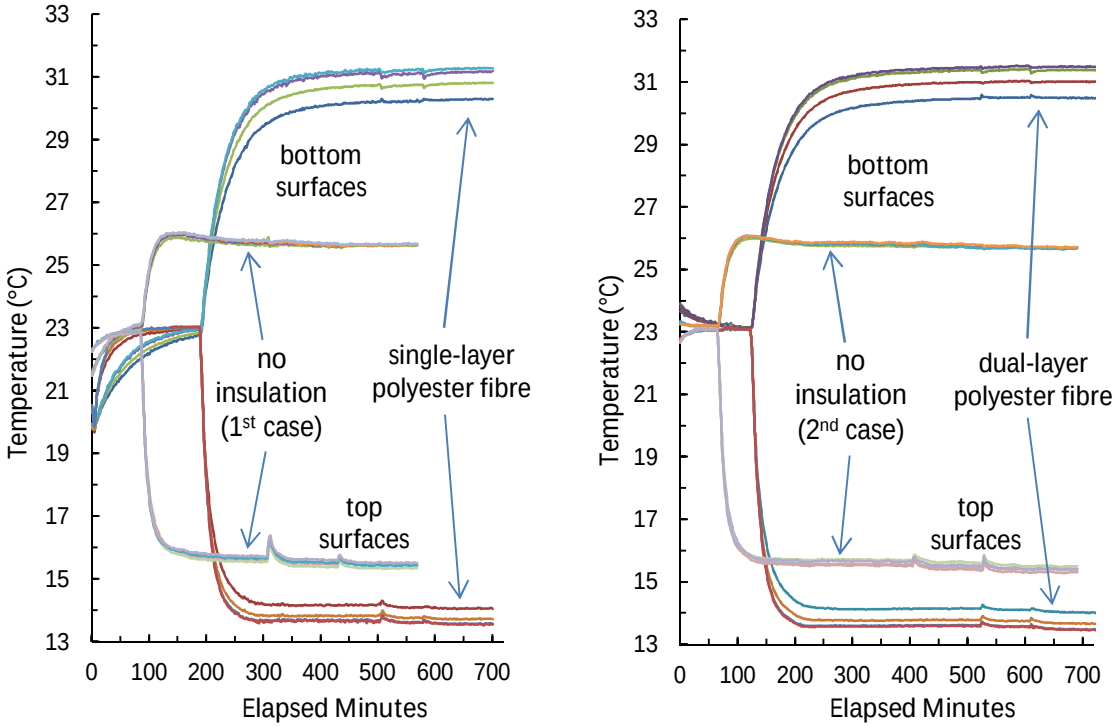

Figure 6.4. Panel surface temperatures during transient measurement. Values were almost independent of location in the case of the uninsulated panels. For the insulated panels, temperatures closer to the web were lower at the bottom surface and higher at the top surface.

Measurement reproducibility for the Fox-600 apparatus with uniform specimens is typically better than 0.2%, suggesting that the bulk of the difference in the case of this panel is due to spatial variation. However, for slowly-stabilizing measurements, the apparatus software introduces some additional variability through its imperfect determination of the appropriate end point.

Table 6.2. Thermal resistance results of the test panel for each insulation case at three different physical positions within the heat flow meter apparatus.

Insulation description	Measurement position	Thermal resistance (m^2.K/W)			Standard deviation (%)
		Total (with buffers)	Specimen only	Specimen (mean of 3)	
Uninsulated (earlier measurement)	1	0.377	0.211	0.211	0.1
	2	0.377	0.211		
	3	0.377	0.211		
Uninsulated	1	0.422	0.207	0.209	0.8
	2	0.425	0.209		
	3	0.425	0.210		
Single-layer polyester	1	1.443	1.228	1.251	1.7
	2	1.472	1.257		
	3	1.485	1.270		
Dual-layer polyester	1	1.612	1.397	1.418	1.4
	2	1.638	1.423		
	3	1.651	1.436		
Uninsulated	1	0.426	0.210	0.211	0.4
	2	0.426	0.211		
	3	0.427	0.212		

6.4 Thermal Modelling Results and Analysis

Figure 6.5 provides indicative output from the transient thermal model in terms of spatial temperature profiles for the uninsulated panel (top) and the dual-layer insulated panel (bottom). The figure shows final steady state values with the imposed 13 ºC top and 33 ºC bottom temperatures. A much more uniform temperature profile is evident in the uninsulated case.

Modelled temperature results for the eight defined locations were used to refine those thermal properties values that were not confidently known, specifically those of the magnesium oxide board and the airspaces. The process is indicated in Table 6.3 which gives a comparison of measured and modelled temperature data taken at 630 minutes (10.5 hours). Starting with the single-layer polyester, modelling suggested that the thermal conductivity of the magnesium oxide material was approximately 0.55 W/m.K, this giving the closest agreement between modelled and measured temperatures. This is 12% higher than the value measured in the Fox 600 apparatus for the 8.9 mm facing sheet. However the calculated

measurement uncertainty was 20% (at 95% confidence level) due to the very low thermal resistance. Additionally it is the conductivity of the webs rather than the faces that is more significant for heat flow but the webs were a different, slightly thicker, material. Although density was the same, conductivity might not be, or the material might not be isotropic, recognizing that web heat flow is along, rather than across, the plane.

The next section of Table 6.3 considers the dual-layer polyester insulation and affirms the conductivity value of 0.55 W/m.K for the web, this value providing good agreement with measured temperatures.

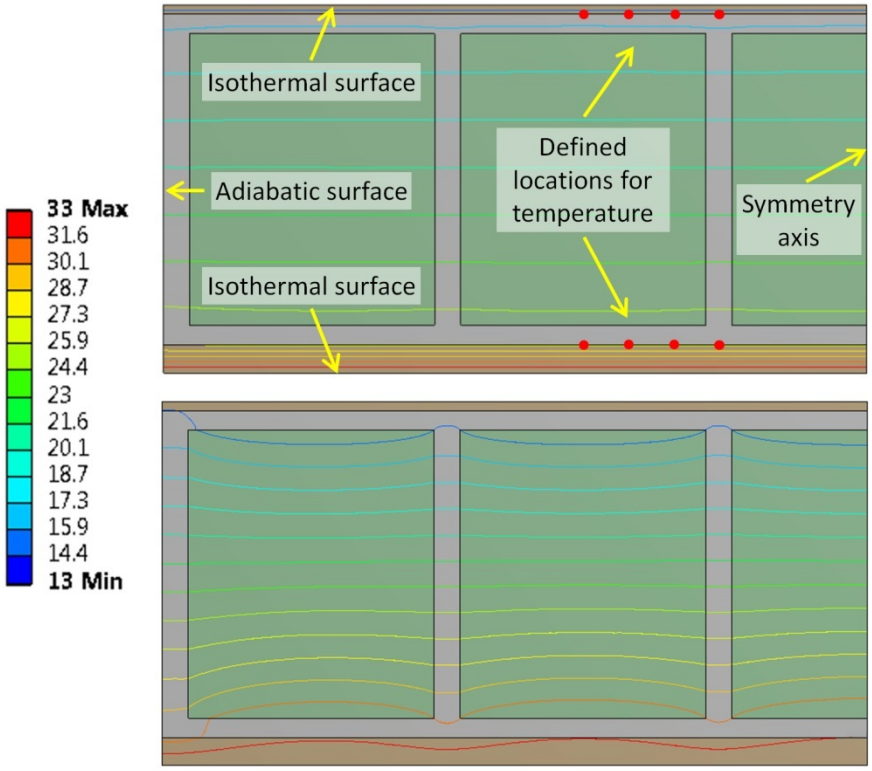

Figure 6.5. Modelling geometry, defined surfaces and locations, and temperature results showing steady-state isotherms for uninsulated panel (top) and dual-layer insulated panel (bottom).

The final section of the table uses the same procedure to arrive at a value for the properties of the uninsulated airspace. In this case, it was not possible to simultaneously obtain close agreement with the top and bottom temperatures. The starting point of 0.76 W/m.K derived from the ISO calculation gave reasonable agreement for the top surface whilst a value of 0.70 W/m.K produced a better overall result averaged over both surfaces with a worst-case disagreement of 0.14 ºC.

Table 6.3. Comparison of measured and modelled temperatures at 630 minutes (10.5 hours) elapsed time, with alternative thermal conductivity values for magnesium oxide board and airspace.

Measured or modelled case using stated thermal conductivity of MgO board and airspace (W/m.K)		Temperature (°C) at specified location			
		1 (web)	2	3	4 (mid-void)
Single-layer polyester fill					
Cold (top)	Measured	14.07	13.72	13.57	13.55
	Modelled, k(MgO)=0.49	14.04	13.69	13.51	13.47
	Modelled, k(MgO)=0.55	14.11	13.73	13.53	13.48
	Modelled, k(MgO)=0.60	14.16	13.76	13.54	13.49
Hot (bottom)	Measured	30.29	30.81	31.17	31.27
	Modelled, k(MgO)=0.49	30.46	30.92	31.23	31.32
	Modelled, k(MgO)=0.55	30.32	30.81	31.14	31.24
	Modelled, k(MgO)=0.60	30.21	30.72	31.08	31.18
Dual-layer polyester fill					
Cold (top)	Measured	14.05	13.69	13.50	13.49
	Modelled, k(MgO)=0.55	14.07	13.65	13.44	13.38
Hot (bottom)	Measured	30.50	31.02	31.40	31.49
	Modelled, k(MgO)=0.55	30.51	31.05	31.41	31.52
Uninsulated airspace					
Cold (top)	Measured	15.41	15.32	15.43	15.51
	Modelled, k(MgO)=0.55, k(air)=0.76	15.44	15.48	15.51	15.50
	Modelled, k(MgO)=0.55, k(air)=0.60	15.25	15.26	15.26	15.26
	Modelled, k(MgO)=0.55, k(air)=0.70	15.38	15.41	15.42	15.42
Hot (bottom)	Measured	25.70	25.70	25.68	25.73
	Modelled, k(MgO)=0.55, k(air)=0.76	25.43	25.38	25.34	25.34
	Modelled, k(MgO)=0.55, k(air)=0.60	26.09	26.07	26.06	26.06
	Modelled, k(MgO)=0.55, k(air)=0.70	25.66	25.62	25.59	25.59

Modified conductivity values derived by the above process are qualified improvements over the starting values because they rely on surface temperature measurement and the presumption that the plates are isothermal. Routine calibration requires agreement within 0.1 ºC between the embedded plate thermocouples and the external system. This is easily met over the 13 ºC to 33 ºC range for calibration performed at the centre of the plates in an isothermal environment (both plates at the same temperature). The apparatus plates are highly conductive but the extent of spatial temperature variation, particularly in the presence of a non-homogeneous specimen, has not been carefully studied. In addition, thermal attachment methods and the properties of covering tapes can affect measurement of surface temperature under an applied temperature gradient. Certainly each set of temperature

measurements is highly consistent and agrees well with the spatial trend predicted by modelling.

Using the modified conductivity values from Table 6.3, the transient model was run to compare measured and modelled temperatures over the duration of the measurement. Results for the second uninsulated case and for dual-layer polyester insulation are shown in Figure 6.6. Results for the single-layer polyester insulation were similar. Considering the uncertainty in thermal properties, including specific heat, overall agreement is very good. However, as expected, the experimentally-measured temperature overshoot at the bottom surface of the uninsulated panel was not predicted. Probably for a related reason, modelled temperatures were also lower on the top side over the period following the initial transient. The presence of lateral heat flow due to insufficient edge insulation was considered to be a possibility so the model was run with the left boundary set to a fixed temperature of 23 ºC (instead of adiabatic). This produced a distorted temperature field near this boundary but there was little change at the reference points with no prediction of an overshoot following the initial transient. The most plausible explanation is transient convective flow within the airspace. A closer study of confined airspace behaviour using computational fluid dynamics might be informative but is beyond the scope of this study, especially since the overshoot is not a factor in the final heat flow values based on steady state correlations. Ridouane et al. (2005) and Ouertatani et al. (2008) have studied natural convention in rectangular enclosures with heat from below. However the transient nature and the existence of multiple adjacent enclosures in this case would result in significant computational complication.

The modelled spatial profile of steady-state heat flux between the centerline of one web and the next is shown in Figure 6.7. The near-uniform flux for the uninsulated panel is apparent, indicating that the thermal resistance of the airspace is commensurate with that of the web. In contrast, for the dual-layer polyester case there is a variation of approximately 2:1 between mid-web and mid-void heat flows at the bottom and a ratio of closer to 3:1 at the top. This exemplifies the averaging effect of the buffers, with a smaller variation associated with a larger buffer resistance. The data presented is for a run time of 18 hours (1080 minutes), by which time steady state had been reached in all cases. The model was also run for periods matching each individual measurement because of concerns that steady state might not quite have been reached (given the shapes of the stabilization curves). Detailed results are presented in Table 6.4 using mean heat flow as the basis of comparison between experimental and modelled results.

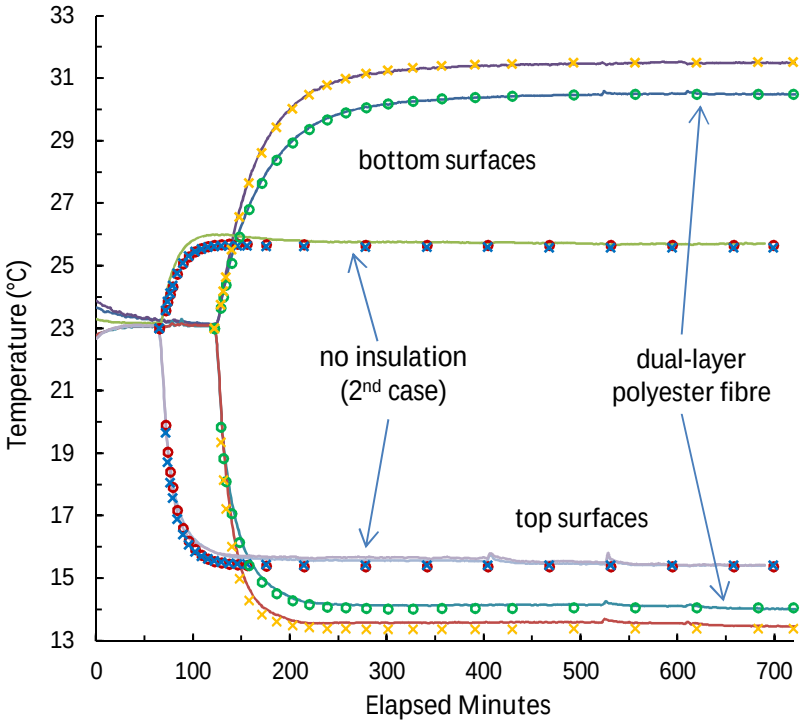

Figure 6.6. Comparison of measured (continuous line) and modelled (marker) panel surface temperatures for the uninsulated panel and for the panel insulated with the double layer of polyester fibre insulation. Temperatures shown are for mid-web and mid-void only.

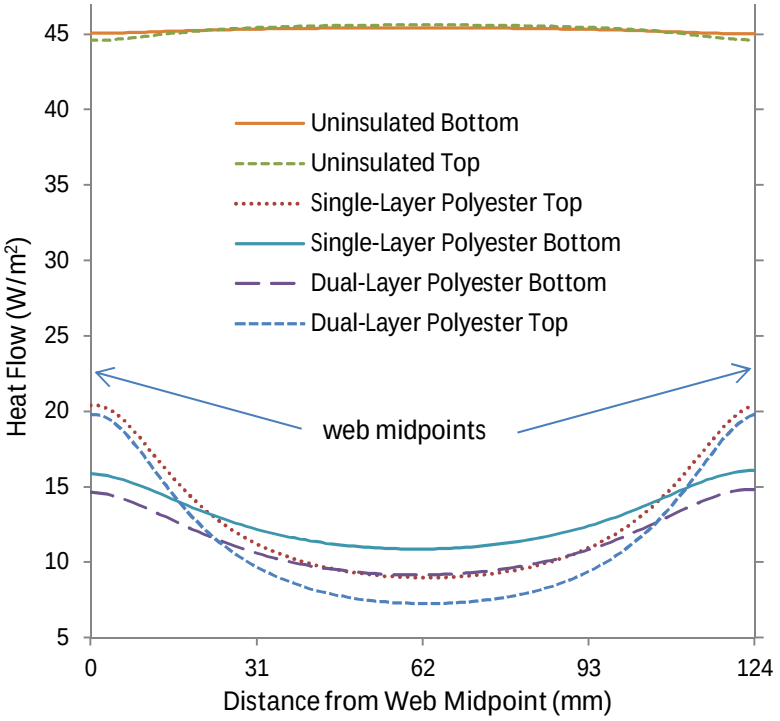

Figure 6.7. Modelled steady-state heat flow profile across a single void from web to web for the three insulation configurations.

The final column of Table 6.4 shows the model prediction that steady state had indeed not been reached for the two insulated cases which have long stabilization times. The largest error was 1.8% in bottom heat flow for the single-layer polyester fibre. However the errors in the top and bottom heat flows were similar and in opposite directions for both insulated cases so that the greatest mean error, along with that for the single-layer polyester, was only 0.4%.

Table 6.4 also shows significant differences between measured and modelled heat flows, the largest individual value being 11.3% for the first measurement of the bottom heat flow of the single-layer polyester. Significantly, all measured heat flows were higher than predicted and almost all fell in value from the first, through the second, to the third measurement. This was not due to the measurement order. Rather, as is evident from Figure 6.4, heat flow tended to stabilize at a lower value for each incrementing position. This then would seem to indicate a uniformity limitation with the HFTs, albeit a small one in overall terms. As is evident from Figure 6.7, the two lateral steps (62 mm totally) resulted in a worst-case change in heat flow over some locations on the top plate by a factor of almost three. A simple geometric analysis shows that three measurements experience close to the largest possible variation if they are spaced apart at one quarter of the repeating web dimension and they increase one to the next. For a spatial heat flow profile following a sinusoidal form, the minimum indicated difference over all three values would be 71% of the peak amplitude, occurring when any two values are very similar. On the presumption that the profile form will be at least roughly sinusoidal, the results suggest a maximum possible variation in indicated average heat flow of approximately 4% associated with the positioning of either of the insulated panels relative to the heat flux sensors.

Heat flow data from Table 6.4 was used to calculate mean thermal resistance at both the end time of measurement and at steady state. Mean thermal resistance was also calculated using the isothermal planes (ITP) and parallel heat flow paths methods, the two common procedures for calculating the effective thermal resistance when there is non-uniform or bridging heat flow (ASHRAE, 2013). Because of the simple panel geometry, these calculations were straightforward. These results, along with the thermal resistance values reported by the Fox 600 apparatus are given in Table 6.5. All values are total thermal resistance, including the contributions of the two buffers as notional surface resistance, analogous to results for overall thermal resistance from a hot box measurement. The measured results are the average of the three measurements for each insulation case.

Table 6.4. Comparison of measured and modelled mean heat flows at both the time of measurement time and at steady state, for top and bottom heat flows, as well as the average. Each set of three values is for panel locations 1, 2 and 3 in succession.

Insulation description	Measured by HFT	Calculated at run end time	Calculated at steady state	Difference between measured and calculated at run end time	Difference between calculations at steady state and run end time
	Top heat flow (W/m^2)			Top heat flow (%)	
Nil test 1	48.58	45.35	45.29	7.1	-0.1
	48.08			6.0	-0.1
	47.85			5.5	-0.1
Nil test 2	48.37	45.30	45.29	6.8	0.0
	48.35			6.7	0.0
	48.12			6.2	0.0
Poly 1 layer	13.16	12.68	12.82	3.8	1.1
	13.10			3.3	1.1
	13.18			4.0	1.1
Poly 2 layer	12.16	11.21	11.29	8.5	0.7
	12.05			7.5	0.7
	12.12			8.1	0.7
	Bottom heat flow (W/m^2)			Bottom heat flow (%)	
Nil test 1	46.20	45.23	45.27	2.2	0.1
	46.15			2.0	0.1
	46.22			2.2	0.1
Nil test 2	45.64	45.27	45.27	0.8	0.0
	45.46			0.4	0.0
	45.51			0.5	0.0
Poly 1 layer	14.56	13.08	12.84	11.3	-1.8
	14.08			7.6	-1.8
	13.75			5.1	-1.8
Poly 2 layer	12.65	11.43	11.32	10.7	-1.0
	12.37			8.3	-1.0
	12.11			6.0	-1.0
	Mean heat flow (W/m^2)			Mean heat flow (%)	
Nil test 1	47.39	45.29	45.28	4.6	0.0
	47.12			4.0	0.0
	47.04			3.9	0.0
Nil test 2	47.01	45.28	45.28	3.8	0.0
	46.91			3.6	0.0
	46.82			3.4	0.0
Poly 1 layer	13.86	12.88	12.83	7.6	-0.4
	13.59			5.5	-0.4
	13.47			4.5	-0.4
Poly 2 layer	12.41	11.32	11.30	9.6	-0.2
	12.21			7.9	-0.2
	12.12			7.0	-0.2

Table 6.5. Comparison of total thermal resistance values as measured by the Fox 600 apparatus, modelled at measurement time and at steady state, and as determined by two calculation methods.

Total thermal resistance (m^2.K/W)					
Core material	HFT measurement (average of 3)	Model at measurement time	Model at steady state	Calculated parallel paths	Calculated isothermal planes
Air (1^{st})	0.424	0.442	0.442	0.442	0.442
Air (2^{nd})	0.426	0.442	0.442	0.442	0.442
Single-layer polyester	1.470	1.553	1.559	1.803	1.506
Double-layer polyester	1.630	1.767	1.770	2.132	1.693

In the case of the uninsulated panel, the two calculation methods and the modelled results were all in close agreement. However the HFT-measured value was 4% lower on average. For the two insulated cases, the calculation methods diverged from each other, with the modelled result lying between them but close to the ITP value in both cases. The ITP value is generally regarded as a lower bound but to be closer to the actual value for cases with layers of high lateral conduction (Van Geem, 1986; Trethowen, 2000). Jones and Jones (1999) propose using weighted combination of the two values, again one that is inclined heavily towards the ITP result for walls with layers of high lateral conductance such as the webbed panel. The modelled results therefore remain consistent with the appropriate calculation, as well as with surface temperature measurement. Given the very simple panel design, with few uncontrolled geometric factors, these results must be regarded as providing good estimates of overall thermal resistance. Averaged over both HFTs, results were lower for both insulation cases, by 6% for the single-layer polyester and 8% in the double-layer case.

The cause of these differences is not clear. The HFT results are internally consistent in that higher levels of non-uniformity and higher thermal resistance are associated with correspondingly lower results, relative to modelling and computation. It is possible that the HFTs do have significant sensitivity to lateral heat flows, as observed previously. However, bias due to this effect should have a value of zero when averaged over all panel positions and so is not consistent with measured heat flow values being low at every test location. The HFTs may simply produce higher output for spatially-variable heat flows than for uniform heat flow of the same mean value (as applies at calibration). Error may also be attributed to the different nature of the specimen. Including buffers, the measurement assembly had a total thickness of 167 mm, towards the upper limit of the apparatus range. In addition, the panel was very non-isotropic, particularly in relation to the presence of the highly conductive top and bottom sheets. Under such conditions, the apparatus may provide measurement results

that are not consistent with calibration performed with a thin isotropic reference material. Ultimately it will require additional study to determine the cause of the generally-higher heat flow readings for the panel with the Fox 600 apparatus.

Uncertainties such as those given in Table 6.1 are only meaningful when there is confidence in the extent to which extraneous factors may introduce bias. In the case of the uninsulated panel, allowing the assumption that perpendicular heat flow is almost spatially uniform and ignoring the other non-homogeneities, our standard calculation procedure produces an uncertainty of 8% in the measured value of thermal resistance at 95% confidence level. This is much higher than the 2-3% achieved with many measurements because of the substantial thickness of the webbed panel and the requirement for a difference calculation. In light of this larger uncertainty figure, the measured results are not inconsistent with the modelling and calculation results, considering the difference of only 4%. In the case of the insulated panels, there is considerable spatial variation in heat flow, both in the perpendicular direction because of the conductive webs and also in the transverse direction because of the two conductive facing panels. Reliable uncertainty calculation is therefore precluded. However, uncertainty is potentially a lot larger than the measured worse-case disagreement of 8% between the HFT-based measurement and the modelling results. Estimation of the uncertainty associated with the modelling results is not straightforward and has not been attempted. Given the consistency between modelling and calculation values and the simple geometry of the panel, it may be little higher than the uncertainty in measurement of the thermal properties of the more-significant component materials, which is around 4-5%.

6.5 Conclusions

The heat flow meter method has proved capable of producing results for the measurement of a thick, non-homogeneous panel that substantially agree with thermal modelling and standard calculation, although suggesting a lower thermal resistance by a small and consistent amount. Differences have ranged from about 4% for a fairly uniform uninsulated panel to 8% for panel of the same thickness with highly non-uniform heat flow due to the presence of insulation between conducting webs. The uninsulated-panel results suggest that factors other than non-homogeneity, such as the relatively high measurement thickness, may have contributed to the lower indicated thermal resistance.

Uncertainty in thermal measurement exceeds the above percentage values to the extent that it is able to be calculated. In the case of the insulated panels containing conductive webs, the non-homogeneity precludes such calculation. Thermal modelling results have agreed well

with calculation using standard methods. Although uncertainty is difficult to formally estimate, modelled results are judged to be the most reliable estimates of thermal resistance in this particular case where panel geometry is simple.

Multiple measurements in different locations of a panel with a spatial variance in heat flow exceeding 200% have resulted in heat flow variations of only ± 2%, suggesting that the HFTs used in the Fox 600 apparatus provide an effective averaging capability. Results with other apparatus may differ.

Accepting that thermal measurement results for the panel derived from the heat flow meter measurements are of uncertain accuracy, the apparatus has nevertheless been instrumental in obtaining modelling results in which there can be greater confidence in two separate ways. In the first instance, heat flow meter measurements have provided essential data on the components of the test assembly. Additionally, with the panel set up in the heat flow meter apparatus in conjunction with buffer materials, measurement of panel surface temperatures has allowed model data to be refined and the predictions of the model to be verified.

The buffer materials have played an important role. In decoupling the specimen surface from the isothermal hot and cold plates, the presence of the buffers has allowed surface temperature profile to be a measurable indicator of heat flow for validation of modelling. By matching their thermal resistance to appropriate values of surface coefficient, the buffers have also facilitated the establishment of heat flow profiles that are representative of in-service conditions.

Stabilization times for thermal measurement have proved difficult to determine automatically when they exceed several hours. On an individual plate basis, errors due to premature measurement completion have exceeded 1% despite conservative detection settings. Numerical modelling obviates this problem.

Good agreement has been achieved between modelling and measurement of surface temperatures and between modelling and analytical calculation of heat flux and overall thermal resistance for insulated and uninsulated versions of the panel. The analytical calculations have been practical in this case due to the very simple rectilinear geometry.

Analytical calculations would not be practical for many more-complex shapes. The results have however demonstrated the value of thermal modelling and suggested that it may be very usefully supported and validated through measurement of surface temperature adjacent to thermal buffer materials in a heat flow meter apparatus. Results from the apparatus heat flux transducers might not be highly reliable but modelling results acquired in this way could

provide an alternative solution when applied to complex or irregular building components for which direct experimental determination of thermal performance is otherwise impractical, especially in regions where hot box test facilities are not readily available.

6.6 References

ASHRAE. (2013) 2013 ASHRAE Handbook - Fundamentals (SI Edition). American Society of Heating, Refrigerating and Air-Conditioning Engineers, Inc., 25, 7-8.

ASTM. (2011) ASTM E1530 - 11. "Test Method for Evaluating the Resistance to Thermal Transmission of Materials by the Guarded Heat Flow Meter Technique.". *Annual Book of ASTM Standards, Vol. 14.02.* ASTM International, DOI: 10.1520/E1530-06

ASTM. (2013a) ASTM C177 - 13. "Test Method for Steady-State Heat Flux Measurements and Thermal Transmission Properties by Means of the Guarded-Hot-Plate Apparatus.". *Annual Book of ASTM Standards, Vol. 04.06.* ASTM International, DOI: 10.1520/C0177

ASTM. (2015) ASTM C518 - 15. "Test Method for Steady-State Thermal Transmission Properties by Means of the Heat Flow Meter Apparatus.". *Annual Book of ASTM Standards, Vol. 04.06.* ASTM International, DOI: 10.1520/C0518-15

Bomberg M. (1994) A Workshop on Measurement Errors and Methods of Calibration of a Heat Flow Meter Apparatus. *Journal of Building Physics* 18: 100-114. DOI: 10.1177/109719639401800202

Bomberg M and Solvason KR. (1983) Comments on Calibration and Design of a Heat Flow Meter *ASTM STP789 Thermal Insulation, Materials, and Systems for Energy Conservation in the '80s.* ASTM International, DOI: 10.1520/stp29452s

Clarke RE, Pianella A, Shabani B, et al. (2016a) Steady-state thermal measurement of moist granular earthen materials. *Journal of Building Physics* Prepublished May 23 2016, DOI: 10.1177/1744259116637864

Clarke RE, Shabani B and Rosengarten G. (2016b) A difference technique to avoid interface errors in measurement of high-conductance thermal insulation. *Journal of Building Physics* Prepublished May 23 2016, DOI: 10.1177/1744259116637863

De Ponte F. (1985) Present and Future Research on Guarded Hot Plate and Heat Flow Meter Apparatus *ASTM STP879 Guarded Hot Plate and Heat Flow Meter Methodology.* ASTM International, DOI: 10.1520/stp32902s

De Ponte F and Maccato W. (1980) The Calibration of Heat Flow Meters *ASTM STP718 Thermal Insulation Performance.* ASTM International, DOI: 10.1520/stp29277s

Desjarlais AO and Tye RP. (1990) Research and Development Data to Define the Thermal Performance of Reflective Materials Used to Conserve Energy in Building Applications. Oak Ridge National Laboratory.

Desjarlais AO and Yarbrough DW. (1991) Prediction of the Thermal Performance of Single and Multi-Airspace Reflective Insulation Materials *ASTM STP1116 Insulation Materials: Testing and Applications, 2nd Volume.* ASTM International, DOI: 10.1520/stp16338s

Fricker JM and Yarbrough DW. (2011) Review of reflective insulation estimation methods. *Proceedings of Building Simulation, 12th Conference of International Building Performance Simulation Association.* Sydney

Gossard D, Lartigue B and Sambou V. (2012) Nusselt number correlations for laminar convection in three-dimensional air-filled cavities. *Journal of Building Physics* 35: 327-337. DOI: 10.1177/1744259111423086

Graves RS and Yarbrough DW. (1993) The Use of an Array of Heat Flux Transducers to Study Thermal Property Variations. *Journal of Building Physics* 17: 171-181. DOI: 10.1177/109719639301700108

Han BJ, Yarbrough DW and Han SM. (1986) Thermal Resistance of Wall Cavities Containing Reflective Insulation. *Journal of Solar Energy Engineering* 108: 338-341. DOI: 10.1115/1.3268116

ISO. (2007) ISO 6946:2007 Building components and building elements - Thermal resistance and thermal transmittance - Calculation method. *ISO 6946*. Geneva, Switzerland: International Organization for Standardization

Jones GF and Jones RW. (1999) Steady-state heat transfer in an insulated, reinforced concrete wall: theory, numerical simulations, and experiments. *Energy and buildings* 29: 293-305. DOI: 10.1016/S0378-7788(98)00072-3

Kosny J and Childs P. (2002) Accuracy of Hot Box Testing of Steel Stud Walls *ASTM STP1426 Insulation Materials: Testing and Applications: 4th Volume*. ASTM International, DOI: 10.1520/stp11010s

Miyake Y and Eguchi K. (1985) Development of a Large Area Heat Flow Meter *ASTM STP879 Guarded Hot Plate and Heat Flow Meter Methodology*. ASTM International, DOI: 10.1520/stp32907s

Ouertatani N, Ben Cheikh N, Ben Beya B, et al. (2008) Numerical simulation of two-dimensional Rayleigh–Bénard convection in an enclosure. *Comptes Rendus Mécanique* 336: 464-470. DOI: 10.1016/j.crme.2008.02.004

Pavlík Z, Jerman M, Trník A, et al. (2014) Effective thermal conductivity of hollow bricks with cavities filled by air and expanded polystyrene. *Journal of Building Physics* 37: 436-448. DOI: 10.1177/1744259113499214

Ridouane EH, Hasnaoui M and Campo A. (2005) Effects of surface radiation on natural convection in a rayleigh-benard square enclosure: steady and unsteady conditions. *Heat and Mass Transfer* 42: 214-225. DOI: 10.1007/s00231-005-0012-7

Robinson HE and Powlitch FJ. (1954) The thermal insulating value of airspaces. Housing research paper no. 32. Washington, DC: US Government Printing Office.

Saber HH. (2013) Practical correlations for thermal resistance of horizontal enclosed airspaces with upward heat flow for building applications. *Building and Environment* 61: 169-187. DOI: 10.1016/j.buildenv.2012.12.016

Sambou V, Lartigue B, Monchoux F, et al. (2016) Modeling of the thermal performance of air-filled partitioned enclosures: Effects of the geometry and thermal properties. *Journal of Building Physics* 39: 321-341. DOI: 10.1177/1744259114561578

TA Instruments. (2016) *Thermal Conductivity Test Instruments*. Available at: **http://www.tainstruments.com/products/thermal-conductivity-meter/**.

Trethowen H. (1986) Measurement errors with surface-mounted heat flux sensors. *Building and Environment* 21: 41-56. DOI: 10.1016/0360-1323(86)90007-7

Trethowen HA. (2000) Validating the isothermal planes method for R-value predictions. Porirua [N.Z.]: Building Research Association of New Zealand.

Tye RP, Coumou KG, Desjarlais AO, et al. (1987) Historical Development of Large Heat Flow Meter Apparatus for Measurements of Thermal Resistance of Insulations *ASTM*

STP922 Thermal Insulation: Materials and Systems. Dallas, Texas, USA: ASTM International, DOI: 10.1520/STP18510S

Van Geem MG. (1986) Thermal Transmittance of Concrete Block Walls with Core Insulation. *Journal of Building Physics* 9: 187-210. DOI: 10.1177/109719638600900302

Yarbrough DW. (1983) Assessment of Reflective Insulations for Residential and Commerical Applications, ORNL/TM-8891. Oak Ridge, Tennessee: Oak Ridge National Laboratory.

7 DISCUSSION AND CONCLUSIONS

7.1 Overview

Through the progression of experimental work described through chapters 2 to 6, and the associated analysis of findings, an improved insight into high-conductance measurement using the heat flow meter apparatus has developed. It can be said that there are deficiencies in the provisions of the standard methods which are important since these methods provide more than just guidance. They also have formal status in building regulations in Australia, New Zealand and indeed in many countries. It is not surprising that the initial development of standard methods for measuring the thermal properties of insulation materials fitted in with the requirements of the time. For the insulation industry through the mid-late 20th century, the use insulation at modest thickness and the limited availability of exotic low conductivity materials (such as vacuum panels) meant that there was an expectation of a median thermal resistance of about 1 m^2.K/W, evidenced by the fact that available reference materials were centred around this value. It is also not surprising that, in the intervening years, commercial interest has expanded into the high-performance end of the spectrum. This is the visible cutting edge, represented by materials such as aerogels, vacuum-insulated panels and the foamed plastics. Markets are clearly following in this direction. There are many current applications in which better-insulating materials would be preferable, ranging in scale from buildings and industrial storage tanks to miniature electronics and protective garments. In the case of long-established products such as glass fibre, further performance improvement might be slight but there is steady increase in the use of higher-thickness products.

The development of measurement techniques has lagged behind the marketplace. This is perhaps inevitable in cases where standardized methods are in operation within changing industries. It is apparent in the most recent ASTM Special Technical Publication on thermal properties measurement ASTM STP1574, Next-Generation Thermal Insulation Challenges and Opportunities (ASTM, 2014). Many of the papers from this symposium do consider new materials whilst Noonan and Jonas (2014) discuss measurements at full thickness in excess of 300 mm, achieved through stacking of thinner calibrated transfer specimens. In the same publication, Zarr and Leigh (2014) report on the performance of glass fibre reference materials just 26 mm thick. Taken together, these two papers underscore the limitations that exist in the measurement of high-thickness, low conductance materials.

Something of the same situation applies at the other end of the spectrum, in the measurement of thermal resistance that is lower than the traditional insulation mainstream. Commercial testing laboratories have an increasing frequency of measurement requests for high-conductance products and yet very little recent research information is available. The drivers for interest in these materials may not be glamorous but are nevertheless significant. They include the need to characterize building components and elements, including those of high conductance, for design modelling, and the requirements of regulation both for thermal performance and for fire-retardant or thermal-barrier performance.

The lower thermal resistance limits contained within ASTM C 177 and C 518 remain as cautionary reference points although ISO standards point out that errors, chiefly related to interface resistance, may occur at thermal resistances well about these limits. ASTM E 1530 serves a very useful role in covering the measurement of engineering materials, including metals. It demonstrates that pathways to circumvent interface resistance are available. The standard does however target the characterization of engineering materials as distinct from insulations. It is inherently not a “full thickness” method as there is an a priori presumption that the measurement specimen will be a carefully-prepared, machined-flat test piece, able to withstand a high clamping force. It therefore cannot accommodate a large percentage of materials that have limited compressibility, layered or composite construction, or surface roughness that is inherently part of the product. It is also significant that the method is not proposed for use above 0.04 m^2.K/W, a limitation that would exclude many highly-conducting building products.

Aspects of ASTM C 518 are also non-optimum in their consideration of highly conducting specimens. In the section pertaining to test procedures for rigid and high-conductance specimens, it specifies that the surfaces should be made flat and parallel and that plate-

embedded temperature sensors may be adequate if the interface resistance is sufficiently low. It therefore skirts the problem of specimens that cannot be practically made flat and it does not give guidance as to how to assess whether or not interface resistance will be sufficiently low. Furthermore it gives no guidance as to techniques for surface temperature measurement, except to say that thermocouples set into the surfaces of specimens should be no greater than 0.25 mm diameter. It is not surprising that commercial apparatus seldom feature an external thermocouple facility. Certainly the prescribed lower measurement limit of 0.1 m^2.K/W is a much clearer statement although it is not linked to interface issues in the text.

A relatively small percentage of laboratories utilize purpose-built apparatus and might therefore have a capability for measuring specimen surface temperature using external sensors. For these laboratories, surface temperature measurement could be a practical proposition, accepting the additional preparation time it entails. However it is not practical with loose fills or with many rough surfaces. In the case of materials with hard incompressible surfaces that are smooth enough for sensors such as thermocouples to be attached, the concurrent use of some type of interface material is required for accommodating the sensor wires unless grooves can be set into the specimen surface for this purpose. Such grooves might disturb the heat flow profile in a thinner specimen and are also likely to mean that the temperature sensor is effectively providing measurement of a region below, rather than at, the specimen-buffer interface, since it would be required to sit fully beneath the surface. Utilizing buffers instead of grooves, a simple solution is that described in Chapter 6 where the use of very-fine thermocouple wire allows measurement to be confidently localized at a point very close to the specimen surface.

A larger question however is the representativeness of temperature readings from only one or just a few locations. Corsan and Williams (1980) discuss the large temperature variations that occur as a result of thickness non-uniformities (and the resultant airspaces). Appropriate spatial averaging would require a significant number of sensors. The variations between sensors can be higher than intuitively expected simply because the unwanted airspaces have a disproportionate effect due to their low conductivity relative to that of the test specimen. This further means that the presumption of uniform and unidirectional heat flow through the specimen is similarly compromised. As noted in Chapter 6, heat flux transducers are not designed for non-uniform heat flow and might not measure it with any accuracy.

Interface buffer materials provide for a prospect of greatly improving heat flow uniformity by replacing the airspace voids with a filler such as a flexible foamed plastic having a thermal conductivity much higher than air. However, as considered in detail in Chapter 5, a

compromise is involved since the buffer needs to have significant thickness in order to have the level of compressibility required to achieve airspace-free contact over the whole area of a typical non-flat specimen. The end result is therefore that the presence of the buffer simultaneously provides for much more uniform temperature difference as measured at the specimen surface, but a lower overall value since some of the gradient will be taken up by the buffer. Corsan and Williams found that the buffer provided overall benefit and should be as soft as possible.

ASTM C 518 proposes buffers (described as thin sheets of a suitable homogeneous material) for those rigid specimens where it is not possible to obtain good surface contact. It adds that the thermal resistance of the thin sheet should be low relative to the specimen and that it should be measured separately by ASTM C 177, with the specimen thermal resistance determined by subtraction. This paragraph would seem to be deficient in several interrelated ways. In the first place, it does not foreshadow the option of surface temperature sensors, the use of which would obviate the need for the subtraction calculation. It is therefore inconsistent with the earlier inference that surface sensors would be required where good surface contact with the plates did not occur. The only quality mentioned for the thin sheet is homogeneity. Flexibility and compressibility are much more relevant: a rigid incompressible sheet would not be useful. In suggesting that the thin sheet should be measured by ASTM C 177 there is an implied suggestion that this method offers superior measurement performance at low thermal resistance. This might be the case only to a small degree, C 177 having a nominal lower limit of 0.06 m^2.K/W compared with the 0.1 m^2.K/W of C 518. Clearly a C 177 measurement would not be suitable for determining the thermal resistance of a thin sheet having a thermal resistance that was low relative to a specimen that itself had a thermal resistance close to 0.1 m^2.K/W. Finally, as considered above, a buffer must have significant thickness and compressibility in order to function correctly. With a high-conductance specimen, this may be incompatible with the C 518 requirement that the thermal resistance of the buffer should be low relative to that of the test specimen. The existence of this restriction would seem reasonable only in the presumption that the testing laboratory was not intending to undertake an uncertainty analysis that included the errors associated with difference measurement, many of which are correlated. However laboratories engaged in commercial measurement should be routinely doing such analyses. Nevertheless finding buffer materials that retained high compressibility but also offered higher thermal conductivity would be beneficial.

The role of buffer materials in the measurement of high-conductance specimens has been a recurrent theme in this dissertation. In the case of Chapters 2 to 4, the use of buffer materials

has been considered largely in terms of the minimization interface resistance. In Chapter 5, interface resistance has been associated with surface roughness and therefore viewed, in part, as an extrinsic property of the specimen, dependent also upon buffer hardness. The buffer therefore also fulfils a role of setting a boundary condition of appropriate hardness. In Chapter 6, the buffers are employed to provide a thermal resistance in series between a building element and an isothermal environment, providing an analogue of the heat transfer surface coefficients employed in classical calculation of the overall thermal performance of building components. These three aspects of high-conductance measurement are considered separately in the following sections.

7.2 Interface Resistance in High-Conductance Measurements

Chapter 2 introduced the concept of using soft, compressible buffers in conjunction with the difference technique in the measurement of highly-conducting materials. It reports on a study of twelve such materials in conjunction with four candidate buffer materials using the Fox 600 apparatus. The test specimens covered a cross section of high-conductance materials ranging from aluminium sheet (0.00001 m^2.K/W) to 0.08 m^2.K/W for a fluted plastic board. All specimens were therefore of a resistance technically below the ASTM C 518 minimum. The buffers ranged from 3 mm thick PVC foam (0.04 m^2.K/W) to 7 mm thick nitrile foam (0.2 m^2.K/W). For the majority of measurements, the buffer was of higher thermal resistance than the test specimen, which amounts to a further technical non-compliance with ASTM C 518. Multiple re-measurement of specimen-buffer combinations, individual buffers and individual specimens (with no interface material) established the repeatability levels and demonstrated some characteristic differences. Silicone sponge was identified as the most consistent and nitrile as the least consistent by a large margin. Compression studies placed the buffer materials in the same ranking in terms of resiliency and low hysteresis. The nitrile also had the highest thermal resistance, in part due to the fact that it was also the thickest. Its combination of attributes rendered its use impractical, relative to the other three. With any of the other three buffers, it was found that thermal resistance was typically lower by between 0.003 and 0.01 m^2.K/W through use of the difference method to remove the contribution of interface resistance.

The highest reproducibility of all measurements in the study was with direct measurement of the two fluted boards. For each of these, the three measurements were within 0.5% of each other. Reproducibility with direct measurement was lower for all other specimens, with some inconsistency probably due to variable reproducibility of interface resistance from

measurement to measurement. Although measurement by difference produced lower results by eliminating contact resistance, variability was higher. For the best-performing silicone sponge, with the eight specimens exceeding 0.01 m^2.K/W in thermal resistance, variability between the three measurements ranged from 2% to 7%. These values are low enough to suggest that the technique is generally viable, recognizing that results depend in part upon the on the choice of buffer, which it may be possible to optimize for particular specimen properties (such as flatness).

An analysis contained in Chapter 2 accounted for all of the thermal resistance contributions algebraically and demonstrated that the simple subtraction of thermal resistance results for measurement of buffers "alone" from results for "specimen plus buffers" contained residual interface resistance terms. A solution to this was proposed in Chapter 3, based on the buffers measurement including a known reference specimen (in place of the test specimen). A required assumption is that the interface resistance between buffer and specimen is similar to that between buffer and reference material. Subsequent work with rough materials described in Chapter 5 suggests that this is a very reasonable assumption provided that both are reasonably smooth and that the buffers are reasonably soft. It is hereafter described as the "referenced difference method".

Chapter 3 reports on an experimental program designed to validate the referenced difference method and to extend the work of Chapter 2 in two specific areas. The first was an extension into a thermal resistance range a little above the nominal lower limit of ASTM C 518 in order to demonstrate the presence of interface resistance in measurements where it might not have been anticipated. Two test specimens were chosen, EPS (polystyrene foam) and PMMA (acrylic). These materials are both commonly used as reference materials, a fact which enhances the value of such a demonstration. The second area concerned buffer properties. Whilst the silicone sponge had performed well, significant uncertainty was attributable to the substantial thermal resistance of the material. As discussed, ASTM C 518 states that the buffer should have a low thermal resistance relative to the test specimen. Since both test materials appeared to be very flat, a somewhat thinner silicone sponge buffer, 4.2 mm thick, was chosen as one candidate. The other was the most conductive buffer that was thought to be potentially practical, a 1.7 mm thick sheet of solid silicone rubber. Its thermal resistance of 0.01 m^2.K/W compared with 0.05 m^2.K/W for the sponge material.

With each buffer type, multiple measurements were performed with and without thin sheets of phenolic board, this material being selected as the favoured reference material for a referenced difference measurement. Repeatability was approximately 0.2% for all

measurements. This was a good result in that it demonstrated not only the reproducibility of measurements involving buffers but also the capability of the Fox 600 apparatus to extend well below the nominal limit of 0.1 m^2.K/W which was required for measurements involving the 1.7 mm solid buffers. As with the Chapter 2 study, multiple measurements were then performed with the permutations of specimen and buffer, individually and together. Results for direct measurement were compared with those from difference measurement, calculated either by simple subtraction or by the referenced difference method. There was a constant separation between the two alternative difference-measurement methods for the same buffer, with results for the referenced difference method being always lower, as expected since the method factors out certain interface terms that have a nett positive value.

The results obtained for the previous study (Chapter 2) were also assessed in terms of the referenced difference method, taking advantage of the constant separation between results for the difference methods. The twelve earlier results were consistent with the two Chapter 3 results. Across all fourteen specimens, thermal resistance values obtained by the referenced difference method were lower by between 0.008 m^2.K/W and 0.016 m^2.K/W. This may therefore be regarded as a representative range of interface resistances. The error so introduced, as a percentage, depends upon the actual thermal resistance of the specimen. Amongst those studied, it was least for the 11 mm thick EPS board where the interface resistance amounted to 3.4%. This would be quite significant if such a specimen was being used as a reference material. The variability of individual measurements and of calculated difference values was not significantly greater with the thicker, softer silicone sponge over the five measurements performed of each. The calculated uncertainty was slightly higher due to the subtraction of more-similar numbers. For measurement of a thermal resistance of approximately 0.1 m^2.K/W, the uncertainties for a coverage factor of two and conservative assumptions would be approximately 4% compared with 3% for the thin, hard buffer. As thermal resistance reduces to 0.03 m^2.K/W, so the calculated uncertainty rises to 15% for measurement with the thicker buffer. Whilst this is high in relation to most reported measurements, it would be acceptable for many building-industry requirements. It would also be reduced by use of a thinner buffer of higher conductance.

Chapters 2 and 3 both make comment about an Asia-Pacific (APLAC) round robin of 27 laboratories which included a specimen of 15mm cast PMMA, having a nominal thermal resistance slightly below 0.1 m^2.K/W. It appears likely that many or most laboratories performed direct measurement and obtained results for conductivity that were too low. Whilst the generic thermal conductivity of cast PMMA in the 0.18-0.19 W/m.K range, the median result was 0.16 W/m.K with only five laboratories reporting values above 0.18

W/m.K. This highlights a general lack of awareness of high-conductance issues, even in terms of the initial planning since the specimens were technically outside the specified range of ASTM C 518 in the first instance.

Chapter 4 reports on the measurement of 30 specimens of loose-fill earth as part of an investigation into their potential use in green roofs. The use of buffer materials for the control of interface resistance and rigid-sided holding frames with stiff bases (reinforced phenolic board) were both central to successful measurement although both were at variance to ASTM C 518 and ASTM C 687, the measurement standard for loose fill materials. The rigid frames and stiff bases allowed specimens to be prepared in the frames with a small amount of compaction, with flat top surfaces, and with the facility remain intact during transfer into and out of the test apparatus. The top surfaces were quite rough compared to most insulation materials since the loose fill materials approximately equivalent to a fine gravel. The main program of measurements involved a set of three different compositions, each at three moisture contents and each represented by three specimens prepared to be as close to identical as possible. Specimens were sealed with cling plastic to prevent a change in their moisture content and measured with soft silicone sponge buffer sheets top and bottom over a time period of approximately 24 hours. The difference measurement included a specimen of the phenolic board between the two buffers and was therefore equivalent to the referenced difference method. Results were very consistent with all sets of three measurements closely grouped and all sets displaying a linear dependence on moisture content. The highest thermal resistance, for a dry scoria formulation, was 0.4 m^2.K/W. The lowest, for wet crushed terracotta was 0.08 m^2.K/W. An additional study was made of a specimen based on a dry commercial formulation having a thermal resistance of approximately 0.45 m^2.K/W. This specimen was re-measured ten times using alternating direct and difference methods (the latter with buffers). The indicated thermal resistance was higher by an average of 0.023 m^2.K/W with direct measurement. This is suggestive of an interface resistance higher than any of the values reported from the studies of Chapters 2 and 3. However the upper surface of the loose fill was also much rougher than any from these studies. It was also notable that the five direct measurements were less consistent than the five difference measurements even though these contained additional randomness accruing through the subtraction of two measurement results. This would seem to be a consequence of the poor surface contact afforded with direct measurement which would be particularly variable in the case of a loose fill specimen, with individual high points being constantly repositioned as a consequence of handling.

Chapter 4 also included a review of measurement methods for loose fills. The conclusions were that the ASTM and ISO steady-state test methods for loose-fill building insulations were targeted at compressible materials and do contain adequate provisions for dense, high-conductivity loose fills such as granular earths. This is despite the fact that some incompressible materials such as perlite are included in their coverage. However the transient methods are currently unable to achieve the low uncertainties required for test methods acceptable to regulatory authorities. Their performance has improving as a result of research and development but the issues are complex since the heat flows are transient and the geometries much more complex than the unidirectional heat flow ideal of the steady state methods. Measurements on the same specimens were also performed using a two-needle transient probe. As part of a separate research program, the alternative approaches are compared and are presented in Pianella et al. (2016). The steady-state results were found to be significantly more consistent within the groups of three alike specimens. There was also a general tendency for the indicated thermal conductivity to be higher with heat flow meter measurements. We found reason to suggest that these higher values were more representative of actual properties.

Achieving a satisfactory result with the heat flow meter apparatus involved the use of rigid-sided holding frames with a stiff base, higher than standard contact pressure, buffers top and bottom with the top recessed so as to confine contact to the loose fill surface as distinct from the frame, and use of the referenced difference method. Improvements to standards, particularly ASTM C 687 to accommodate incompressible and high-conductance loose fills were suggested.

7.3 Surface Roughness in High-Conductance Measurements

Interface resistance between abutting surfaces, whether electrical or thermal, is widely associated with surface roughness. However the studies described in Chapters 2 to 4 have demonstrated the successful use of flexible buffers to reduce thermal interface resistance in the first instance and to allow its effect to be factored out through difference measurement. A complication noted in Chapter 3 was that when the buffers were a harder material, in that case a 1.7 mm thick solid (un-foamed) silicone rubber sheet, the indicated thermal resistance tended to be slightly higher. Through the course of ongoing measurements it was found that this effect appeared to be associated with surface roughness and that it could be very significant for cases where very rough surfaces were combined with very high conductance.

In these cases the use of harder buffers appeared to be associated with both higher measured thermal resistance and higher measured overall thickness.

The choice of buffer thickness and hardness is a compromise that it is important to optimize. A key feature of thicker, softer buffers is their perceived ability to produce low interface resistance when adjacent to hard surfaces by adapting to the small non-uniformities that would otherwise limit contact to just the high points. However the inherent thermal resistance of thick, soft buffer materials is likely to be higher, reducing the potential precision of a difference measurement. This is especially the case when considering the possible effects of erratic or spatially non-uniform compression, buffer hysteresis, and imprecise clamping pressure. Thin, hard buffers therefore have some potential advantages.

Chapter 5 reports on an experimental study of nine materials, including a number with very rough surfaces, in combination with four silicone buffers ranging from 1.7 mm thick solid sheet to 6.4 mm medium-soft sponge. The dependence on buffer hardness was found to be very predictable with the increases in thermal resistance and apparent specimen thickness being well correlated. Across the range of materials, thermal resistance was higher by up to 0.01 m^2.K/W and thickness by up to 0.5 mm using the hardest buffer relative to the softest. These relative properties are readily measurable with some precision since they are the difference in overall values between results derived with one buffer and another. They have been termed R_x and t_x respectively.

An analytical model was developed to explore the relationship between interface resistance and surface roughness. The model allows roughness to be expressed in a simplified way as a varying fraction of flat hills in contact with the buffer and flat valleys which may be airspaces, depending on their depth, so that heat flow occurs through one of two alternative heat flow paths. The softness of the buffer in combination with the area fraction of the hills that it contacts determines the overall degree to which it is compressed. This in turn affects the extent to which the uncompressed areas extend into the valleys, allowing a valley airspace to exist. The model is not dimensionally sensitive and has been very effective in predicting the effect of roughness on overall thermal resistance and measured thickness, and the way these are correlated.

Roughness of the specimen surfaces was also measured using confocal microscopy. This produced roughness values with a ranking consistent with the rankings in the value of t_x. However roughness, commonly expressed as a mean amplitude, is not directly compatible with the dual terms of area fraction and valley depth employed by the analytical model and amenable to thermal resistance calculation. A geometric procedure was developed so that

generalized roughness could be expressed in terms of the two-zone model, allowing a relationship between roughness and interface resistance to be developed. This was achieved by assuming specimen roughness to have a sinusoidal profile, allowing calculation of the equivalent percentage area of the higher parts of the specimen profile that were in contact with the buffer (the fraction of hills) and the average height of the airspace formed above the lower areas of the sinusoid that were not in contact. Estimates of R_x based on optical roughness measurements with the application of this procedure, agreed well with the measured values.

Using the same procedure for the case of individual measurements, the model predicts that soft buffers may allow contact with the test specimen to be substantially free of interface resistance up to a certain level of roughness. This occurs because the buffer is sufficiently soft and the roughness sufficiently small that there is complete contact. Roughness may be defined using the three-dimensional mean absolute amplitude, S_a. With the softest 6.4 mm thick silicone sponge buffer, the threshold for the onset of interface resistance was predicted to be at a roughness of 60 μm. Beyond this threshold, interface resistance increases in direct proportion to roughness. Hard buffers exhibit the same proportionality but the onset threshold is at virtually zero roughness and interface resistance may exceed 0.010 m^2.K/W for an S_a value of 200 μm.

One of the materials studied, a thick specimen of PMMA, had a very smooth surface but significant thickness variation as determined by 48 edge measurements. Its behaviour was similar to a rough-surfaced material in terms of the value of R_x. It is notable that the analytical model is scale independent, reflecting the fact that even if different techniques are required in order to measure them, large-scale and small-scale thickness variations may have similar consequences in terms of interface resistance. The values of R_x and t_x were as well correlated for this specimen as for any of the others. Since t_x is directly measurable (by making multiple thickness measurements in the apparatus using different buffers), it appears to provide a means of predicting R_x and the approximate scale of thickness non-uniformity at all roughness scales.

An important conclusion from the work is the fact that for rough surfaces, thermal measurement results will depend to some extent on the compressibility or softness of the abutting surface. Applications exist where these surfaces could be very soft or very hard. Measurement results would be more consistent and useful if the characteristics of abutting surfaces were defined. For characterization of the bulk properties of the specimen, the softest practical buffer should be used as this will be least affected by surface effects.

7.4 Spatial Non-Uniformity in High-Conductance Measurements

Chapter 6 reports on the thermal assessment of webbed hollow-cored building panel. As a non-homogeneous specimen, it is outside the normal scope of the heat flow meter method. However the regular 124 mm web spacing was of smaller dimension than the 254 mm square heat flux transducer, suggesting that non-uniformity might not be severe. An initial series of measurements showed heat flow meter results to be independent of the position of webs relative to the heat flux sensor. This raised important questions concerning the ability of the heat flow meter method to deal with non-homogeneity, leading to further studies where experimental, modelling (using ANSYS) and heat-bridging calculation results for the original panel, and insulated versions, were compared.

Buffers were used in the initial measurements because the panel was composed of hard cementitious boards of high conductance, the buffers serving roles of plate protection as well as interface-resistance control. However the non-uniformity also suggested an additional role for buffers related to creating appropriate boundary conditions. Hot box measurement methods accommodate non-uniform specimens on the presumption that isothermal hot and cold air temperature zones exist on either side of the test specimen, coupled to it through the air films. The measured property is then the overall thermal resistance, including air films. Buffers provide the same functionality in a heat flow meter apparatus, coupling the isothermal hot and cold boundary temperatures to the specimen surface through buffers with appropriately-chosen properties.

Panel surface temperatures were measured at eight places to record panel response to the step function occurring when thermal measurement is commenced and then proceeds to stabilization. This step response was also modelled using ANSYS running in transient thermal analysis mode. This was done for the uninsulated (open-cored) panel as well as for versions filled with two levels of polyester fibre insulation. Modelled heat flow had spatial variations of about 2:1 on one side and 3:1 on the other for the highest insulation case but was only a few percent for the uninsulated panel, largely explaining the invariant nature of the original results. Measured and modelled temperatures agreed well after adjustment to web and airspace thermal properties data based on the comparison. Modelled heat flow also agreed well with analytical calculations which were straightforward due to the simple geometry of the panel. However heat flows indicated by the apparatus flux transducers were consistently higher by about 4% and 8% for the uninsulated and insulated cases respectively. These results are suggestive of some bias due to specimen non-homogeneity although the relatively high thickness may have been a contributing factor. Results do however suggest

that measurement in a heat flow meter apparatus in combination with interface buffers allows for revealing temperature-measurement with non-homogeneous specimens. Such measurements can be applied to the validation of modelling, potentially providing sufficient confidence in results to satisfy regulatory requirements. Since hot box test facilities allowing direct measurement are not readily available in many regions, this may provide an alternative for suitable specimens.

7.5 Recommendations for Future Work

7.5.1 Material Properties of Buffers

The medium-soft grade of silicone sponge used as a buffer for much of the research was found to perform at least adequately in terms of measurement repeatability. Useful properties included an appropriate thermal resistance for setting desired boundary conditions for the work described in Chapter 6. However, in general, measurement uncertainty for difference measurement would be lowest for a material of the highest thermal conductivity. Silicone with conductive loadings is available and this, or other engineered composite materials, might offer improved overall performance. However, high loadings could lead to compression-dependent conductivity and increased stiffness, neither of which would be desirable. Although the silicone sponge that was used had better resilience and lower deformation hysteresis than the other materials trialled, the study was by no means exhaustive. Other silicones, and possible other materials entirely, might be studied to see if they provided a better balance of attributes.

Chapter 5 identified buffer softness as a highly desirable property for measurement of rough-surfaced materials. Softness however also allows a buffer to deflect under load, therefore changing its thickness and thermal resistance. With the same apparatus loading for specimen and reference measurement, these resistance changes should be the same, introducing zero overall error. However differences will exist, especially with uneven specimen surfaces for which compression may be spatially non-uniform. Estimating the errors that this might introduce is a complex task. A study of the useful lower limits to softness would nevertheless be beneficial.

7.5.2 Apparatus Limitations

The study of surface roughness also suggested that for smooth surfaces, interface resistance should be very low if both specimen and apparatus plates are very flat. The consistent existence of a residual interface resistance for all direct measurements suggested

that the flatness of apparatus plates is an issue. The plates are not highly accessible, making careful mapping of plate flatness a non-trivial task. Plate flatness is known to be affected by temperature and also by the reactive force provided by a test specimen. Apart from large-area affects such as overall bowing, more localized effects such as imperfect flatness at the interface between metering and guard areas are potential issues worthy of study, contingent on the availability of suitable flatness-mapping equipment.

7.5.3 Measurement of Non-Homogeneous Specimens

The measured thermal resistance of the non-homogeneous panels reported in Chapter 6 was lower than expected by 8% or less depending on the insulation configuration. The low result has been attributed to heat flow non-uniformity. However, it is not a large error and may be partially due to anisotropy associated with the conductive facings. It was not possible to compare the webbed panel to one having similar facings but a uniform core. A future study might be constructed to specifically isolate such factors and determine more precisely the HFT response to spatially-varying heat flow alone. A greater level of instrumentation, including an array of sensors for plate surface temperature, would also be helpful.

7.5.4 Validation and Standards

The approach to high-conductance measurement consistently presented in this dissertation is that of using buffer materials at the specimen-plate interface, and difference measurement (preferably the procedure described as the referenced difference method) for determination of specimen thermal resistance. It has been described for a wide range of highly-conductive specimens, for two less-conductive specimens, for rigid loose fill materials, for materials with rough surfaces and for a non-homogeneous webbed panel. However it is an approach that has not been reported by other workers. Perhaps there is reluctance to move beyond the guidance of an existing standard, despite the alternative being a potential failure to account for errors due to interface resistance. It would be most useful if this issue and the methodology presented in this dissertation were critically investigated by others, with the expectation that findings would be corroborative. It would appear that there are clear weaknesses in ASTM C 518, ASTM C 177 and ASTM C 687. At the very least, they have limitations in the measurement of high-conductance materials which, if properly addressed, might lead to improved measurement performance in this area. However, consistent research findings from numerous sources would be required in order to instigate change. Hopefully the work described in this dissertation can be a catalyst for this to occur.

8 REFERENCES (COMPLETE)

AIRAH. (1978) *AIRAH Design Data Manual,* Parkville, Vic.: Australian Institute of Refrigeration Air Conditioning and Heating

AIRAH. (2013) AIRAH Technical Handbook. Australian Institute of Refrigeration, Air-Conditioning and Heating Inc.

Al-Ajlan SA. (2006) Measurements of thermal properties of insulation materials by using transient plane source technique. *Applied Thermal Engineering* 26: 2184-2191. DOI: 10.1016/j.applthermaleng.2006.04.006

Albers MA and Pelanne CM. (1983) An Experimental and Mathematical Study of the Effect of Thickness in Low-Density Glass-Fiber Insulation *Thermal Conductivity 17/ Thermal Expansion 8.* Gaithersburg, MD (USA): Springer Science + Business Media, DOI: 10.1007/978-1-4899-5436-7_44

Almanza O, Rodríguez-Pérez MA and De Saja JA. (2004) Applicability of the transient plane source method to measure the thermal conductivity of low-density polyethylene foams. *Journal of Polymer Science Part B: Polymer Physics* 42: 1226-1234. DOI: 10.1002/polb.20005

APLAC. (2010) APLAC TO53. Final Report, Thermal Insulation Proficiency Testing Program. Abbotsford, Vic, Australia: Asia Pacific Laboratory Accreditation Cooperation.

ASHRAE. (2013) 2013 ASHRAE Handbook - Fundamentals (SI Edition). American Society of Heating, Refrigerating and Air-Conditioning Engineers, Inc., 25, 7-8.

ASTM. (1985) *ASTM STP879 Guarded Hot Plate and Heat Flow Meter Methodology*: ASTM International, DOI: 10.1520/stp879-eb

ASTM. (2007) ASTM D1056 - 07 "Specification for Flexible Cellular Materials--Sponge or Expanded Rubber.". *Annual Book of ASTM Standards, Vol. 08.01.* ASTM International, DOI: 10.1520/D1056-07

ASTM. (2009) ASTM D5930 - 09 "Test Method for Thermal Conductivity of Plastics by Means of a Transient Line-Source Technique.". *Annual Book of ASTM Standards, Vol. 08.03.* ASTM International, DOI: 10.1520/d5930-09

ASTM. (2010a) ASTM C177 - 10. "Test Method for Steady-State Heat Flux Measurements and Thermal Transmission Properties by Means of the Guarded-Hot-Plate

Apparatus.". *Annual Book of ASTM Standards, Vol. 04.06.* ASTM International, DOI: 10.1520/c0177-10

ASTM. (2010b) ASTM C518 - 10. "Test Method for Steady-State Thermal Transmission Properties by Means of the Heat Flow Meter Apparatus.". *Annual Book of ASTM Standards, Vol. 04.06.* ASTM International, DOI: 10.1520/c0518-10

ASTM. (2011) ASTM E1530 - 11. "Test Method for Evaluating the Resistance to Thermal Transmission of Materials by the Guarded Heat Flow Meter Technique.". *Annual Book of ASTM Standards, Vol. 14.02.* ASTM International, DOI: 10.1520/E1530-06

ASTM. (2012) ASTM C687 - 12. "Standard Practice for Determination of Thermal Resistance of Loose-Fill Building Insulation.". *Annual Book of ASTM Standards, Vol. 04.06.* ASTM International, DOI: 10.1520/c0687-12

ASTM. (2013a) ASTM C177 - 13. "Test Method for Steady-State Heat Flux Measurements and Thermal Transmission Properties by Means of the Guarded-Hot-Plate Apparatus.". *Annual Book of ASTM Standards, Vol. 04.06.* ASTM International, DOI: 10.1520/C0177

ASTM. (2013b) ASTM C1113 / C1113M - 09 (2013) "Standard Test Method for Thermal Conductivity of Refractories by Hot Wire (Platinum Resistance Thermometer Technique).". *Annual Book of ASTM Standards, Vol. 15.01*. ASTM International, DOI: 10.1520/c1113_c1113m

ASTM. (2013c) ASTM E1461 - 13. "Test Method for Thermal Diffusivity by the Flash Method.". *Annual Book of ASTM Standards, Vol. 14.02.* ASTM International, DOI: 10.1520/E1461

ASTM. (2014) *ASTM STP1574 Next-Generation Thermal Insulation Challenges and Opportunities*: ASTM International, DOI: 10.1520/stp1574-eb

ASTM. (2015) ASTM C518 - 15. "Test Method for Steady-State Thermal Transmission Properties by Means of the Heat Flow Meter Apparatus.". *Annual Book of ASTM Standards, Vol. 04.06.* ASTM International, DOI: 10.1520/C0518-15

Barned JR. (1946) Thermal Conductivities of Building Materials. *Report R2.* Melbourne: CSIRO, Division of Building Research.

Barned JR and O'Brien LF. (1970) Thermal Conductivity of Building Materials. *Report R2.* CSIRO, Division of Building Research.

Bentz DP, Peltz MA, Durán-Herrera A, et al. (2011) Thermal properties of high-volume fly ash mortars and concretes. *Journal of Building Physics* 34: 263-275. DOI: 10.1177/1744259110376613

Bobeth M and Diener G. (1982) Upper bounds for the effective thermal contact resistance between bodies with rough surfaces. *International Journal of Heat and Mass Transfer* 25: 1231-1238. DOI: 10.1016/0017-9310(82)90217-4

Bomberg M. (1994) A Workshop on Measurement Errors and Methods of Calibration of a Heat Flow Meter Apparatus. *Journal of Building Physics* 18: 100-114. DOI: 10.1177/109719639401800202

Bomberg M and Solvason KR. (1983) Comments on Calibration and Design of a Heat Flow Meter *ASTM STP789 Thermal Insulation, Materials, and Systems for Energy Conservation in the '80s.* ASTM International, DOI: 10.1520/stp29452s

Booth JR, Graves RS and Yarbrough DW. (1995) Aging of Thin-Slices of PIR Foams Manufactured with Alternative Blowing Agents. *Journal of Building Physics* 19: 118-131. DOI: 10.1177/109719639501900203

Brzezinski A and Tleoubaev A. (2002) Effects of Interface Resistance on Measurements of Thermal Conductivity of Composites and Polymers *Proceedings of the 30th Annual Conference on Thermal Analysis and Applications (NATAS).* Pittsburgh: B&K Publishing

BSI. (2001) BS EN 12664:2001. "Thermal performance of building materials and products. Determination of thermal resistance by means of guarded hot plate and heat flow meter methods. Dry and moist products of medium and low thermal resistance". British Standards Institution

Campbell GS, Huffaker EM, Wacker BT, et al. (2005) Use of the line heat source method to measure thermal conductivity of insulation and other porous materials *Thermal Conductivity 27/ Thermal Expansion 15*. Knoxville, TN: DEStech Publications, Inc., Lancaster, PA, U.S.A.

Campbell R and Rose M. (2013) Thermal Conductivity Measurements of Concrete Using the Heat Flow Meter (HFM) and Guarded Hot Plate (GHP) Methods. **http://www.netzsch-thermal-analysis.com:** NETZSCH Instruments North America.

Cha J, Seo J and Kim S. (2012) Building materials thermal conductivity measurement and correlation with heat flow meter, laser flash analysis and TCi. *Journal of Thermal Analysis and Calorimetry* 109: 295-300.

Clarke RE and Delsante AE. (1993) Moisture adsorption in thermal conductivity samples and its effect on equilibration time *Thermal Conductivity 22, Proceedings of the 22nd International Thermal Conductivity Conference.* Phoenix, Arizona: Technomic Publishing

Clarke RE, Pianella A, Shabani B, et al. (2016a) Steady-state thermal measurement of moist granular earthen materials. *Journal of Building Physics* Prepublished May 23 2016, DOI: 10.1177/1744259116637864

Clarke RE, Rosengarten G and Shabani B. (2014) Flexible Buffer Materials to Reduce Contact Resistance in Thermal Insulation Measurements *Thermal Conductivity 32 / Thermal Expansion 20, Proceedings of the 32th International Thermal Conductivity Conference and 20th International Thermal Expansion Symposium.* West Lafayette, Indiana: Purdue University Scholarly Publishing Services, DOI: 10.5703/1288284315544

Clarke RE, Shabani B and Rosengarten G. (2016b) A difference technique to avoid interface errors in measurement of high-conductance thermal insulation. *Journal of Building Physics* Prepublished May 23 2016, DOI: 10.1177/1744259116637863

Corsan JM and Williams I. (1980) Errors associated with imperfect surfaces in standard hot-plate thermal conductivity measurements. In: Metrology NPLDoQ (ed) *NPL Report QU57.* National Physical Laboratory, Teddington, Middlesex, TW11 OLW, UK.

De Ponte F. (1984) Standard Reference Materials in the European Community. *Journal of Building Physics* 8: 94-106. DOI: 10.1177/109719638400800204

De Ponte F. (1985) Present and Future Research on Guarded Hot Plate and Heat Flow Meter Apparatus *ASTM STP879 Guarded Hot Plate and Heat Flow Meter Methodology.* ASTM International, DOI: 10.1520/stp32902s

De Ponte F and Maccato W. (1980) The Calibration of Heat Flow Meters *ASTM STP718 Thermal Insulation Performance.* ASTM International, DOI: 10.1520/stp29277s

Desjarlais AO and Tye RP. (1990) Research and Development Data to Define the Thermal Performance of Reflective Materials Used to Conserve Energy in Building Applications. Oak Ridge National Laboratory.

Desjarlais AO and Yarbrough DW. (1991) Prediction of the Thermal Performance of Single and Multi-Airspace Reflective Insulation Materials *ASTM STP1116 Insulation Materials: Testing and Applications, 2nd Volume.* ASTM International, DOI: 10.1520/stp16338s

Dong Y, McCartney JS and Lu N. (2015) Critical Review of Thermal Conductivity Models for Unsaturated Soils. *Geotechnical and Geological Engineering* 33: 207-221. DOI: 10.1007/s10706-015-9843-2

Farrell C, Mitchell RE, Szota C, et al. (2012) Green roofs for hot and dry climates: Interacting effects of plant water use, succulence and substrate. *Ecological Engineering* 49: 270-276. DOI: 10.1016/j.ecoleng.2012.08.036

Filla BJ and Slifka AJ. (1997) Thermal Conductivity Measurements of Pyroceram 9606 Using a High-Temperature Guarded-Hot-Plate *Thermal Conductivity 24 / Thermal Expansion 12, Proceedings of the 24th International Thermal Conductivity Conference and 12th International Thermal Expansion Symposium.* Pittsburgh, PA: Technomic

Fricker JM and Yarbrough DW. (2011) Review of reflective insulation estimation methods. *Proceedings of Building Simulation, 12th Conference of International Building Performance Simulation Association.* Sydney

Gossard D, Lartigue B and Sambou V. (2012) Nusselt number correlations for laminar convection in three-dimensional air-filled cavities. *Journal of Building Physics* 35: 327-337. DOI: 10.1177/1744259111423086

Graves RS and Yarbrough DW. (1993) The Use of an Array of Heat Flux Transducers to Study Thermal Property Variations. *Journal of Building Physics* 17: 171-181. DOI: 10.1177/109719639301700108

Hall JA, Ceckler WH and Thompson EV. (1987) Thermal properties of rigid polymers. I. Measurement of thermal conductivity and questions concerning contact resistance. *Journal of Applied Polymer Science* 33: 2029-2039. DOI: 10.1002/app.1987.070330615

Han BJ, Yarbrough DW and Han SM. (1986) Thermal Resistance of Wall Cavities Containing Reflective Insulation. *Journal of Solar Energy Engineering* 108: 338-341. DOI: 10.1115/1.3268116

Hollingsworth M. (1980) Experimental Determination of the Thickness Effect in Glass Fiber Building Insulation *ASTM STP718 Thermal Insulation Performance.* ASTM International, DOI: 10.1520/stp29278s

Hust JG and Smith DR. (1989) Interlaboratory Comparison of Two Types of Line-Source Thermal-Conductivity Apparatus Measuring Five Insulating Materials. Boulder, Colorado: NIST.

ISO. (1991) ISO 8301:1991 Ed 1 Thermal insulation. Determination of steady-state thermal resistance and related properties. Heat flow meter apparatus. Geneva, Switzerland: International Organization for Standardization

ISO. (2007) ISO 6946:2007 Building components and building elements - Thermal resistance and thermal transmittance - Calculation method. *ISO 6946.* Geneva, Switzerland: International Organization for Standardization

ISO. (2008) ISO/IEC Guide 98-3:2008 Uncertainty of measurement -- Part 3: Guide to the expression of uncertainty in measurement (GUM:1995). Geneva, Switzerland: International Organization for Standardization

Jackson RL, Bhavnani SH and Ferguson TP. (2008) A Multiscale Model of Thermal Contact Resistance Between Rough Surfaces. *Journal of Heat Transfer* 130: 081301-081301. DOI: 10.1115/1.2927403

Jones GF and Jones RW. (1999) Steady-state heat transfer in an insulated, reinforced concrete wall: theory, numerical simulations, and experiments. *Energy and buildings* 29: 293-305. DOI: 10.1016/S0378-7788(98)00072-3

Kamai T, Kluitenberg GJ and Hopmans JW. (2015) A Dual-Probe Heat-Pulse Sensor with Rigid Probes for Improved Soil Water Content Measurement. *Soil Science Society of America Journal* 79: 1059. DOI: 10.2136/sssaj2015.01.0025

Kosny J and Childs P. (2002) Accuracy of Hot Box Testing of Steel Stud Walls *ASTM STP1426 Insulation Materials: Testing and Applications: 4th Volume.* ASTM International, DOI: 10.1520/stp11010s

Lavrykov SA and Ramarao BV. (2012) Thermal Properties of Copy Paper Sheets. *Drying Technology* 30: 297-311. DOI: 10.1080/07373937.2011.638148

Le Goic G, Brown CA, Favreliere H, et al. (2013) Outlier filtering: a new method for improving the quality of surface measurements. *Measurement Science and Technology* 24: 015001. DOI: 10.1088/0957-0233/24/1/015001

Liu G and Si BC. (2011) Single- and Dual-Probe Heat Pulse Probe for Determining Thermal Properties of Dry Soils. *Soil Science Society of America Journal* 75: 787. DOI: 10.2136/sssaj2010.0241

Miyake Y and Eguchi K. (1985) Development of a Large Area Heat Flow Meter *ASTM STP879 Guarded Hot Plate and Heat Flow Meter Methodology.* ASTM International, DOI: 10.1520/stp32907s

Narumanchi S, Mihalic M, Kelly K, et al. (2008) Thermal interface materials for power electronics applications *11th Intersociety Conference onThermal and Thermomechanical Phenomena in Electronic Systems, 2008. ITHERM 2008.* Orlando, Florida, DOI: 10.1109/ITHERM.2008.4544297

Netzsch. (2015) *Netzsch Thermal Analysis*. Available at: https://**www.netzsch-thermal-analysis.com/**.

Noonan PM and Jonas TR. (2014) Full-Thickness Thermal Testing of Fiberglass Insulation Using an ASTM C518-10 Heat Flow Meter Apparatus *ASTM STP1574 Next-Generation Thermal Insulation Challenges and Opportunities.* ASTM International, DOI: 10.1520/stp157420130099

Ouertatani N, Ben Cheikh N, Ben Beya B, et al. (2008) Numerical simulation of two-dimensional Rayleigh–Bénard convection in an enclosure. *Comptes Rendus Mécanique* 336: 464-470. DOI: 10.1016/j.crme.2008.02.004

Pavlík Z, Jerman M, Trník A, et al. (2014) Effective thermal conductivity of hollow bricks with cavities filled by air and expanded polystyrene. *Journal of Building Physics* 37: 436-448. DOI: 10.1177/1744259113499214

Pianella A, Clarke RE, Williams NSG, et al. (2016) Steady-state and transient thermal measurements of green roof substrates. *Energy and buildings* 131: 123-131. DOI: 10.1016/j.enbuild.2016.09.024

Rennex B. (1985) Summary of Error Analysis for the National Bureau of Standards 1016-mm Guarded Hot Plate and Considerations Regarding Systematic Error for the Heat Flow Meter Apparatus *ASTM STP879 Guarded Hot Plate and Heat Flow Meter Methodology.* ASTM International, DOI: 10.1520/stp32900s

Rides M, Morikawa J, Halldahl L, et al. (2009) Intercomparison of thermal conductivity and thermal diffusivity methods for plastics. *Polymer Testing* 28: 480-489. DOI: 10.1016/j.polymertesting.2009.03.002

Ridouane EH, Hasnaoui M and Campo A. (2005) Effects of surface radiation on natural convection in a rayleigh-benard square enclosure: steady and unsteady conditions. *Heat and Mass Transfer* 42: 214-225. DOI: 10.1007/s00231-005-0012-7

Robinson HE and Powlitch FJ. (1954) The thermal insulating value of airspaces. Housing research paper no. 32. Washington, DC: US Government Printing Office.

Robinson HE and Watson TW. (1952) Interlaboratory Comparison of Thermal Conductivity Determinations with Guarded Hot Plates *ASTM STP119 Symposium on Thermal Insulating Materials.* Cincinnati, Ohio, USA: ASTM International, DOI: 10.1520/stp119-eb

Saber HH. (2013) Practical correlations for thermal resistance of horizontal enclosed airspaces with upward heat flow for building applications. *Building and Environment* 61: 169-187. DOI: 10.1016/j.buildenv.2012.12.016

Sailor DJ and Hagos M. (2011) An updated and expanded set of thermal property data for green roof growing media. *Energy and buildings* 43: 2298-2303. DOI: 10.1016/j.enbuild.2011.05.014

Salmon DR and Tye RP. (2009) An Inter-Comparison of Two Methods for Measuring the Thermal Conductivity of Low-Density Masonry Materials *Thermal Conductivity 30: Thermal Expansion 18.* Pittsburgh, Pennsylvania, USA: DESTech Publications, Inc

Salmon DR and Tye RP. (2011) An inter-comparison of a steady-state and transient methods for measuring the thermal conductivity of thin specimens of masonry materials. *Journal of Building Physics* 34: 247-261. DOI: 10.1177/1744259109360060

Sambou V, Lartigue B, Monchoux F, et al. (2016) Modeling of the thermal performance of air-filled partitioned enclosures: Effects of the geometry and thermal properties. *Journal of Building Physics* 39: 321-341. DOI: 10.1177/1744259114561578

Sandberg PI. (1995) Thermal Conductivity of Moist Masonry Materials. *Journal of Building Physics* 18: 276-288. DOI: 10.1177/109719639501800307

Shirtliffe CJ. (1980) Effect of Thickness on the Thermal Properties of Thick Specimens of Low-Density Thermal Insulation *ASTM STP718 Thermal Insulation Performance.* ASTM International, DOI: 10.1520/stp29265s

Stacey C, Parfitt MJ, Simpkin AJ, et al. (2014) Design of a Guarded Hot Plate for Measuring Thin Specimens of Polymer and Composite Materials *Thermal Conductivity 32 / Thermal Expansion 20, Proceedings of the 32th International Thermal Conductivity Conference and 20th International Thermal Expansion Symposium.* West Lafayette, Indiana, DOI: 10.5703/1288284315551

Standards Australia. (2003) AS 3743:2003 Potting Mixes. Sydney: Standards Australia

Standards Australia. (2006) AS/NZS 4859.1:2002 Materials for the thermal insulation of buildings - General criteria and technical provisions. Sydney: Standards Australia, Standards NZ

Stovall T. (2014) Evaluation of Homogeneity Qualification Criteria in the Accelerated Aging of Closed-Cell Foam Insulation, Results after Five Years of Full-Thickness Aging *ASTM STP1574 Next-Generation Thermal Insulation Challenges and Opportunities.* ASTM International, DOI: 10.1520/stp157420130104

Symons JG, Clarke RE and Peirce JV. (1995) The Thermal Performance of Several Australian Fibrous Insulating Materials. *Journal of Building Physics* 19: 72-88. DOI: 10.1177/109719639501900107

TA Instruments. (2016) *Thermal Conductivity Test Instruments*. Available at: **http://www.tainstruments.com/products/thermal-conductivity-meter/**.

Tleoubaev A and Brzezinski A. (2007) Errors of the Heat Flow Meter Method Caused by Thermal Contact Resistance *Thermal Conductivity 29 / Thermal Expansion 17, Proceedings of the 29th International Thermal Conductivity Conference and 17th International Thermal Expansion Symposium.* Birmingham, Alabama: DEStech Publications

Trethowen H. (1986) Measurement errors with surface-mounted heat flux sensors. *Building and Environment* 21: 41-56. DOI: 10.1016/0360-1323(86)90007-7

Trethowen HA. (2000) Validating the isothermal planes method for R-value predictions. Porirua [N.Z.]: Building Research Association of New Zealand.

Tye RP. (1990) Measurements of thermal insulation performance: The challenge of the next decade. *International Journal of Thermophysics* 11: 315-327. DOI: 10.1007/BF01133564

Tye RP, Coumou KG, Desjarlais AO, et al. (1987) Historical Development of Large Heat Flow Meter Apparatus for Measurements of Thermal Resistance of Insulations *ASTM STP922 Thermal Insulation: Materials and Systems.* Dallas, Texas, USA: ASTM International, DOI: 10.1520/STP18510S

Tye RP and Salmon DR. (2001) Thermal Conductivity Certified reference Materials: Pyrex 7740 and Polymethlymethacrylate *Thermal Conductivity 26 / Thermal Expansion 14, Proceedings of the 26th International Thermal Conductivity Conference and 14th International Thermal Expansion Symposium.* Cambridge, Massachusetts: DEStech Publications

Van Geem MG. (1986) Thermal Transmittance of Concrete Block Walls with Core Insulation. *Journal of Building Physics* 9: 187-210. DOI: 10.1177/109719638600900302

Wegger E, Jelle BP, Sveipe E, et al. (2011) Aging effects on thermal properties and service life of vacuum insulation panels. *Journal of Building Physics* 35: 128-167. DOI: 10.1177/1744259111398635

Williamson TJ. (2013) Designing houses for the Australian climate: the early research. *Architectural Science Review* 56: 197-207. DOI: 10.1080/00038628.2013.807218

Yarbrough DW. (1983) Assessment of Reflective Insulations for Residential and Commerical Applications, ORNL/TM-8891. Oak Ridge, Tennessee: Oak Ridge National Laboratory.

Yu M, Sui X, Peng X, et al. (2009) Influence of moisture content on measurement accuracy of porous media thermal conductivity. *Heat Transfer-Asian Research* 38: 492-500. DOI: 10.1002/htj.20272

Zarr RR. (2001) A history of testing heat insulators at the National Institute of Standards and Technology. *ASHRAE Transactions* 107: 661.

Zarr RR. (2010) Assessment of Uncertainties for the NIST 1016 mm Guarded-Hot-Plate Apparatus: Extended Analysis for Low-Density Fibrous-Glass Thermal Insulation. *Journal of Research of the National Institute of Standards and Technology* 115: 23-59.

Zarr RR, Heckert NA and Leigh SD. (2014) Retrospective Analysis of NIST Standard Reference Material 1450, Fibrous Glass Board, for Thermal Insulation Measurements. *Journal of Research of the National Institute of Standards and Technology* 119: 296. DOI: 10.6028/jres.119.012

Zarr RR and Leigh SD. (2014) Standard Reference Material 1450d, Fibrous Glass Board, for Thermal Insulation Measurements *ASTM STP1574 Next-Generation Thermal Insulation Challenges and Opportunities.* ASTM International, DOI: 10.1520/stp157420130063

Zsembery S, Clarke RE and McNeilly T. (1996) Thermal transmission properties of Australian clay bricks. *Masonry International* 10: 30-34